Reduced Stress

Jeffrey R. Keaton
Amec Foster Wheeler, Los Angeles, CA, USA

Definition

Reduced stress is very much like stress, only smaller (Fig. 1). Find the term “stress” in the *Encyclopedia of Engineering Geology* (Bobrowsky and Marker 2018). Copy the definition, paste it into a word processing application, and then make the font smaller. Individuals who follow these steps will experience reduced stress.

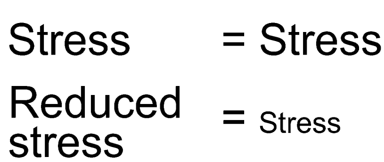

Reduced Stress, Fig. 1 Reduced stress

Cross-References

► Stress

References

Bobrowsky PT, Marker BR (eds) (2018) Encyclopedia of engineering geology. Springer Online, https://link.springer.com/referencework/10.1007%2F978-3-319-12127-7. Accessed 29 Jan 2018

Remote Sensing

Janusz Wasowski[1], Daniele Giordan[2,3] and Vern Singhroy[4]
[1]CNR-IRPI (National Research Council – Institute for Geohydrological Protection), Bari, Italy
[2]Research Institute for Hydrogeological Prevention and Protection, Torino, Italy
[3]CNR-IRPI, Torino, Italy
[4]Natural Resources Canada, Canada Centre for Remote Sensing, Ottawa, ON, Canada

Definition

Remote sensing – “The science and art of obtaining information about an object, area, or phenomenon through the analysis of data acquired by a device that is not in contact with the object, area, or phenomenon under investigation,” as defined by Lillesand et al. (2015) in their textbook on remote sensing and image interpretation.

Introduction

The first uses of remote sensing in engineering geology practice date back to the late 1920s and early 1930s, when aerial photo interpretation and photogrammetry methods assisted engineers in terrain reconnaissance and site evaluation, flood control surveillance, and topographic mapping (Barr 1984). Since then the use of information retrieved from remotely sensed data by research and professional engineering geologists has become more diversified and more common. However, the application potential of remote sensing in ground engineering is still considered to be little explored in comparison to the uses of remotely sensed data by

P. T. Bobrowsky, B. Marker (eds.), *Encyclopedia of Engineering Geology*,
https://doi.org/10.1007/978-3-319-73568-9

geologists or applied geomorphologists. We foresee an increasingly greater uptake of remotely sensed data by engineering geologists in the near future, because presently, the new-generation high-resolution optical and radar sensors and the improved digital image processing techniques developed in this century are now capable of delivering more rapidly high-quality information that is sufficiently detailed (and cost-effective) for many practical engineering applications.

We focus on the new tools and techniques of Earth surface sensing, which hold the most promise for profitable exploitation in engineering geology research and practice. The emphasis is on selected space and airborne, as well as ground-based, imaging systems, where the most innovation has been taking place since the beginning of this century.

Furthermore, we consider the wide field of engineering geology, ranging from the traditional ground engineering to the multidisciplinary socioeconomic domains (e.g., natural hazards, environmental protection, and sustainable development), in which the applied geologists and geotechnical engineers have become increasingly more involved in the recent decades (Juang et al. 2016). We highlight both the well-recognized as well as currently little-exploited opportunities offered by innovative remote sensing techniques.

For details on remote sensing principles and digital image processing and interpretation, the interested reader is referred to selected textbooks and manuals (Drury 2001; Khorram et al. 2016; Lillesand et al. 2015; Njoku 2014). We also provide references to review articles on specific applications of new remote sensing techniques in engineering geology.

New Remote Sensing Tools and Applications

Very-High-Resolution Optical Satellites

The availability of high-quality imagery provided initially (since the early 2000s) at about 1 m resolution by the first commercial satellites (e.g., IKONOS, QUICKBIRD) can be considered as a major breakthrough in the practical applicability of spaceborne optical sensing to geological engineering. Such resolution meant that the level of detail of information obtained from satellite imagery is comparable to that attainable from high-quality digital aerial photography. The trend toward improving resolutions (sub-0,5 m as of 2015, e.g., WorldView-3) and decreasing prices of the imagery and the growing number of satellite constellations that can offer daily (or even intraday) revisits of the area of interest and rapid data products delivery through web-based access imply the greater and more profitable use of space imagery.

In addition to detailed terrain and site characterization or mapping natural hazards (e.g., floods, landslides), which until recently relied only on aerial photo interpretation, satellite imagery can be uniquely exploited for disaster management and post-event damage assessment (e.g., Bally 2013). One important limitation of the use of satellite optical data in emergency situations (especially flood events) is the presence of persistent cloud cover in certain regions (e.g., tropical regions with long rainy seasons).

Unmanned Aerial Vehicles (UAV)

These inexpensive airborne platforms, also called unmanned aerial systems (UAS), remotely piloted aircraft systems (RPAS), or simply drones, are usually operated by a person on the ground (Barnhart et al. 2012). They can carry sophisticated imaging sensors but most often include light digital cameras used to acquire very-high-resolution (cm-dcm) images. This, as well as the flexibility in survey scheduling, makes UAV technology particularly attractive for rapid response and initial surveys of damaging natural or human-made hazards (e.g., Giordan et al. 2015). With UAV flight endurance on the order of several hours or more, a nearly all-day surveillance capability can be assured for management of evolving hazards.

UAV are typically low-flying platforms and can also acquire imagery even in the presence of low-altitude clouds. However, the presence of strong wind can preclude or restrict their use. The use of UAV is also limited by stringent aviation regulations. In comparison to wide-area coverage typical of satellites, UAV are best fitted to acquire very-high-resolution imagery over smaller areas and are well suited for engineering applications (e.g., Nex and Remondino 2014).

Spaceborne Synthetic Aperture Radar (SAR) Multi-temporal Interferometry (MTI)

MTI refers to a series of advanced synthetic aperture radar differential interferometry (DInSAR) techniques, including Permanent/Persistent Scatterers Interferometry – PSInSAR™/PSI and similar methods – as well as Small Baseline Subset, SBAS, and related/hybrid approaches. Simply stated, with radar satellites periodically revisiting the same area, DInSAR and MTI are used to provide information on distance changes between the onboard radar sensor and targets on the ground (e.g., rock outcrops and bare ground, human-made structures such as buildings, roads, and corner reflectors).

In settings with limited vegetation cover, these techniques can deliver precise (mm-cm resolution), spatially dense information (from hundreds to thousands measurement points/km^2) on slow rate (mm-dcm/year) deformations affecting the ground or engineering structures. Radar satellites guarantee wide-area coverage (thousands km^2); the sensors that actively emit electromagnetic radiation can “see” through the clouds, and the deformation measurements are rarely affected by bad weather conditions. Since 2008 the application potential of MTI has increased thanks to the improved capabilities of the new radar sensors (COSMO-SkyMed constellation and TerraSAR-X) in terms of resolution (from 3 to 1 m) and revisit time (from 11 to 4 days).

Recent literature reviews (e.g., Wasowski and Bovenga 2014a, b) suggest that so far MTI has been mostly used in research-oriented engineering geology investigations, especially those regarding slope and subsidence hazards. However, MTI is also often employed to assist in management of oil/gas field operations (e.g., Ferretti 2014; Singhroy et al. 2015), especially for monitoring ground instabilities induced by the fluid/gas injection and withdrawal. With the steadily growing number of radar satellites, the global coverage and free data availability offered by the recent (2014) European Space Agency Sentinel-1 mission, and continuous improvements of radar data processing methods, MTI is expected to become soon a standard operational tool (like Global Positioning System – GPS) for detecting and monitoring ground deformations and structural distress.

Ground-Based Interferometric SAR (GBInSAR)

As with InSAR or DInSAR, the GBInSAR (also called GBSAR) technology relies on a synthetic aperture radar imaging and exploits the principles of interferometry. In a common operating setup, GBInSAR consists of a radar sensor that moves along a fixed rail (up to 2–3 m long) while sending microwaves toward the target area (e.g., quarry slope) and receiving back the reflected radar signal. Radar images repeatedly acquired in this mode can be used to retrieve very detailed surface morphology of a target area and detect possible deformations. In comparison to MTI techniques, the unique feature of GBInSAR is the capability to provide precise measurements for a wide range of deformation rates (from mm/year to m/hour).

GBInSAR systems achieve millimeter measurement precision and are suitable for local-scale or site-specific monitoring, with up to few kilometer remote surveying range. With its high-frequency (minutes) measurements, day/night and all-weather operational capability, and very rapid processing and delivery of measurement results (within hours), GBInSAR can be exploited for near real-time monitoring and early warning. The equipment, however, is expensive and requires human assistance in the field. Therefore, GBInSAR is most cost-effective for high-risk, short-term (e.g., daily–weekly) monitoring, high-value infrastructure (e.g., dams, bridges), and human activities (e.g., mining).

More information on the principles of ground-based interferometry, data acquisition modes, and processing is available in recent review articles of Monserrat et al. (2014) and Caduff et al. (2015). These works also discuss different examples of ground and structure deformation monitoring via GBInSAR.

LiDAR (Light Detection and Ranging)

Tratt (2014) offers a comprehensive overview of LiDAR technology. LiDAR technique is based on a laser beam scanning which results in spatially “continuous” very-high-resolution imagery (clouds of points) of the ground surface and associated natural and artificial features. A distinction is made between airborne laser scanner (ALS), also called airborne laser swath mapping (ALSM), and terrestrial laser scanner (TLS) applications, as this implies differences in scale (regional or local to site specific) of investigation and in data resolution. ALS and TLS attain, respectively, dcm and cm spatial resolutions and dcm and sub-cm measurement precisions. Importantly, useful results can be obtained even in the presence of dense vegetation.

ALS can be used to generate high-resolution topographic maps and digital elevation models (DEM) for local to large-area investigations; often high-resolution optical imagery is contemporaneously acquired (using digital cameras) during airborne LiDAR surveys. By repeating TLS or ALS surveys, change detection is possible and, e.g., ground surface displacements or soil erosion volume estimates can be obtained (e.g., DeLong et al. 2012).

TLS setup on the ground is relatively easy, but human assistance is also required during the scanning operations. The ALS and TLS instrumentation is expensive. Furthermore, significant costs of airborne surveys tend to preclude the use of ALS for frequent/systematic repetition of measurements.

Summary

New remote sensing technologies can now provide very high spatial resolution imagery for producing detailed topographic maps and DEM. Very-high-precision measurements of ground surface and infrastructure deformations can also be obtained. Spaceborne radar sensors offer great potential for multi-scale (from regional scale to site specific) deformation monitoring because of wide-area coverage and regular schedule with increasing revisit frequency, while maintaining high spatial resolution and millimeter precision of measurement. The high resolutions of the new-generation satellite sensors imply now the possibility to derive very detailed information that fits the requirements of engineers and is relevant to many engineering geology investigations, both in research and practice. For example, remotely sensed data can assist in:

– Terrain mapping (e.g., for lifeline routing)
– Site selection and characterization
– Natural resource mapping and characterization
– Natural hazard (geologic and hydrologic) assessment and monitoring (e.g., subsidence, landslides, ground deformations in general, floods)
– Monitoring human-induced hazards (e.g., landfill deformations, subsidence due to groundwater withdrawal)
– Monitoring engineering structures (e.g., stability of transportation infrastructure, dams)

R

– Monitoring mining operations (e.g., slope instability issues in opencast mines)
– Monitoring and management of oil/gas field operations (e.g., addressing ground instability issues)
– Engineering structure damage assessment (e.g., building structural damage after an earthquake)

Remote sensing technologies are only starting to gain significant visibility within the engineering geology community. Therefore, a greater opening of the profession to closer multidisciplinary collaborations is needed to fully benefit from the enormous quantities of information the innovative remote sensing can now produce. New collaborations have to be established, particularly with physicists and electronic engineers specializing in advanced image/signal processing and big data management, and geologists with expertise in interpretation of digital remotely sensed data.

Cross-References

► Aerial Photography
► InSAR
► LiDAR
► Photogrammetry

References

Bally P (ed) (2013) Satellite earth observation for geohazard risk management – the Santorini Conference – Santorini, Greece, 21–23 May 2012. ESA Publication STM-282. doi:10.5270/esa-geo-hzrd-2012
Barnhart RK, Hottman SB, Marshall DM, Shappee E (2012) Introduction to unmanned aircraft systems. CRC Press, Boca Raton, FL, USA, 234 p
Barr (1984) Applied geology. In: Finkl CW (ed) Encyclopedia of earth sciences series, vol 3. Springer, ISSN: 1388–4360.
Caduff R, Schlunegger F, Kos A, Wiesmann A (2015) A review of terrestrial radar interferometry for measuring surface change in the geosciences. Earth Surf Process Landf 40:208–228
DeLong SB, Prentice CS, Hilley GE, Ebert Y (2012) Multitemporal ALSM change detection, sediment delivery, and process mapping at an active earthflow. Earth Surf Process Landf 37:262–272
Drury SA (2001) Image interpretation in geology, 3rd edn. Nelson Thornes, Cheltenham
Ferretti A (2014) Satellite InSAR data: reservoir monitoring from space. EAGE Publications bv, Houten, 160 p
Giordan D, Manconi A, Facello A, Baldo M, Dell'Anese F, Allasia P, Dutto F (2015) Brief communication: the use of an unmanned aerial vehicle in a rockfall emergency scenario. Nat Hazards Earth Syst Sci 15:163–169
Juang CH, Carranza-Torres C, Crosta G, Dong JJ, Gokceoglu C, Randall W, Jibson RW, Shakoor A, Tang H, van Asch TWJ, Wasowski J (2016) Engineering geology – a fifty year perspective. Eng Geol 201:67–70
Khorram S, van der Wiele CF, Koch FH, Nelson SAC, Potts MD (2016) Principles of applied remote sensing. Springer International Publishing, Cham/Heidelberg/New York/Dordrecht/London, 307 p
Lillesand TM, Kiefer RW, Chipman JW (2015) Remote sensing and image interpretation, 7th edn. Wiley, Hoboken, 768 p
Monserrat O, Crosetto M, Luzi G (2014) A review of ground-based SAR interferometry for deformation measurement. ISPRS J Photogramm Remote Sens 93:40–48
Nex F, Remondino F (2014) UAV for 3D mapping applications: a review. Appl Geomatics 6:1–15
Njoku EG (ed) (2014) Encyclopedia of remote sensing – encyclopedia of earth sciences series. Springer International Publishing, Cham/Heidelberg/New York/Dordrecht/London, 939 p
Singhroy V, Li J, Charbonneau F (2015) High resolution rapid revisit InSAR monitoring of surface deformation. Can J Remote Sens 41:458–472
Tratt DM (2014) Emerging technologies, LiDAR. In: Njoku EG (ed) Encyclopedia of remote sensing. Springer International Publishing, Cham/Heidelberg/New York/Dordrecht/London, pp 177–185
Wasowski J, Bovenga F (2014a) Investigating landslides and unstable slopes with satellite multi temporal interferometry: current issues and future perspectives. Eng Geol 174:103–138
Wasowski J, Bovenga F (2014b) Remote sensing of landslide motion with emphasis on satellite multitemporal interferometry applications: an overview. In: Davies T (ed) Landslide hazards, risks and disasters. Elsevier, pp 345–403. doi:10.1016/B978-0-12-396452-6.00011-2

Reservoirs

Saeid Eslamian[1], Ali Reza Gohari[1], Kaveh Ostad-Ali-Askari[2] and Negin Sadeghi[3]
[1]Department of Water Engineering, Isfahan University of Technology, Isfahan, Iran
[2]Department of Civil Engineering, Isfahan (Khorasgan) Branch, Islamic Azad University, Isfahan, Iran
[3]Urban Engineering Department, Isfahan (Khorasgan) Branch, Islamic Azad University, Isfahan, Iran

Definition

Reservoirs are typically artificial water bodies that are constructed behind a dam or they are natural water storage entities such as lakes and rivers that are used for different purposes including drinking, irrigation, and industry.

Introduction

Water is recognized as the most important factor for economic and social development in developed and less developed countries around the world. Given that there is an inconsistency between the rainfall seasons and high water demand in arid and semi-arid regions, groundwater resources are the primary water source to satisfy various water demands. Surface water reservoirs are constructed to collect and store water during seasons of high rainfall and river flow when there is relatively lower water uses.

Due to water-related problems around the world and the potential for severe drought conditions in the future, proper design of new water reservoirs as well as the utilization and conservation of current reservoirs are crucial. A dam is defined as an engineered structure constructed across a valley or natural depression to create a water storage reservoir. Such reservoirs are required for three main purposes: (1) provision of a dependable water supply for domestic and/or irrigation use, (2) flood mitigation, and (3) generation of electric power (Best 1998). In addition, a reservoir is also a place where many aquatic and nonaquatic animals exist and thrive (Thornton et al. 1996).

Reservoirs are mainly used to hold a water resource for domestic, industrial, and agricultural use but also to control unexpected floods, so they can be found in those areas that have problems caused either by an excess of water or water scarcity. In arid areas where water resources are limited, reservoirs are used to collect and protect available water for applications such as drinking and agriculture during periods with high water demand. On the other hand, during periods of flooding, reservoirs can play an important role in the control of floodwater and reduction or even prevention of damage in downstream regions (Thornton et al. 1996).

Note that a reservoir system is fed by annual precipitation including rain and snow melt, runoff, and river flow. In contrast, water loss may be caused through evaporation of water, which is a common problem especially in arid areas, and also by percolation through the reservoir bed (Dettinger and Anderson 2015; Takemon 2006).

In providing a water supply, the reservoir is filled during periods of above-average stream flow, thus ensuring a steady supply of water during periods of little or no stream flow. For flood mitigation, the storage reservoir is kept nearly empty during drought and periods of low rainfall, so that, when the flood-generating rainstorms occur, the storage volume available in the reservoir provides a buffer against severe flooding in the river valley downstream of the dam (Best 1998).

The earliest known reservoir was constructed in about 3000 BC for the purposes of irrigation and watering of crops (UNEP 1991; Smith et al. 2006).

Location

Reservoirs can be classified into two types, based on situation. Reservoirs can be located either below the ground surface (like aquifers) or at the surface (such as impounded water behind a dam, natural lakes, wetlands, etc.) according to the regional climatic and geological conditions. Each of these reservoirs has advantages and disadvantages. Most drinking water reservoirs are designed above the ground and may be vulnerable to contamination from chemicals, harmful sediments, human activities, and so on. Also, water loss (evaporation) from open-air reservoirs is considered an important challenge especially in arid and semi-arid areas when they need to be covered to prevent and reduce evaporation.

Nevertheless, open air reservoirs have some benefits, including beautifying the environment, contributing to the growth of plants and animals, boosting the ecosystem, adjusting local temperature, etc.

Underground water reservoirs like aquifers are important water resources for the collection and storage of rainwater for different purposes such as irrigation. Given that they are not directly in contact with atmospheric air, their water losses (evaporation) are much lower than in surface reservoirs. Other positive points of these reservoirs include less water pollution, higher temperature stability, etc. But, difficulty of access is the most important problem of these reservoirs.

Construction

Reservoirs can also be classified according to their method of construction into two categories: natural reservoirs and artificial (man-made) reservoirs. The most important natural reservoirs are seas and lakes, wetlands, and aquifers. Artificial water reservoirs include lakes created behind dams, artificial wetlands, and flood-spreading sites.

Natural reservoirs were more important in the past, but today artificial water reservoirs are more useful for humans in order to store and use water. Some reservoirs are used to supply electricity, but, such reservoirs must also be of a sufficiently high quality for use in agriculture, industry, and even drinking (the need for a treatment plant to operate such reservoirs is a prerequisite). The most important problems of artificial reservoirs are their gradual salinization, as well as sediment buildup, and the need for dredging.

Geological Issues

The most important factors are foundation conditions and the porosity of construction materials. Therefore, selecting the best method for reservoir design as well as estimating construction costs should be based on a holistic view of the geological knowledge of the prospective dam site and its environs, including the nature and distribution of the various rock types in the area, the weathering profile, and details of the structural geology. The required information can be obtained through the site investigation programs by using various data-gathering techniques, including outcrop mapping, bulldozed trenching to expose bedrock below overburden, diamond core drilling, water pressure testing, geophysical surveys, joint surveys, and laboratory testing of rock samples. By integrating this geological and physical information, a geo-mechanical site model is then formed, which provides the engineers with a realistic and quantitative knowledge on which the reservoir and its associated structures will be designed. Collecting the relevant geological information and presenting them in an applicable and useful form for the engineers are the main functions of the engineering geologist (Rezaei et al. 2017).

Two criteria must be satisfied during the design of large dams: (1) they should be reasonably watertight, and (2) they should be stable. Such dams are constructed of impermeable materials (e.g., concrete) or impermeable membranes (e.g., an Earth core) are incorporated in their structures to achieve the first criteria. Moreover, the dams' foundations must be made watertight by using grouting or other means. To achieve the second criteria, the movement and deformation of the dams and their foundations cannot be ignored and must be considered through the design procedure.

Types of Dams

There are several basic types of dams that can be selected by engineers during the designing phase for a particular location. Figs. 1 and 2 show the summary of the layout and characteristics of these basic types of dams. At some dam sites, the most economical design has been a composite of two or more basic dam types. One particular type of composite concrete dam is the multiple arch design, which consists of several cylindrical arches supported by buttresses. This type is well suited to sites with geologically variable foundations. The buttresses are located on strong zones of the foundations, whereas the arches are located to bridge weak parts in the foundations.

Reservoir Foundations

According to the dam types shown in Figs. 1 and 2, there is a progressive decline in the foundation area for a given dam height between the Earth dam (largest area) to the double curvature arch dam (smallest area). This also means that the bearing pressure which must be supported by the foundations progressively increases from a minimum for the Earth dam to a maximum for the arch dam (Best 1998). Thus, the sequence of dam types from (1) to (6) in Figs. 1 and 2 requires progressively stronger foundations. It follows that foundation geology at a proposed dam site is an important factor in deciding the most economic type of dam for the site.

<table>
<tr><th>Type</th><th>Cross section</th><th>Plan</th><th>Main characteristics</th></tr>
<tr><td>Earth Dam</td><td>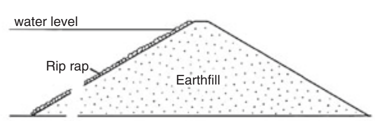
</td><td>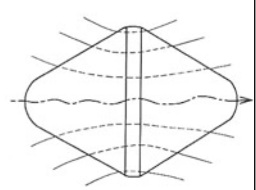</td><td>Has gentle slopes, and hence a large volume and foundation area.

Made of compacted earth.</td></tr>
<tr><td>Earth Cored Rock fill Dam</td><td>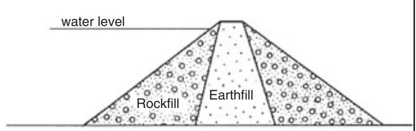
</td><td>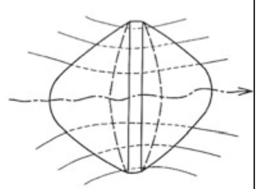</td><td>Impermeable earth core, supported by outer zones of compacted broken rock. Steeper slopes than an earth dam. Similar effect may be achieved by an impermeable membrane of concrete, bitumen, steel, or other materials at or near the upstream face.</td></tr>
<tr><td>Concrete Gravity Dam</td><td>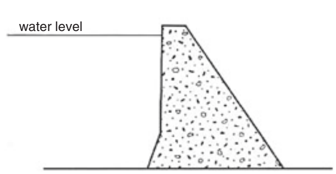
</td><td>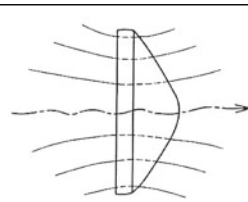</td><td>Water held back by the weight of the structure (hence the name) Construction material (concrete) easier for engineers to control than earth and rock</td></tr>
</table>

Reservoirs, Fig. 1 Basic type of dam designs (Modified after Best 1981)

Construction Materials

Reservoirs are constructed from large volumes of naturally occurring Earth materials – broken rock for rockfill and concrete aggregate, sand, gravel, and slopewash or highly weathered regolith for the earth core. Such construction materials must be available near the dam site in order to reduce construction costs (Best 1981). Therefore, the location and cost of construction materials and their extraction are other important factors in determining the type of dam. For instance, a site with highly weathered bedrock is likely to be only suitable for the foundations of an Earth dam. If the overburden close to the site is thin and suitable bedrock occurs at depth, it may well be more economical to excavate the foundations to a depth suitable for a concrete dam than to transport earth material over a long distance to the site.

Choice of Dam Type

During the design stage, several types of dam are considered and quantities of materials, cost of materials, amount of foundation excavation, type and amount of foundation treatment, and so on are estimated for each type. The final decision for dam type is based on a cost-benefit analysis to design the lowest estimated construction cost and the safest standards. In general, there are three factors which control this final decision: (1) topography of the dam site and reservoir area; (2) strength and variability of the foundations; and (3) availability and suitability of construction materials. These factors are largely controlled by the geological structure and history of the site. The final decision needs considerable geological data analysis and interpretation, particularly for factors (2) and (3), presented in a manner which the engineer can use in design calculations (Rezaei et al. 2017).

Water Quality

The climate characteristics, the quantity and quality of water inflow to the reservoirs, as well as the evaporation rate in the reservoir surface are the most important parameters affecting water quality, including physical, chemical, and biological issues in reservoirs.

Because, lakes and water reservoir dams are considered as important sources of drinking water supply, agriculture, and industry for human societies, the optimal use of these resources requires proper water quality according to factors

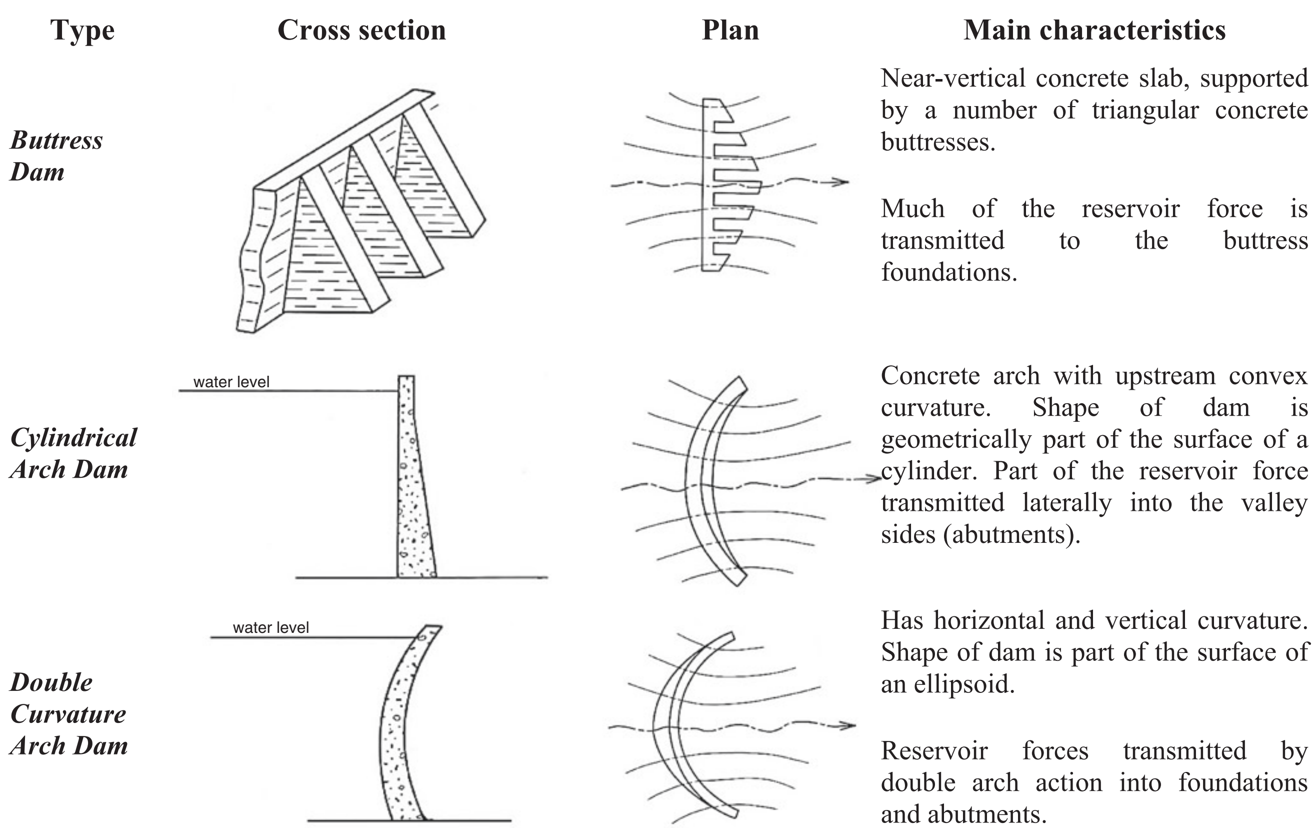

Reservoirs, Fig. 2 Basic type of dam designs (Modified after Best 1981) such as nitrate, nitrite, dissolved oxygen, electrical conductivity, and pH. Salinity and concentration of inlet sediment are also important aspects to evaluate water quality in the reservoirs, especially for drinking and irrigation uses. Thus, it is important to know the details of water quality changes in the dam which must be achieved before any corrective action and operation.

Reservoir Management

As a result of population growth, socioeconomic development, coupled with occurrence of severe drought, there are widespread serious problems facing water security especially in reservoirs.

One of the main problems, especially in arid areas, is high values of evaporation from water bodies, increasing the concentration of salt and decreasing the quality of water. In many cases, the reduction of evaporation is much cheaper than collecting and storing the same amount of water from other sources.

Sedimentation is always one of the main challenges for dam operation. Various methods are proposed to predict the sedimentation and reduction of sediment deposited in dams (Piri et al. 2011). It reduces the effective storage volume of the reservoir, adds to a decline in dam stability, as well as disruptions in functioning of the lower valves.

Important parameters of reservoir water quality are salinity, the amount of sediment entering the reservoir (turbidity), and chemical contamination that confronts the use and exploitation of the reservoir with many difficulties and limitations.

Summary

Reservoirs are typically artificial water bodies that are constructed behind a dam or they are natural water storage entities such as lakes and rivers that are used for different purposes including drinking, water irrigation, and industry. It is necessary to manage extraction of water (from lakes and rivers) and apply effective strategies to optimal operation of artificial reservoirs. Notably, salinity and concentration of inlet sediment are important factors to evaluate in relation to water quality in reservoirs, so, the parameters relating to salinity of the reservoir and the increase of sediment inputs to these resources should be constantly addressed. Dam site selection is an extremely important issue in terms of dam safety and environmental impact. A detailed knowledge of the geology of the dam site and the future reservoir, as well as its catchment area, is necessary before the dam site is selected; acquiring such knowledge is vital in the siting, design, and construction (Best 1981).

Cross-References

▶ Catchment
▶ Climate Change
▶ Dams
▶ Desert Environments
▶ Desiccation
▶ Erosion
▶ Fluid Withdrawal
▶ Groundwater
▶ Hydraulic Action
▶ Hydrogeology
▶ Hydrology
▶ Infiltration
▶ Instrumentation
▶ Lacustrine Deposits
▶ Land Use
▶ Levees
▶ Pollution
▶ Pressure
▶ Risk Assessment
▶ Sabkha
▶ Saline Soils
▶ Saturation
▶ Sequence Stratigraphy
▶ Site Investigation
▶ Soil Field Tests
▶ Soil Mechanics
▶ Strain
▶ Strength
▶ Stress
▶ Tailings
▶ Water
▶ Water Testing

References

Best EJ (1981) The influence of geology on the location, design and construction of water supply dams in the Canberra area. BMR J Aust Geol Geophys 6:161–179

Best E (1998) Dams. In: Encyclopedia of hydrology and lakes. Springer, pp 149–153

Dettinger MD, Anderson ML (2015) Storage in California's reservoirs and snowpack in this time of drought: San Franc Estuary Watershed Sci 13(2)

Piri M, Hesam M, Dehghani AA, Meftah HM (2011) Experimental study on the effect of physical and chemical approach in reducing the evaporation from water surface. J Water Soil Conserv 17(4):141–154

Rezaei A, Karimi H, Zhan H (2017) The importance of understanding the hydrogeology and geochemistry of karst terrains for safely siting dams. J Cave Karst Stud 79(1):48–58

Takemon Y (2006) Ecological impacts of reservoir dams on river ecosystems in tail waters. Asia Oceania Geosciences Society (AOGS), Singapore

Thornton J, Steel A, Rast W (1996) Reservoirs. In: Chapman D (ed) Water quality assessment, World Health Organization. E & FN Spon, London, pp 369–412
UNEP (1991) Freshwater pollution, UNEP/GEMS environment library, no 6. United Nations Environment Programme, Nairobi, 36 pp

Residual Soils

Isabel M. R. Duarte[1] and Carlos M. G. Rodrigues[2]
[1]GeoBioTec Research Centre (UID/GEO/04035/2013), Department of Geosciences, School of Sciences and Technology, University of Évora, Évora, Portugal
[2]CONSTRUCT Institute of R&D in Structures and Construction (UP), School of Technology and Management, Polytechnic Institute of Guarda (IPG), Guarda, Portugal

Synonyms

Alteration products; Lateritic soils; Saprolites; Weathering products

Definition

Residual soil is the material resulting from the *in situ* weathering of the parent rock.

Residual soils are distributed throughout many regions of the world, such as Africa, South Asia, Australia, Southeastern North America, Central and South America, and considerable regions of Europe. The largest areas and thickness of these soils occur normally in humid tropical regions, such as Brazil, Nigeria, South India, Singapore, and the Philippines.

Characteristics

According to Duarte (2002), the diversity exhibited by residual soils is due, not so much to the lithology of the original rock, but mainly to external factors such as climate, topography, and vegetation cover; factors that provide distinctive weathering processes and, consequently, distinctive weathering products – the residual soils. At the first International Conference on Tropical Residual Soils, it was proposed to divide such soils into two classes (Brand and Phillipson 1985): (i) Lateritic soils are those that belong to a higher level, well drained and leached, in which the predominant clay belongs to the kaolinite group and contain hydrated iron oxides that give them a reddish color. Generally these do not include primary minerals, and the structure of the parent rock has been totally destroyed. (ii) Saprolite or saprolitic soils, sometimes referred to as young soil, are the residual soils that maintain relic structures from the parent rock, which generally are situated in the levels directly above the original rock, usually contain small amounts of clay minerals, and include primary minerals.

Lateritic residual soils predominate in tropical regions, within latitudes 30° N and 30° S, whereas saprolitic soils are common in temperate regions, for instance, in Portugal, France, Turkey, Piedmont (eastern USA), or in subtropical regions (e.g., Hong Kong and South Africa). The formation of saprolites, which is essentially related to granular rocks, includes primary and secondary minerals in its silt-clay fraction, the nature and quantity of which depends upon parent rock characteristics and on degree of weathering achieved.

The specific characteristics of residual soils in contrast to those of transported soils, are generally attributed either to the presence of clay minerals specific to residual soils (physical composition and mineralogical composition), or to particular structural characteristics of soil in its undisturbed *in situ* state, such as: (i) Macrostructure: includes the presence of unweathered or partially weathered rock, and relic discontinuities or other weakness planes and structures inherited from the original rock mass; Microstructure – includes rock fabric, interparticle bonds or cementation, particle aggregates, dimension and shape of micropores (Vaughan 1988; Duarte 2002; Wesley 2010). These specific characteristics influence the geotechnical behavior *in situ*, thus permeability is governed by the micro and macro-structure, as well as the strength and deformability of the residual soil masses (Townsend 1985; Blight 1997).

According to Gomes (1988), the clay of residual soils formed in temperate climates are intermediate, sharing characteristics both of soils from cold or desert climates, where physical weathering prevails, through the disintegration (mechanical breakdown) of phyllosilicates (mica and chlorite) from the parent rock, and those of tropical climates, where chemical weathering prevails, producing kaolinite, gibbsite or smectite, depending upon local conditions. In regions of temperate climate, soils can be derived from either mechanical weathering or chemical weathering. These soils show little evolution, since precipitation and temperature facilitate the moderate hydrolysis of silicates. In the weathering profiles, both neoformed and transformed clay minerals may be present (Fig. 1).

Cross-References

▶ Alteration
▶ Biological Weathering
▶ Chemical Weathering
▶ Classification of Rocks
▶ Classification of Soils
▶ Collapsible Soils

Residual Soils, Fig. 1 Weathering profile of a granitic massif in southern Portugal, under temperate climate, with a saprolitic residual soil cover of about 10 m thick (Photo by I. Duarte)

▶ Landslide
▶ Physical Weathering
▶ Sediments
▶ Soil Mechanics
▶ Soil Properties

References

Blight GE (1997) In: Blight GE, Technical committee 25 on the properties of Tropical and Residual Soils of the International Society for Soil Mechanics and Foundation Engineering (eds) Mechanics of residual soils. Balkema, Rotterdam

Brand EW, Phillipson HB (1985) In: Technical committee 25 on the properties of Tropical and Residual Soils of the International Society for Soil Mechanics and Foundation Engineering (ed) Sampling and testing of residual soils. A review of international practice. Scorpion Press, Hong Kong

Duarte IMR (2002) Solos residuais de rochas granitóides a Sul do Tejo. Características geológicas e geotécnicas [Residual soils of granitoid rocks to south of the Tagus River. Geological and geotechnical characteristics]. (Unpublished Doctoral Dissertation, in Portuguese). University of Évora, Évora, Portugal

Gomes CF (1988) Argilas. O que são e para que servem. [Clays. What they are and what they are for]. Gulbenkian Foundation, Lisboa

Townsend FC (1985) Geotechnical characteristics of residual soils. J Geotech Eng 111(1):77–94

Vaughan PR (1988) Characterising the mechanical properties of in-situ residual soil. In: Proceedings of the II international conference on geomechanics in tropical soils, Singapore, vol 2, pp 469–487

Wesley LD (2010) Fundamentals of soil mechanics for sedimentary and residual soils. Wiley, New Jersey

Restoration

Jerome V. De Graff
College of Science and Mathematics, Department of Earth and Environmental Sciences, California State University, Fresno, CA, USA

Synonyms

Rehabilitation; Restoration

Definitions

1. "...the combined process of land treatment that minimizes water degradation, air pollution, damage to aquatic or wildlife habitat, flooding, erosion, and other adverse effects from surface mining operations...so that mined lands are reclaimed to a useable condition which is readily adaptable for alternative land uses and create no danger to public health or safety" (OMR 2015).
2. To make "........land capable of more intensive use by changing its general character, as by drainage of excessively wet land; irrigation of arid or semiarid land; or recovery of submerged land from seas, lakes and rivers" (EEA 2015).

Restoration, Fig. 1 Reclamation at Wishon Quarry in the foothills of the central Sierra Nevada, California (USA) involved filling excavated shallow pit following removal of rock for facing an earthen dam. Stockpiled soil is being applied to a refilled section of the pit. (Photo by J. De Graff)

Restoration, Fig. 2 Kinderdijk, a UNESCO World Heritage site between Rotterdam and Dordrecht, Netherlands, preserves windmills, pumping stations, low and high storage basins ("boezems"), dikes, ditches, and sluices which have kept the low-lying peat land of the Alblasserwaard dry since 1758. This polder landscape illustrates land reclamation through water management over a nearly 1000-year period (Photo by J. De Graff)

R

Characteristics

Mining is one of the primary human activities responsible for disturbing land to an extent that reclamation is necessary. Disturbance is due to the extraction of near-surface deposits of metallic and nonmetallic mineral resources or from activities incidental to underground mining such as ore storage, ore processing, and stockpiling of tailings and waste rock (Fig. 1).

Reclamation is needed for abandoned or inactive mined areas and for those areas where mining is actively being undertaken. Re-establishing natural drainage patterns, preventing accelerated erosion, especially slope instability, and promoting desirable vegetation growth are all important aspects in reclaiming abandoned and inactive mined area (Newton and Claassen 2003). An especially important component of reclamation for surface disturbance at underground mines is ensuring effective closure of hazardous mine openings. The need for building materials including sand, gravel, and crushed rock near expanding urban areas is typically satisfied by nearby active surface mining operations. Whereas reclamation of rock quarries can be difficult, sand and gravel can be infilled with soil generated from pit development or restored as wetland areas. This is an important aspect of local land use planning to ensure access to needed aggregate resources and subsequent utilization of the mined areas (Arbogast et al. 2000).

Altering the natural landscape to increase its suitability for human activities is a form of reclamation with a long history. Arguably, one of the most extensive reclamation efforts is the dike and polder system in The Netherlands (Fig. 2). From the twelfth century to present, the Dutch have created extensive areas of arable land while providing flood control along rivers and the shoreline of the North Sea. Urban locations along coast such as Rio de Janeiro and Cape Town and islands like Singapore and Hong Kong have commonly modified their nearshore environments to accommodate additional buildings, port facilities, airport runways, or other amenities. Boston provides a good example of how coastal artificial fills placed without regard to material properties and subsurface conditions can even create unintended hazards, for example, liquefaction potential (Brankman and Baise 2008). Natural landscape reclamation can require engineering geologic information ranging from general aspects such as site subsurface conditions or characteristics of geologic materials present or being used in construction work to more specific ones such as the stability of an engineered slopes or seepage conditions within an embankment.

Cross-References

- ► Land Use
- ► Liquefaction
- ► Mining
- ► Tailings

References

Arbogast BF, Knepper DH Jr, Langer WH (2000) The human factor in mining reclamation. US Geol Surv Circ 1191:28

Brankman CM, Baise LG (2008) Liquefaction susceptibility mapping in Boston, Massachusetts. Environ Eng Geosci 14:1–16

EEA (2015) Land reclamation. In: Environmental Terminology and Discovery Service (ETDS). European Environment Agency. http://glossary.eea.europa.eu/terminology/concept_html?term=land%20reclamation. Accessed 28 Dec 2015

Newton GA, Claassen VP (2003) Rehabilitation of disturbed lands in California: a manual for decision making. California Department of Conservation, California Geological Survey Special Publication 123

OMR (2015) Reclamation. In: Definitions, California Statutes and Regulations for the Office Mine Reclamation, Sacramento. http://www.conservation.ca.gov/index/Documents/omr-regs2015.pdf. Accessed 28 Dec 2015

Retaining Structures

Rosalind Munro
Amec Foster Wheeler, Los Angeles, CA, USA

Synonyms

Retaining walls

Definition

Retaining structures are walls, dams, barriers, or bins that hold Earth materials or water in place or keep Earth materials or water from encroaching into an area. Retaining structures also are used to create stable surfaces for building pads, roads, bridge abutments, or wharves. Retaining structures can be used to limit the volume of excavations or to allow utilization of space near the boundary of a particular piece of land. Other structures that appear to be earth-retaining structures may have erosion protection as their primary purpose.

Introduction

Retaining structures commonly are engineered features that are designed and constructed to hold soil or water in place. Structures that retain water are called dams, levees, or flood walls; structures that retain Earth are called earth-retaining structures or retaining walls, which are described here. Retaining structures can be installed at a site prior to excavation as structures that become retaining walls as excavation progresses (Fig. 1) or they can be constructed on sloping ground or to provide a terraced configuration with soil backfill placed behind the walls (Fig. 2). Descriptions and design guidance is provided by NAVFAC (1986), USACE (1989), and USACE (1994).

Stability of retaining walls is provided by simple mass, mass created by mechanically stabilized Earth systems, cantilevered overturning resistance, anchored lateral

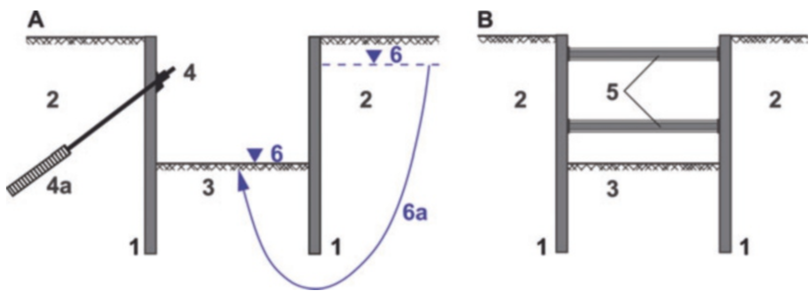

Retaining Structures, Fig. 1 Schematic diagram showing elements of retaining structures for stabilizing excavations. (**a**) Sheet pile or soldier pile retaining structure; (**b**) Braced retaining structure. Notations: *1* Retaining element (sheet pile for soft ground, driven or drilled H-pile with lagging placed as excavation progresses); *2* Retained soil. *3* Soil below excavated bottom. *4* Tieback element. *4a* Anchor on tieback. *5* Bracing struts or elements. *6* Groundwater level in retained soil and at bottom of excavation (sump pump would be required to remove water from excavation). *6a* Hypothetical groundwater flow line

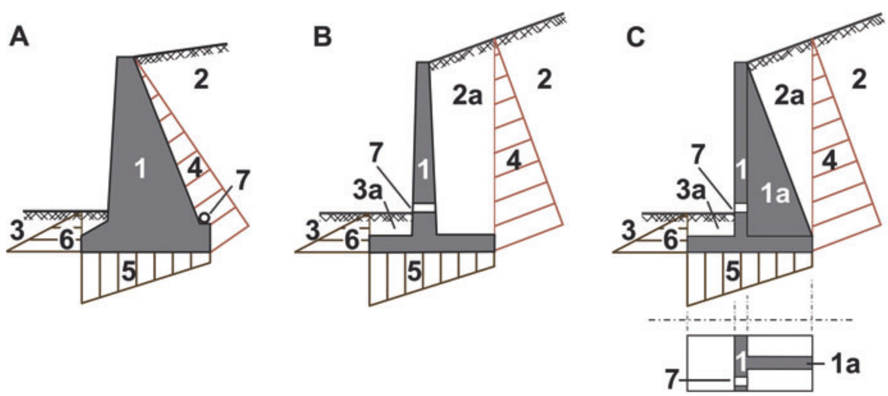

Retaining Structures, Fig. 2 Schematic diagram showing elements of earth-retaining walls. (**a**) Concrete gravity retaining wall; (**b**) Concrete cantilevered retaining wall; (**c**) Concrete counterfort retaining wall. Notations: *1* Primary concrete element of wall. *1a* Counterfort element. *2* Retained soil backfill. *2a* Part of retained soil backfill directly over wall foundation element that contributes to the mass of the wall system. *3* Soil backfill or native soil that contributes to sliding resistance of the wall system. *3a* Part of the soil backfill directly over the wall foundation element that contributes to the mass of the wall system. *4* Representation of geostatic stress that contributes to "active" Earth pressure on the wall system. *5* Representation of bearing capacity that resists overturning tendency of retained earth. *6* Representation of "passive" earth pressure that resists sliding tendency of retained Earth. *7* Drainage pipe or conduit to limit the hydrostatic stress that can occur behind the retaining wall

resistance, and braced lateral resistance. Examples of a variety of earth retaining systems are illustrated in Fig. 3. Gravity walls (Fig. 2a) rely on the mass of stable material to resist sliding and overturning. The mass of material can be stacked stones (Fig. 3a), mortared stones (Fig. 3b), stacked sacks of soil-cement mixtures (Fig. 3c) or sacks of pre-mixed concrete (Fig. 3d); interlocking concrete elements filled with soil (crib wall; Fig. 3e); or steel, concrete, or synthetic material cells filled with soil (bin wall; Fig. 3f); gabion baskets filled with durable rock fragments (Fig. 3g, h, i, and j); and stabilizing layers of welded wire or high-density polyethylene (HDPE) that creates mechanically stabilized Earth systems (Fig. 3g, h, and i). Retaining walls also can be cast-in-place reinforced concrete with decorative rock finishing (Fig. 3k) or soldier-pile and lagging systems with tiebacks and bracing elements (Fig. 3l). The stabilizing mass in a gravity retaining wall is designed to resist lateral Earth pressures, including the hydrostatic effects of groundwater and transient impulse effects of earthquake shaking. Geosynthetic filter fabric commonly is used to prevent migration of soil particles from the subgrade into pore space in gabion baskets or to prevent migration of soil particles from crib walls or bin walls into the subgrade, depending upon the grain size distributions. The examples of welded-wire walls, welded-wire steepened slope, and gabion baskets (Fig. 3g, h, i, and l) are discussed in Keaton et al. (2011).

Sheet pile and soldier pile walls (Fig. 1a) rely on the stiffness of the structural wall element to resist lateral Earth pressures and hydrostatic pressures, as well as effects of earthquake shaking. Soldier pile walls typically are constructed with steel H-beams spaced 1–3 m apart that are driven into the ground vertically, or placed into drilled holes that are then backfilled with concrete. The H-configuration is controlled so that the open ends are aligned to permit placement of timber elements, called lagging, into the slot created by the aligned H-piles that retains the soil. After the H-piles

R

are in place, an excavation is advanced incrementally and lagging timbers placed to retain the soil. For shallow excavations in soft soils, relatively short-cantilevered retaining walls may be made of steel sheet piles. Anchored retaining walls are similar to cantilevered walls with anchor elements supplementing the stiffness of the structural wall elements. Some retaining systems can use soil nails that stabilize the soil mass with increased shear resistance rather than lateral resistance provided by anchors for structural wall elements. Soil nail systems may have surface elements or coatings, such as shotcrete, for erosion control.

Mechanically stabilized Earth (MSE) retaining walls use reinforcing elements in soil backfill to create a mass of stable soil that acts partly as a gravity wall and partly like a soil nail wall. Reinforcing elements can be strips or grids of galvanized or coated steel, or high-density polyethylene (HDPE)

Retaining Structures, Fig. 3 (continued)

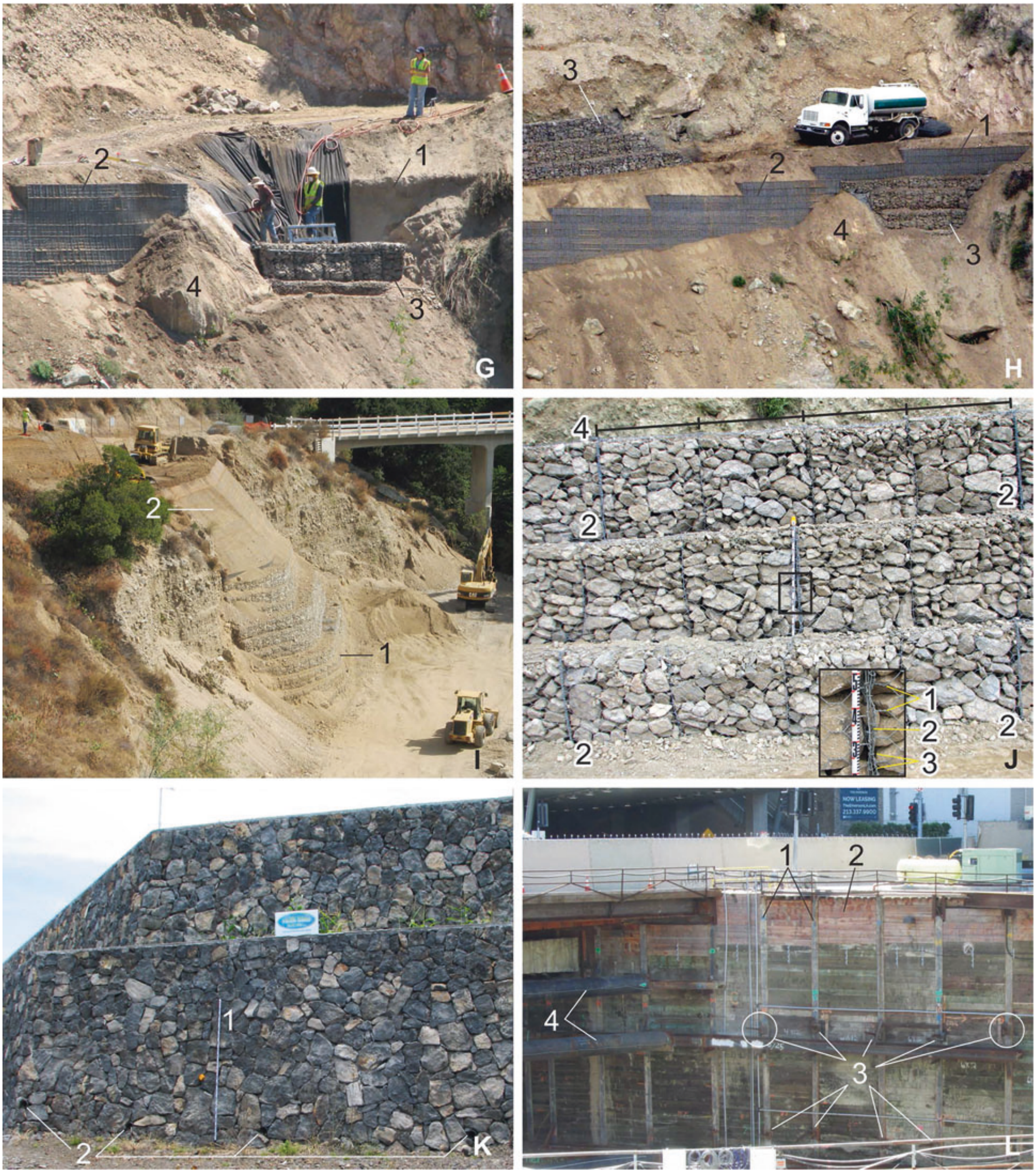

Retaining Structures, Fig. 3 Photographs of a variety of earth-retaining walls. (**a**) Hand-placed dry-stacked stone wall with two rows of fired bricks at the top. (**b**) Hand-placed stone-and-mortar wall. (**c**) Hand-placed sacks of soil-cement mixtures; original sacks probably were burlap fabric that has rotted away over several decades of exposure (concrete feature is bridge abutment placed in 1945). (**d**) Hand-placed paper sacks of commercially available dry pre-mixed concrete. (**e**) Concrete crib walls forming an inside corner adjacent to an unsurfaced road. (**f**) Galvanized steel bin wall. (**g**) and (**h**) Retaining systems composed of an old cast-in-place concrete (*1*), new welded-wire wall elements (*2*), and new gabion baskets (*3*), to enable restoration of vehicle access on an unsurfaced road across a landslide; complications were caused by the presence of a large block of rock (*4*) which was left in place. (**i**) Gabion-basket wall (*1*) topped by welded-wire steepened-slope elements (*2*). (**j**) Detail of gabion basket wall visible in panel **h**; notations: (*1*) hexagonal double-twist galvanized wire basket; (*2*) separation between gabion baskets; (*3*) pneumatically secured wire fasteners that hold baskets together into an integrated wall; (*4*) line defining a single, four-compartment gabion basket that is 91 mm high, 91 mm deep, and 4 × 91 mm long (3 ft × 3 ft × 12 ft in U.S customary units). (**k**) Cast-in-place concrete wall with hand-placed decorative stone facing; 2 m long ruler (*1*), drain hole outlets (*2*). (**l**) Soldier-pile and lagging retaining wall; steel H-beam soldier piles (*1*); timber lagging (*2*); tieback elements (*3*), and pipe struts used as corner bracing elements (*4*) (All photographs by Jeffrey Keaton) grid elements. MSE walls require facing elements that can be precast concrete panels, wire mesh, or ultra violet-resistant HDPE grid elements. Geosynthetic filter fabric is needed behind mesh and grid facings to prevent soil particles from moving through the facing.

Cross-References

▶ Bearing Capacity
▶ Cofferdam
▶ Foundations
▶ Gabions
▶ Geostatic Stress
▶ Geotechnical Engineering
▶ Geotextiles
▶ Groundwater
▶ Lateral Pressure
▶ Pore Pressure
▶ Soil Nails

References

Keaton JR, Perry DL, Kim PW (2011) Repair of Storm-damaged slopes, Lower Mount Wilson Road, Los Angeles County, California. Transp Res Rec: J Transp Res Board 2204, Low-volume roads, vol 2: 242–250. https://doi.org/10.3141/2204-30. Accessed 15 Oct 2016

NAVFAC (1986) Foundations and earth structures. Naval Facilities Engineering Command, U.S. Department of the Navy, Alexandria, Virginia. Design Manual 7.02. http://www.geotechnicaldirectory.com/publications/Dm702.pdf. Accessed 15 Oct 2016

USACE (1989) Retaining and flood walls. U.S. Army Corps of Engineers, Washington, DC. Engineer Manual EM 1110-2-2502. http://www.publications.usace.army.mil/Portals/76/Publications/EngineerManuals/EM_1110-2-2502.pdf. Accessed 15 Oct 2016

USACE (1994) Design of sheet pile walls. U.S. Army Corps of Engineers, Washington, DC. Engineer Manual EM 1110-2-2504. http://www.publications.usace.army.mil/Portals/76/Publications/EngineerManuals/EM_1110-2-2504.pdf. Accessed 15 Oct 2016

Risk Assessment

Rüdiger Escobar-Wolf, El Hachemi Bouali and Thomas Oommen
Department of Geological and Mining Engineering and Sciences, Michigan Technological University, Houghton, MI, USA

Definition

Risk assessment is a fundamental step in the management and reduction of risks. Risk assessments require inputs from experts in different hazard-related fields, and in the case of risks associated to geologic hazards, will involve engineering geologists in this process. Risk assessments also involve assessing vulnerabilities and finally the potential losses that may occur, as well as their associated likelihood. The risk assessment process therefore integrates multidisciplinary efforts, aiming to produce a result that is useful for decision-making on how to manage the risk.

Risk, Hazard, and Vulnerability

Risk can be broadly defined as the possibility of the potential loss of something of value. Assessing the risk involves identifying, describing, and, when possible, measuring the potential for such loss. The loss could be of human lives, public or private property, and other less tangible societal or natural assets. The potential loss is caused by a hazard phenomenon or event. In the context of engineering geology, hazards are related to particular Earth processes, like earthquakes, volcanic activity, landslides, etc. Assessing the potential loss also requires knowledge of the entities (people, communities, etc.) that may suffer the loss, that is, the vulnerable system or elements. The vulnerability encompasses the characteristics and conditions that may contribute to an increased risk and, therefore, potential losses. Many formal definitions and conceptions of risk have been proposed by a variety of authors involving the concepts of hazard and vulnerability and other variables (Wisner et al. 2012). Often the definition of risk is presented in the form of an equation. A general form of the risk equation is:

$$\text{Risk} = f(\text{Hazard}, \text{Vulnerability}, \text{other variables}) \qquad (1)$$

The functional type for Eq. 1 can adopt many forms, but it is often defined as a product, as:

$$\text{Risk} = H \; x \; V \qquad (2)$$

In this definition, the H and V variables are usually assumed to be positive numbers measuring the intensity, probability, severity, or some other aspect of the hazard and vulnerability, respectively. The central idea behind this definition is to show that the risk increases with both hazard and vulnerability, but if one of the variables (H or V) decreases or becomes zero, the risk will also decrease or become zero, even if the other variable does not change. What this shows is that risk can be reduced (or increased) by either reducing (or increasing) the hazard, the vulnerability, or both.

Graphically, the concept of risk can also be illustrated as shown in Fig. 1 (Wood 2011). Risk only exists when vulnerability (or a vulnerable entity) intersects with (i.e., is exposed to) a hazard. The risk will be modulated by the magnitude of the hazard and the vulnerability, but it is also important to

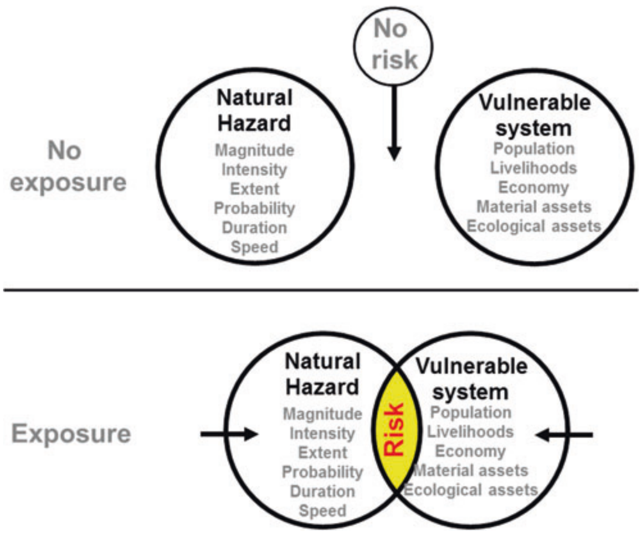

Risk Assessment, Fig. 1 Graphical representation of the relationship between risk, hazard, and vulnerability. Risk arises from the intersection of hazards and vulnerabilities, when vulnerable systems are exposed to natural hazards. Modified from Wood 2011

notice that the extent of the intersection or exposure will also determine the risk, even if the hazard or magnitude does not change individually.

These definitions emphasize the role of vulnerability in contributing to risk generation. Historically, the hazard variable, and natural hazards in particular, has received most of the attention in both theoretical risk work and practical applications of risk assessment and management (White et al. 2001).

The vulnerability analysis usually falls outside the field of engineering geology and is undertaken within other disciplines of engineering, social sciences, economics, etc. For that reason, involvement of engineering geologists is usually limited to the hazard assessment component of risk assessment. It is, however, important for the engineering geologist to be aware of the broader context.

Risk Assessment and the Risk Management Process

Risk assessment has a crucial role in the risk management process, and it is in this broader context that the importance of risk assessment should be understood and appreciated. Risk management is defined by the United Nations Office for Disaster Risk Reduction as "The systematic approach and practice of managing uncertainty to minimize potential harm and loss" (UNISDR 2016); the stated goal in this definition is to minimize harm and loss, but this has to be done in a context of uncertainty. Risk always implies uncertainty (Rougier et al. 2013). The uncertainty factor is unavoidable in risk management; however, a minimum knowledge of the potential causes for loss and their associated likelihoods is necessary to implement any risk management process. The risk assessment provides basic information and knowledge about the problem and sets the stage for potential courses of action (i.e., solutions to the problem) in the management process. The risk management process can be illustrated by the diagram shown in Fig. 2, in which the risk assessment is a fundamental component.

The risk management process involves decision-making on whether to invest or spend resources to reduce a given risk or not. For instance: Is the cost of designing and building more earthquake-resistant structures justified? or Is hardship and potential economic losses from the evacuations of population due to a potential volcanic risk necessary? The risk assessment aims to inform such a decision-making process by providing estimates of the potential losses that would result from different risk scenarios, for example, earthquakes of different magnitudes, occurrence of different volcanic hazards, etc.

The decision-making process does not only depend on the information provided by the risk assessment but also depends on the value judgements that society, or whoever represents its interests in the decision-making process (e.g., the authority), make about the different potential outcomes (Fischhoff and Lichtenstein 1984). This is reflected in the definition of criteria such as acceptable risk levels, the precautionary principle, etc.

Uncertainty in risk assessment is unavoidably transferred to the risk management decision-making process. Reducing uncertainty in risk assessment is therefore highly desirable, but doing so may come at a high cost (e.g., collecting more data, doing more analysis), and will be constrained at some point by practical and even fundamental limits (Rougier et al. 2013). Being unavoidable, uncertainty has to be represented and formalized in an adequate way in the risk assessment. Usually this is done through probabilistic analysis, in which the probabilities of different risk scenarios or outcomes are estimated through some appropriate model. In the decision-making process, the losses for each potential outcome or scenario are weighted by their estimated probability of occurrence to obtain an expected loss. Sometimes an "event" or "probability tree" formalization is used for that effect.

Assessing Hazard and Vulnerability and Integrating Them into a Risk Assessment

In the context of engineering geology, the hazard assessment methodologies depend on the type of geologic processes or phenomena involved, but they often share general characteristics. A source process is usually identified at the beginning of the assessment, be it a seismic source, unstable slope area, volcanic system, etc. A consideration of potential scenarios for the process is then defined, usually considering a range of

R

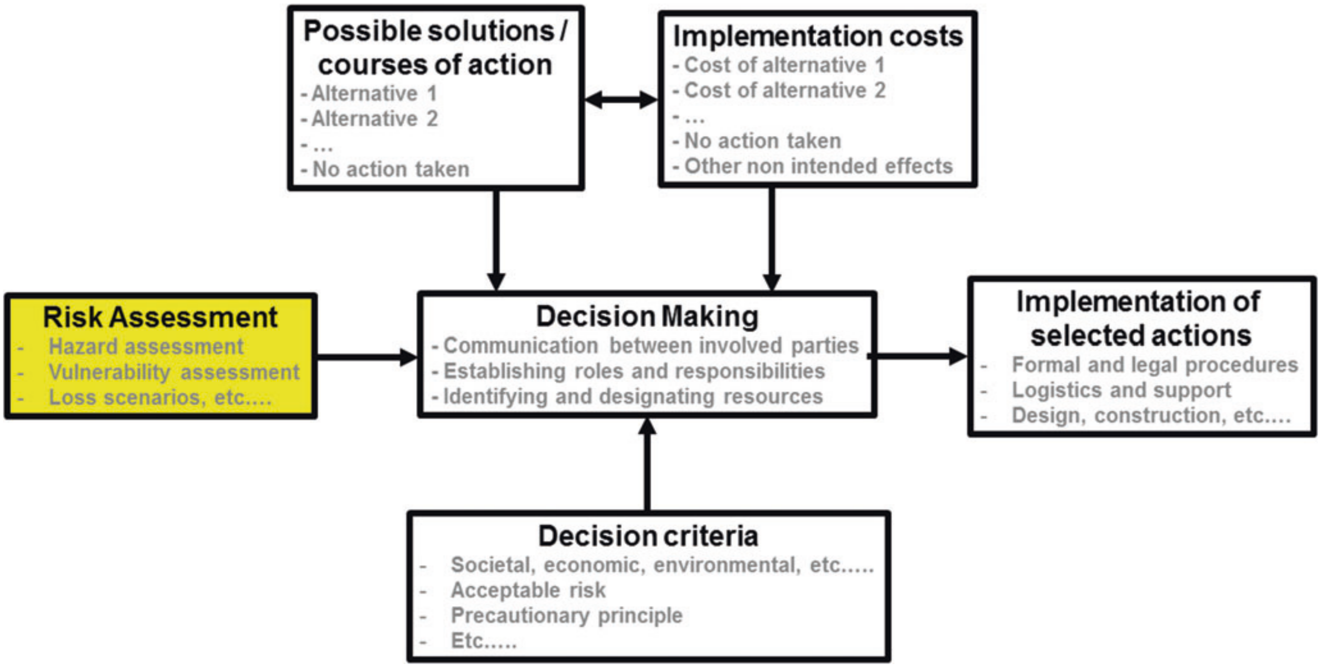

Risk Assessment, Fig. 2 Risk management process

different magnitudes and locations for the phenomena involved. Different types of phenomena and their interactions can also be considered, for instance, landslides triggered by earthquakes. A source process may be of limited areal extent, but its effects could propagate over a much more extensive area; therefore, a model for propagation is usually also involved. Using the source locations and propagation models, it may be possible to map the geographic extent of the area that could potentially be impacted by the hazard. Figure 3 shows a schematic diagram of this process.

Multiple scenarios, assuming different conditions for the source and propagation models, can be defined. If probabilities can be attached to each of them, a full probabilistic analysis may be possible (Rougier et al. 2013). Probabilistic analysis strategies may involve the random sampling of the input variables and parameters for the source and propagation models to produce a Monte Carlo simulation for the output of the models, that is, a probabilistic hazard map. Choosing the right distribution for the input parameters can be difficult and usually requires extensive historical data on previous occurrences of the hazard phenomena.

Vulnerability assessment is usually done by professionals in fields other than engineering geology, depending on the type of vulnerability being assessed. Structural vulnerability can be evaluated by structural and civil engineers, such as in terms of expected damage that a structure may experience under a given seismic ground acceleration or the maximum load of volcanic ash that a roof can withstand. It is important to notice that in these examples the structural vulnerability analysis uses information produced by hazard analyses (e.g. ground acceleration, ash loading) as an input; this is usually the case and illustrates the intimate interaction between hazard and vulnerability assessments. Other types of vulnerability, for example, economic, social, etc., could in principle also be assessed in a similar way but are in practice sometimes more difficult to establish in a quantitative manner. Economic vulnerability could be related to people's livelihood through exposure to the hazard, such as agricultural land exposed to landslide hazard, but is often also heavily dependent on the internal dynamics of the economic system in which people are embedded (Blaikie et al. 2004). This results in a less straightforward relationship to the hazards. The situation can be even more complex for other types of vulnerability, resulting in a less interactive analysis with respect to hazards.

Integrating hazard and vulnerability analyses into the risk assessment will depend on the format and nature of the assessment. In a quantitative, probabilistic risk assessment, both hazard and vulnerability inputs need to provide relevant information in that format. When the aim is to assess the geographic distribution of risk, both hazard and vulnerability inputs have to be in a geographic format, such as GIS layers. In other cases, the hazard and, particularly, the vulnerability inputs cannot be provided in an easily quantifiable format, which will result in a risk assessment that is more qualitative in nature.

Summary and Conclusions

Risk assessment involves estimating risks based on an analysis of the relevant hazards and vulnerabilities. The risk assessment

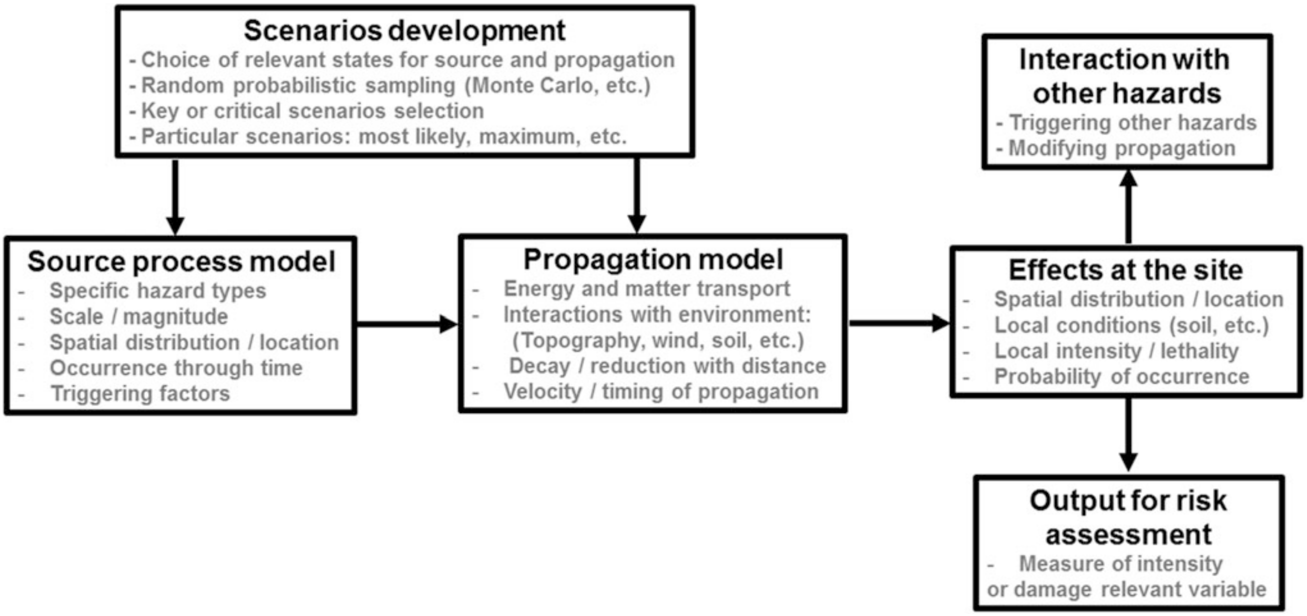

Risk Assessment, Fig. 3 General source-propagation-site process involved in many hazard modeling methods

is a crucial component of risk management, as it provides the input for informed decision-making on risk reduction actions. Uncertainty in risk assessment is unavoidable but should be minimized as much as possible; uncertainty can be incorporated in the analysis by using probabilistic methods and in the final decision-making process. Hazard and risk assessment methodologies produce results that can be integrated into a final risk assessment and, for that purpose, the output from hazard and risk analyses have to be in a compatible format.

Cross-References

- ▶ Earthquake
- ▶ Engineering Geomorphology
- ▶ Geohazards
- ▶ Hazard Assessment
- ▶ Landslide
- ▶ Mass Movement
- ▶ Risk Mapping
- ▶ Subsidence
- ▶ Volcanic Environments

References

Blaikie P, Cannon T, Davis I, Wisner B (2004) At risk: natural hazards, people's vulnerability and disasters. Routledge, London, 469 p

Fischhoff B, Lichtenstein S (1984) Acceptable risk. Cambridge University Press, Cambridge, 204 p

Rougier J, Hill LJ, Sparks S, Sparks RSJ (2013) Risk and uncertainty assessment for natural hazards. Cambridge University Press, New York, 588 p

UNISDR (2016) The United Nations Office for disaster risk reduction terminology on disaster risk reduction. Web Resource. https://www.unisdr.org/we/inform/terminolog. Accessed on May 2016

White G, Kates R, Burton I (2001) Knowing better and losing even more: the use of knowledge in hazards management. Global Environ Change B Environ Hazard 3(3):81–92

Wisner B, Gaillard J, Kelman I (eds) (2012) Handbook of hazards and disaster risk reduction and management. Routledge, London, 912 p

Wood N (2011) Understanding risk and resilience to natural hazards, U.S. Geological Survey Fact Sheet, vol 2011–3008. U.S. Dept. of the Interior, U.S. Geological Survey, Reston, 2 p

Risk Mapping

Cees J. Van Westen
Faculty of Geo-Information Science and Earth Observation (ITC), University of Twente, Enschede, The Netherlands

R

Definition

A process to determine the probability of losses by analyzing potential hazards and evaluating existing conditions of vulnerability that could pose a threat of harm to property, people, livelihoods, and the environment on which they depend (UN-ISDR 2009)

Introduction

The Earth is shaped by endogenic processes, caused by forces from within the Earth, resulting in hazardous events like earthquakes or volcanic eruptions, and exogenic processes, caused by forces related to the Earth's atmosphere, hydrosphere, geosphere, biosphere, and cryosphere and their interactions. Anthropogenic activities have had a very important influence on a number of these processes, especially in the last 200 years, for instance, through the increase of greenhouse gases, leading to global warming, but also through dramatic changes in the land cover and land use and overexploitation of scarce resources. The above mentioned processes from endogenic, exogenic, and anthropogenic sources may lead to potentially catastrophic events, even in locations that may be far away. For instance, earthquakes might trigger landslides which may lead to landslide-dammed lakes that may break out breach and cause flooding downstream. Or the dams of large reservoirs in mountains, constructed for hydropower, irrigation, or drinking water, may fail under an earthquake or extreme rainfall event and cause a similar flood wave.

These potentially harmful events are called hazards. They pose a level of threat to life, health, property, or environment. They may be classified in different ways, for instance, according to the main origin of the hazard: geophysical, meteorological, hydrological, climatological, biological, extraterrestrial, and technological (see Table 1, from Guha-Sapir et al. 2016). Such classifications are always somewhat arbitrary, and several hazard types could be grouped in different categories, for instance, landslides could be caused by earthquakes, extreme precipitation, or human interventions.

Hazards have a number of characteristics that should be understood in order to assess and subsequently reduce their potential damage. Hazards with certain magnitudes may occur with certain frequencies, as small events may occur often and large events seldom. In order to be able to establish a magnitude-frequency relationship for hazard events, it is generally necessary to collect historical data (e.g., from

Risk Mapping, Table 1 Classification of hazard types as used by the International Disaster Database EM-DAT (Guha-Sapir et al. 2016), which is based on and adapted from the IRDR Peril Classification and Hazard Glossary (IRDR 2014)

Main group	Main subgroup	Main type	Subtype
Natural	**Geophysical**: A hazard originating from solid Earth. This term is used interchangeably with the term geological hazard	Earthquake	Ground shaking, tsunami
		Mass movement	
		Volcanic	Ashfall, lahar, pyroclastic flow, lava flow
	Meteorological: A hazard caused by short-lived, micro to mesoscale extreme weather and atmospheric conditions that last from minutes to days	Storm	Extratropical storm, tropical storm, convective storm
		Extreme temperature	Cold wave, heat wave, severe winter conditions
		Fog	
	Hydrological: A hazard caused by the occurrence, movement, and distribution of surface and subsurface freshwater and saltwater	Flood	Coastal flood, riverine flood, flash flood, ice jam flood
		Landslide	Avalanche (snow, debris), mudflow, rockfall
		Wave action	Rogue wave, seiche
	Climatological: A hazard caused by long-lived, meso to macroscale atmospheric processes ranging from intra-seasonal to multi-decadal climate variability	Drought	
		Glacial lake outburst	
		Wildfire	Forest fire, land fire (bush, pasture)
	Biological: A hazard caused by the exposure to living organisms and their toxic substances or vector-borne diseases that they may carry. Examples are venomous wildlife and insects, poisonous plants, and mosquitoes carrying disease-causing agents such as parasites, bacteria, or viruses (e.g., malaria)	Epidemic	Viral , bacterial, parasitic, fungal, prion disease
		Insect infestation	Grasshopper, locust
		Animal accident	
	Extraterrestrial: A hazard caused by asteroids, meteoroids, and comets as they pass near Earth, enter the Earth's atmosphere, and/or strike the Earth and by changes in interplanetary conditions that affect the Earth's magnetosphere, ionosphere, and thermosphere	Impact	
		Space weather	Energetic particles, geomagnetic storm
Technological	Industrial accident		Chemical spills, collapse, explosion, fire, gas leak, poisoning, radiation, others
	Transport accident		Air, road, rail, water
	Miscellaneous accident		Collapse, explosion, fire, others

seismograph, meteorological stations, stream gauges, historical archives, remote sensing, field investigations, etc.) and carry out statistical analysis (e.g., using extreme event analysis such as Gumbel analysis) (Van Westen et al. 2008). The magnitude of the hazard gives an indication of the size of the event, or the energy released, whereas the intensity of a hazard refers to the spatially varying effects. For example, earthquake magnitude refers to the energy released by the ruptured fault (e.g., measured on the Richter scale), whereas the intensity refers to the amount of ground shaking which varies with the distance to the epicenter (e.g., measured on Modified Mercalli scale). The magnitude of floods may be measured as the discharge in the main channel at the outlet of a watershed before leaving the mountainous area, whereas the intensity may be measured as the water height or velocity which is spatially distributed and depends on the local terrain. For some types of hazards, there is no unique intensity scale defined, for instance, for landslides (Corominas et al. 2014).

These events may be potentially harmful to people, property, infrastructure, economy, and activities but also to the environment, which are all grouped together under the term "elements at risk" or assets. Also the term exposure is used to indicate those elements at risk that are subject to potential losses. Important elements at risk that should be considered in analyzing potential damage of hazards are population, building stock, essential facilities, and critical infrastructure. Critical infrastructure consists of the primary physical structures, technical facilities, and systems which are socially, economically, or operationally essential to the functioning of a society or community, both in routine circumstances and in the extreme circumstances of an emergency (UN-ISDR 2009). Elements at risk have a certain level of vulnerability, which can be defined in a number of different ways. The general definition is that vulnerability describes the characteristics and circumstances of a community, system, or asset that make it susceptible to the damaging effects of a hazard (UN-ISDR 2009). There are many aspects of vulnerability, related to physical, social, economic, and environmental conditions (see, e.g., Birkmann 2006). When considering physical vulnerability only, it can be defined as the degree of damage to an object (e.g., building) exposed to a given level of hazard intensity (e.g., water height, ground shaking, impact pressure).

Risk mapping is defined as the probability of harmful consequences or expected losses (deaths, injuries, property, livelihoods, economic activity disrupted, or environment damaged) resulting from interactions between natural or human-induced hazards and vulnerable conditions (UN-ISDR 2009; EC 2011). Risk can be presented conceptually with the basic equation indicated in Fig. 1.

Risk Assessment and Mapping

ISO 31000 (2009) defines risk assessment as a process made up of three processes: risk identification, risk analysis, and risk evaluation. Risk identification is the process that is used to find, recognize, and describe the risks that could affect the achievement of objectives. Risk analysis is the process that is

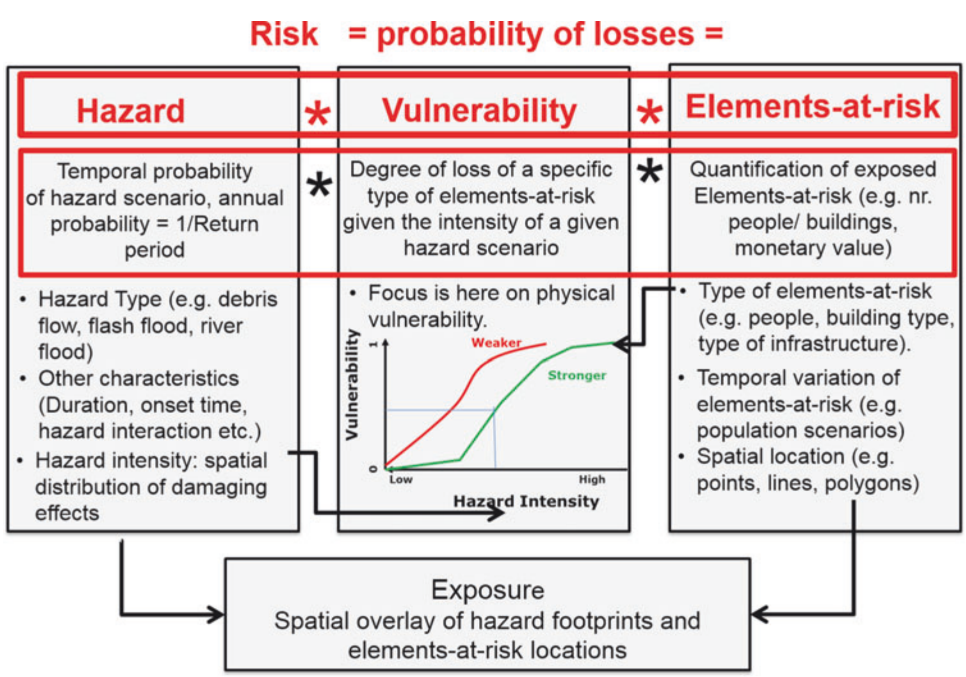

Risk Mapping, Fig. 1 Schematic representation of risk as the multiplication of hazard, vulnerability, and quantification of the exposed elements at risk. The various aspects of hazards, vulnerability, and elements at risk and their interactions are also indicated. This framework focuses on the analysis of physical losses, using physical vulnerability data used to understand the nature, sources, and causes of the risks that have been identified and to estimate the level of risk. It is also used to study impacts and consequences and to examine the controls that currently exist. Risk evaluation is the process that is used to compare risk analysis results with risk criteria in order to determine whether or not a specified level of risk is acceptable or tolerable.

The term risk mapping is often used as being synonymous with risk analysis in the overall framework of risk management. Risk assessments (and associated risk mapping) include a review of the technical characteristics of hazards such as their location, intensity, frequency, and probability; the analysis of exposure and vulnerability including the physical, social, health, economic, and environmental dimensions; and the evaluation of the effectiveness of prevailing and alternative coping capacities in respect to likely risk scenarios (UN-ISDR 2009; EC 2011; ISO 31000 2009). In the framework of natural hazard risk assessment, the term risk mapping also indicates the importance of the spatial aspects of risk assessment. All components of the risk equation (Fig. 1) are spatially varying, and the risk assessment is carried out in order to express the risk within certain areas. To be able to evaluate these components, we need to have spatially distributed information. Computerized systems for the collection, management, analysis, and dissemination of spatial information, so-called Geographic Information Systems (GIS), are used to generate the data on the various risk components and to analyze the risk (OAS 1991; Coppock 1995; Cova 1999; Van Westen 2013). Hazard data are generally the most difficult to generate. For each hazard type (e.g., flooding, debris flow, rockfall), so-called hazard scenarios should be defined, which are hazard events with a certain magnitude/intensity/frequency relationship (e.g., flood depth maps for 10-, 50-, and 100-year return periods). Different types of modeling approaches are required for the hazard scenario analysis, depending on the hazard type, scale of analysis, availability of input data, and availability of models. Generally speaking, a separate analysis is required to determine the probability of occurrence for a given magnitude of events, followed by an analysis of the initiation of the hazard (e.g., hydrological modeling or landslide initiation modeling) and of the runout or spreading of the hazard (e.g., hydrodynamic modeling or landslide run-out modeling). Overviews of hazard and risk assessment methods for landslides, for example, can be found in Corominas et al. (2014) and for floods in Prinos (2008). Elements-at-risk data are very often based on building footprint maps, which represent the location of buildings, with attributes related to their use, size, type, and number of people during different periods of the year (e.g., daytime, night time). Remote sensing is often used to extract these building maps if existing cadastral maps are not available. For other elements at risk like transportation infrastructure and land cover maps, also remote sensing data are used as important inputs. Vulnerability data are often collected in the form of vulnerability curves, fragility curves, or vulnerability matrices, which indicate the relationship between the levels of damage to a particular type of element at risk (e.g., single-story masonry building) given intensity levels of a particular hazard type (e.g., debris flow impact pressure). Generation of vulnerability curves is a complicated issue, as they can be generated empirically from past damage event for which intensity and damage are available for many elements at risk or through numerical modeling (Roberts et al. 2009).

Risk mapping for natural hazard risk can be carried out at a number of scales and for different purposes. Table 2 gives a summary. In the following sections, four methods of risk mapping will be discussed: quantitative risk assessment (QRA), event tree analysis (ETA), risk matrix approach (RMA), and indicator-based approach (IBA).

Quantitative Risk Assessment

If the various components of the risk equation can be spatially quantified for a given set of hazard scenarios and elements at risk, the risk can be analyzed using the following equation:

Risk Mapping, Table 2 Indication of scales of analysis with associated objectives and data characteristics (approaches: *QRA* quantitative risk assessment; *EVA* event tree analysis; *RMA* risk matrix approach; *IBA* indicator-based approach)

Scale of analysis	Scale	Possible objectives	Possible approaches
International, global	<1:1 million	Prioritization of countries/regions; early warning	Simplified RMA and IBA
Small: provincial to national scale	<1:100,000	Prioritization of regions; analysis of triggering events; implementation of national programs; strategic environmental assessment; insurance	Simplified EVA, RMA, and IBA
Medium: municipality to provincial level	1:100,000–1:25,000	Analyzing the effect of changes; analysis of triggering events; regional development plans	RMA/IBA
Local: community to municipality	1:25,000–1:5,000	Land use zoning; analyzing the effect of changes; Environmental Impact Assessments; design of risk reduction measures	QRA/EVA/ RMA IBA
Site specific	1:5,000 or larger	Design of risk reduction measures; early warning systems; detailed land use zoning	QRA/EVA/RMA

$$\text{Risk} = \sum_{\text{All hazards}} \left(\int_{P_T=0}^{P_T=1} P_{(T|HS)} \times \left(\sum_{\text{All EaR}} \left(P_{S|HS} \times \left(A_{ER|HS} \times V_{ER|HS} \right) \right) \right) \right) \quad (1)$$

in which:

$P_{(T|HS)}$ = the temporal probability of a certain hazard scenario (HS). A hazard scenario is a hazard event of a certain type (e.g., flooding) with a certain magnitude and frequency.

$P_{(S|HS)}$ = the spatial probability that a particular location is affected given a certain hazard scenario.

$A_{(ER|HS)}$ = the quantification of the amount of exposed elements at risk, given a certain hazard scenario (e.g., number of people, number of buildings, monetary values, hectares of land).

$V_{(ER|HS)}$ = the vulnerability of elements at risk given the hazard intensity under the specific hazard scenario (as a value between 0 and 1).

The method is schematically indicated in Fig. 2. GIS operations are used to analyze the exposure as the intersection between the elements at risk and the hazard footprint area for each hazard scenario. For each element at risk also, the level of intensity is recorded through a GIS overlay operation. These intensity values are used in combination with the element-at-risk type to find the corresponding vulnerability curve, which is then used as a look-up table to find the vulnerability value. The manner in which the amount of elements at risk are characterized (e.g., as number of buildings, number of people, economic value) also defines the way in which the risk is calculated. The multiplication of exposed amounts and vulnerability should be done for all elements at risk for the same hazard scenario. The results are multiplied with the spatial probability that the hazard footprint actually intersects with the element at risk for the given hazard scenario $P_{(S|HS)}$ to account for uncertainties in the hazard modeling. The resulting value represents the losses, which are plotted against the temporal probability of occurrence for the same hazard scenario in a so-called risk curve. This is repeated for all available hazard scenarios. At least three individual scenarios should be used, although it is preferred to use at least six events with different return periods (FEMA 2004) to better represent the risk curve. The area under the curve is then calculated by integrating all losses with their respective annual probabilities. It is possible to create risk curves for the entire study area, or for different spatial units, such as administrative units, census tracks, road or railway sections, etc. Risk can be presented in a number of different ways, depending on the objectives of the risk assessment (Birkmann 2007). Risk can be expressed in absolute or relative terms. Absolute population risk can be expressed as individual risk (the annual probability of a single exposed person to be killed) or as societal risk (the relation between the annual probability and the number of people that could be killed). Absolute economic risk can be expressed in terms of average annual loss, maximum probable loss, or other indices that are calculated from a series of loss scenarios, each with a relation between frequency and expected monetary losses (Jonkman et al. 2003).

The components that are involved in risk assessment have a high degree of uncertainty. Aleatory uncertainty is associated with the variation of the input data used in the risk assessment, for example, the variations in soil characteristics used to model landslide probability, surface characteristics, building characteristics, etc. These are normally incorporated in probabilistic risk analysis (Bedford and Cooke 2001) which calculates thousands of hazard and risk scenarios taking the variations of the input factors and calculating exceedance probabilities using techniques such as Monte Carlo simulation. Epistemic uncertainty refers to uncertainty associated with incomplete or imperfect knowledge about the processes involved and lack of sufficient data. This is often a serious problem as there may not be enough data available to determine individual hazard scenarios or there are no vulnerability curves for the types of elements at risk within the study area.

Risk assessment is computationally intensive. It can be carried out using conventional GIS systems, although it is advisable to use specific software tools. A number of software tools have been developed for multi-hazard risk assessment, for example, HAZUS in the USA (Schneider and Schauer 2006), RiskScape in New Zealand (Schmidt et al. 2011), CAPRA in Central America (CAPRA 2013), and MATRIX (Garcia-Aristizabal and Marzocchi 2013) and RISK-GIS in Australia (Granger et al. 1999). The common aspect of these software programs is that they are used to analyze damages and replacement costs, casualties, disruption, and number of people affected by various hazards. They differ in terms of the methods used for hazard assessment, asset exposure analysis, and vulnerability assessment and the method for risk calculation. What they also have in common is that these methods are very data demanding.

Event Tree Analysis

One of the difficult issues in natural hazard risk assessment is how to analyze the risk for more than one hazard in the same area and the way they interact. The simplest approach is to consider that the hazards are independent and caused by different triggers. If that is the case, the risk can be calculated by adding the average annual losses for the different types of hazard. Compared to single processes, standard approaches

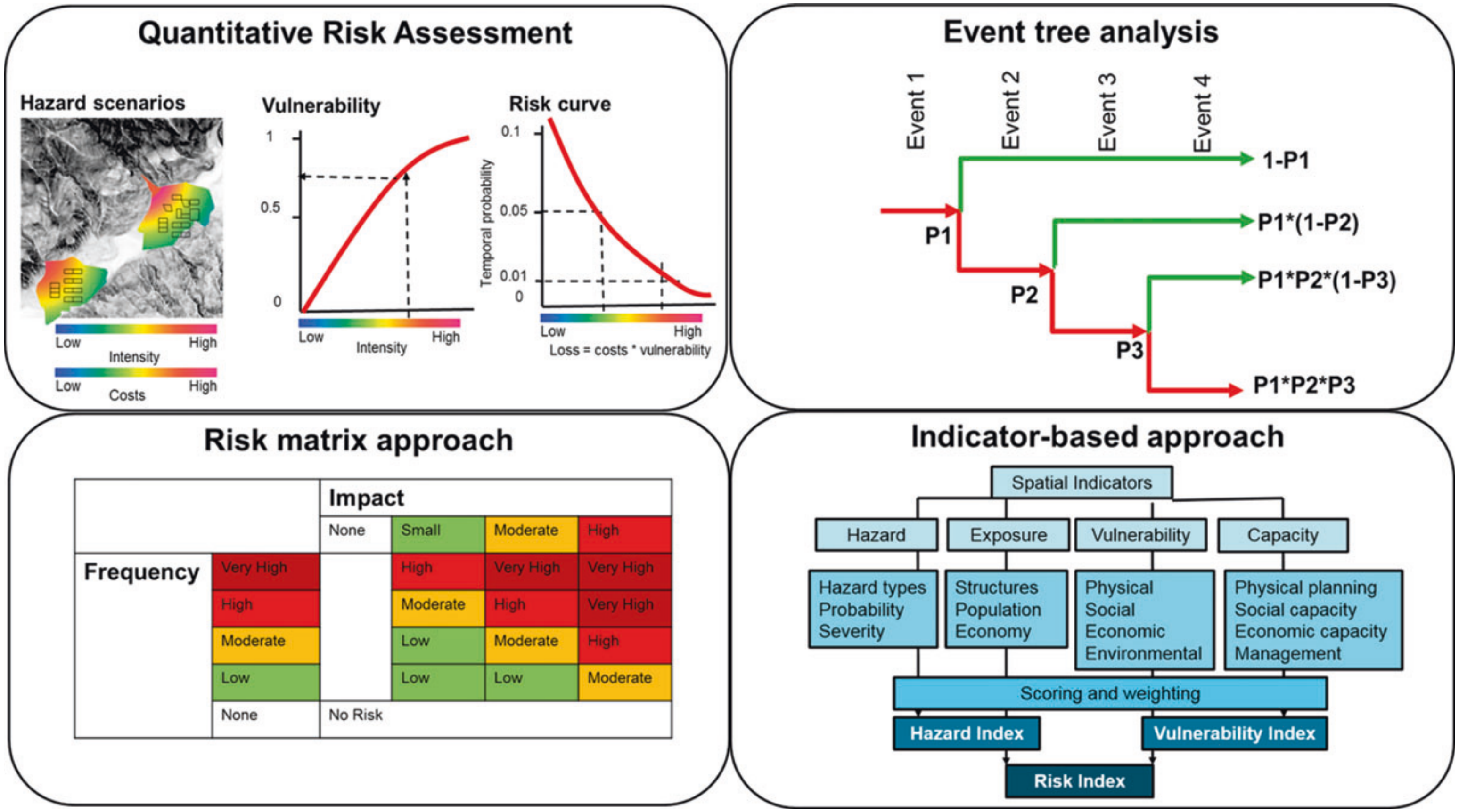

Risk Mapping, Fig. 2 Components relevant for risk assessment and the four major types of risk mapping that are presented in this entry and methodological frameworks for multi-hazard risk assessment are less common in the literature (Kappes et al. 2012), which is related to the complex nature of the interaction between the hazards and the difficulty to quantify these. Hazard may occur in sequence, where one hazard may trigger the next, as is the case in the example mentioned above on earthquake-triggered landslide-dam break-out flooding. These hazard chains or domino effects are extremely difficult to quantify over certain areas, although good results have been obtained at a local level (e.g., Peila and Guardini 2008). Hazards may also occur simultaneously, caused by the same triggering event, and may affect the same area, for example, as flash flooding or debris flows that affect the same area. One hazard may also alter the existing conditions so that a subsequent hazard could occur in different locations and with a higher frequency, for example, the higher hazard for debris flows after forest fires. The best approach for analyzing such hazard chains is to use a so-called event tree. An event tree analysis is a system which is applied to analyze all the combinations (and the associated probability of occurrence) of the parameters that affect the system under analysis. All the analyzed events are linked to each other by means of nodes (see Fig. 2), all possible states of the system are considered at each node, and each state (branch of the event tree) is characterized by a defined value of probability of occurrence.

Risk Matrix Approach

Risk assessments are often complex and do not allow to develop a full numerical approach, since many aspects are not fully quantifiable or have a very large degree of uncertainty. This may be related to the difficulty to define hazard scenarios, map and characterize the elements at risk, or define the vulnerability using vulnerability curves. In order to overcome these problems, the risk is often assessed using so-called risk matrices or consequences-frequency matrices (CFM) (see Fig. 2). They permit the classification of risks based on expert knowledge with limited quantitative data (Haimes 2008; Jaboyedoff et al. 2014). The risk matrix is made of classes of frequency of the hazardous events on one axis and the consequences (or expected losses) on the other axis. Instead of using fixed values, the use of classes allows for more flexibility and incorporation of expert opinion. Such methods have been applied extensively in natural hazard risk assessment, for example, in Switzerland (Jaboyedoff et al. 2014). This approach also permits to visualize the effects and consequences of risk reduction measures and to give a framework to understand risk assessment. The system depends on the quality of the group of experts that are formed to identify the hazard scenarios and that carry out the hazard filtering and ranking in several substages characterized by frequency (probability) and impact classes and their corresponding limits (Haimes 2008).

Indicator-Based Approach

There are many situations where (semi)quantitative methods for risk mapping are not appropriate. This could be because some of the data are lacking, thus making it impossible to quantify the components, such as hazard frequency, intensity, and physical vulnerability, for instance, when the risk assessment is carried out over large areas or in areas with limited data. Another reason is that one would like to take into account a number of different components of vulnerability that are not incorporated in (semi)quantitative methods, such as social vulnerability, environmental vulnerability, and capacity. In those cases, it is common to follow an indicator-based approach to measure risk and vulnerability through selected comparative indicators in a quantitative manner in order to be able to compare different areas or communities. The process of disaster risk assessment is divided into a number of components, such as hazard, exposure, vulnerability, and capacity (see Fig. 2), through a so-called criteria tree, which list the subdivision into objectives, sub-objectives, and indicators. Data for each of these indicators are collected at a particular spatial level, for instance, by administrative units. These indicators are then standardized (e.g., by reclassifying them between 0 and 1) and weighted internally within a sub-objective, and then the various sub-objectives are also weighted among themselves. Although the individual indicators normally consist of quantitative data (e.g., population statistics), the resulting vulnerability, hazard, and risk results are scaled between 0 and 1. These relative data allows to comparison of the indicators for the various administrative units. These methods can be carried out at different levels, ranging from local communities (e.g., Bollin and Hidajat 2006) and cities (Greiving et al. 2006) to countries (Van Westen et al. 2012).

Conclusions

The four methods for risk assessment treated in this chapter all have certain advantages and disadvantages, which are summarized in Table 3. The quantitative risk assessment method is the best for evaluating several alternatives for risk reduction, through a comparative analysis of the risk before and after the implementation followed by a cost–benefit analysis. The event tree analysis is the best approach for analyzing complex chains of events and the associated probabilities. The risk matrix approach is often the most practical approach as basis for spatial planning, where the effect of risk reduction methods can be seen as changes in the classes within the risk matrix. The indicator-based approach, finally, is the best when

Risk Mapping, Table 3 Advantages and disadvantages of the four risk assessment methods discussed

Method	Advantages	Disadvantages
Quantitative risk assessment (QRA)	Provides quantitative risk information that can be used in cost-benefit analysis of risk reduction measures	Very data demanding. Difficult to quantify temporal probability, hazard intensity, and vulnerability
Event tree analysis	Allows modeling of a sequence of events and works well for domino effects	The probabilities for the different nodes are difficult to assess, and spatial implementation is very difficult due to the lack of data
Risk matrix approach	Allows expression of risk using classes instead of exact values and is a good basis for discussing risk reduction measures	The method does not give quantitative values that can be used in cost–benefit analysis of risk reduction measures. The assessment of impacts and frequencies is difficult, and one area might have different combinations of impacts and frequencies
Indicator-based approach	Only method that allows a holistic risk assessment, including social, economic, and environmental vulnerability and capacity	The resulting risk is relative and does not provide information on actual expected losses

there are insufficient data to carry out a quantitative analysis but also as a follow-up of a quantitative analysis as it allows one to take into account other aspects than just physical damage. Even though hazard and risk mapping may have taken place, real risk reduction will only happen when it leads to a reduction in either the hazard frequency and intensity or the number of exposed elements at risk and their vulnerability. This requires integration of risk analysis into a risk management framework, which includes the adoption of policy and regulations and interaction of geoscientists within this process (DeGraff 2012).

Cross-References

▶ Earthquake Magnitude
▶ Hazard Assessment
▶ Risk Assessment

References

Bedford T, Cooke RM (2001) Probabilistic risk analysis: foundations and methods. Cambridge University Press, Cambridge

Birkmann J (ed) (2006) Measuring vulnerability to natural hazards: towards disaster resilient societies. UNU Press, Tokyo/New York

Birkmann J (2007) Risk and vulnerability indicators at different scales: applicability, usefulness and policy implications. Environ Hazards 7:20–31

Bollin C, Hidajat R (2006) Community-based disaster risk index: pilot implementation in Indonesia. In: Birkmann J (ed) Measuring vulnerability to natural hazards – towards disaster resilient societies. UNU Press, Tokyo/New York/Paris

CAPRA (2013) Probabilistic risk assessment program. http://www.ecapra.org/

Coppock JT (1995) GIS and natural hazards: an overview from a GIS perspective. In: Carrara A and Guzzetti F (eds) Geographical information systems in assessing natural hazards. Advances in natural and technological hazards research, vol 5. Kluwer, Dordrecht, pp 21–34

Corominas J, van Westen CJ, Frattini P, Cascini L, Malet J-P, Fotopoulou S, Catani F, van den Eeckhaut M, Mavrouli O, Agliardi F, Pitilakis K, Winter MG, Pastor M, Ferlisi S, Tofani V, Hervas J, Smith JT (2014) Recommendations for the quantitative analysis of landslide risk: open access. Bull Eng Geol Environ 73(2):209–263

Cova TJ (1999) GIS in emergency management. In: Longley PA, Goodchild MF, Maguire DJ, Rhind DW (eds) Geographical information systems: principles, techniques, applications, 2nd edn. Management issues and applications. Wiley, New York

DeGraff JV (2012) Solving the dilemma of transforming landslide hazard maps into effective policy and regulations. Nat Hazards Earth Syst Sci 12:53–60

EC (2011) Risk assessment and mapping guidelines for disaster management. European Commission Commission staff working paper, European Union

FEMA (2004) HAZUS-MH. FEMA's methodology for estimating potential losses from disasters. US Federal Emergency Management Agency. http://www.fema.gov/plan/prevent/hazus/index.shtm

Garcia-Aristizabal A, Marzocchi W (2013) Software for multi-hazard assessment. Deliverable 3.5 of the EU Matrix project: new methodologies for multi-hazard and multi-risk assessment methods for Europe. http://matrix.gpi.kit.edu/downloads/MATRIX-D3.05.pdf

Granger K, Jones TG, Leiba M, Scott G (1999) Community risk in Cairns: a multi-hazards risk assessment. Technical report, Australian Geological Survey Organisation (AGSO). http://www.ga.gov.au/corporate_data/33548/33548.pdf

Greiving S, Fleischhauer M, Lückenkötter J (2006) A methodology for an integrated risk assessment of spatially relevant hazards. J Environ Plan Manag 49(1):1–19

Guha-Sapir D, Below R, Hoyois Ph (2016) EM-DAT: the CRED/OFDA International Disaster Database, Université Catholique de Louvain, Brussels. www.emdat.be

Haimes YY (2008) Risk modeling, assessment, and management, 3rd edn. Wiley, Hoboken, p 1009

IRDR (2014) Integrated research on disaster risk. Peril classification and hazard glossary (IRDR DATA publication no. 1). Integrated research on disaster risk, Beijing. http://www.irdrinternational.org/wp-content/uploads/2014/04/IRDR_DATA-Project-Report-No.-1.pdf

ISO 31000 (2009) Risk management – principles and guidelines. http://www.iso.org/iso/home/standards/iso31000.htm

Jaboyedoff M, Aye ZC, Derron M-H, Nicolet P, Olyazadeh R (2014) Using the consequence – frequency matrix to reduce the risk: examples and teaching. International conference analysis and management of changing risks for natural hazards, Padua, 18–19 Nov 2014

Jonkman SN, Gelder PHAJM, Vrijling J (2003) A Overview of quantitative risk measures for loss of life and economic damage. J Hazardous Materials 99:1–30. https://doi.org/10.1016/S0304-3894(02)00283-2

Kappes MS, Keiler M, Von Elverfeldt K, Glade T (2012) Challenges of analyzing multi-hazard risk: a review. Nat Hazards 64(2): 1925–1958
OAS (1991) Geographic information systems. In: Natural hazard management. Organization of American States. Primer on natural hazard management in integrated regional development planning. www.oas.org/dsd/publications/Unit/oea66e/ch05.htm
Peila D, Guardini C (2008) Use of the event tree to assess the risk reduction obtained from rockfall protection devices. Nat Hazards Earth Syst Sci 8:1441–1450
Prinos P (2008) Review of flood hazard mapping. European community sixth framework programme for European research and technological development, FLOODsite
Roberts NJ, Nadim F, Kalsnes B (2009) Quantification of vulnerability to natural hazards. Georisk Assess Manag Risk Eng Syst Geohazards 3(3):164–173
Schmidt J, Matcham I, Reese S, King A, Bell R, Henderson R, Smart G, Cousins J, Smith W, Heron D (2011) Quantitative multi-risk analysis for natural hazards: a framework for multi-risk modelling. Nat Hazards 58(3):1169–1192
Schneider PJ, Schauer BA (2006) HAZUS, its development and its future. Nat Hazards Rev 7(2):40–44
UN-ISDR (2009) Terminology on disaster risk reduction. https://www.unisdr.org/we/inform/terminology
Van Westen CJ (2013). Remote sensing and GIS for natural hazards assessment and disaster risk management. In: Shroder J, Bishop MP (eds) Treatise on geomorphology. Remote sensing and GIScience in geomorphology, vol 3. Academic, San Diego, pp 259–298
Van Westen CJ, Castellanos Abella EA, Sekhar LK (2008) Spatial data for landslide susceptibility, hazards and vulnerability assessment: an overview. Eng Geol 102(3–4):112–131
Van Westen CJ, Straatsma MW, Turdukulov UD, Feringa WF, Sijmons K, Bakhtadze K, Janelidze T, Kheladze N. (2012) Atlas of natural hazards and risks of Georgia: e-book. Tbilisi, Caucasus Environmental NGO Network (CENN), University of Twente Faculty of Geo-Information and Earth Observation (ITC). ISBN 978-9941-0-4310-9

Rock Bolts

Alberto Ortigao
Terratek, Rio de Janeiro, Brazil

Definition

Tension elements designed to resist tension forces in the rock, usually made of a steel bar installed in pre-drilled hole and grouted.

Characteristics

A rock bolt has the following elements:

- *Head* is the anchor end outside the ground, comprising a plate, a nut, and a bearing plate.
- *Bonded length* is the length that transmits tension forces to the ground.
- *Spacer* is a plastic device, not always used to keep the tendon centered in the drill hole (Fig. 1).

Ortigao and Brito (2004) give additional details of rock bolt characteristics.

Drilling

The most common drilling method is percussion and rotary drilling with pneumatic drill rigs and cutting tools.

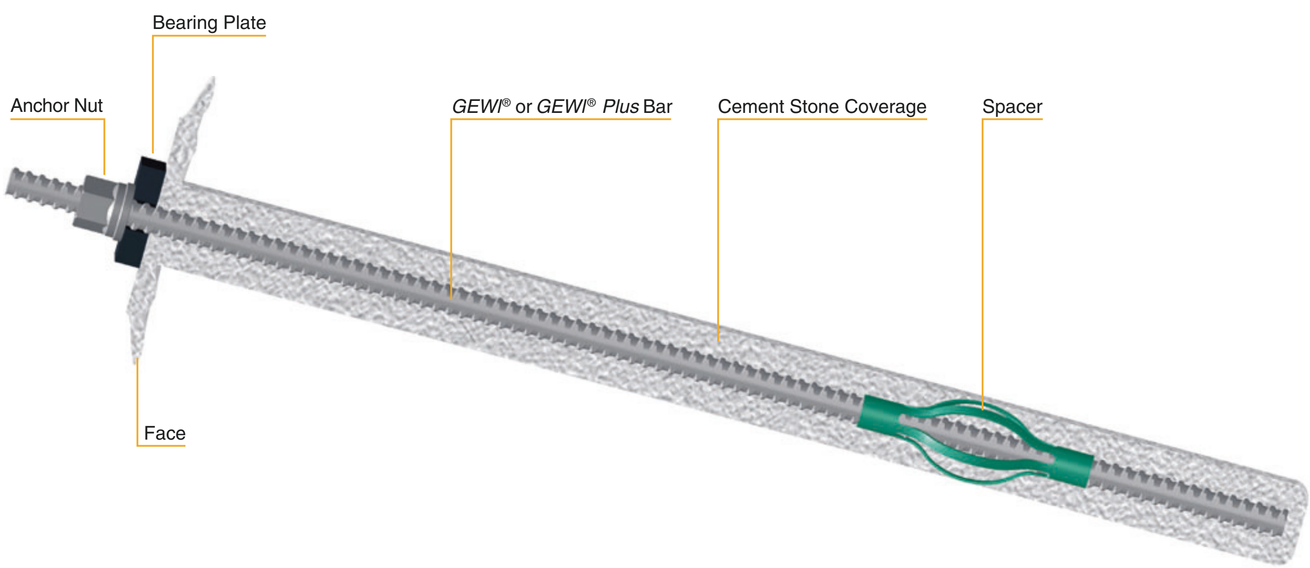

Rock Bolts, Fig. 1 Rock bolt (By courtesy of Dywidag)

R

Grouting

The most common grout is Portland cement grout. However, when rapid setting is needed, as is common in tunneling, resin grout is used.

Cross-References

► Grouting
► Ground Anchors

References

Ortigao JAR, Brito H (2004) Anchors, bolts and nails, Chapter 11. In: Ortigao JAR, Sayao AFSFJ (eds) Handbook of slope stabilisation. Springer, Heidelburg. www.springeronline.com, 478 p

Rock Coasts

Allan Williams[1,2] and Enzo Pranzini[3]
[1]Faculty of Architecture, Computing and Engineering, University of Wales, Swansea, Wales, UK
[2]CICA NOVA, Nova Universidad de Lisboa, Lisbon, Portugal
[3]Department of Earth Science, University of Florence, Florence, Italy

Definition

A rocky coast is one "*that is cliffed and yet composed of consolidated material irrespective of its hardness*" (Sunamura 1992, p. 2), that is, it ranges from very hard rock coasts (e.g., granite, basalt) to soft cohesive fluvial or glacial deposits, and they represent some 75% of the world's coastlines. Erosion on such coasts is irreversible and is a function of wave energy and rock strength (Fig. 1). They are usually high, and consequently there is an inherent danger for injury or even death to coastal visitors, so good signage is important (Fig. 1).

Cliff Erosion

Erosion is becoming an acute problem within the coastal zone, and because of global warming/sea level change, *El Nino* effects and greater storminess are likely to increase the risk of cliff failure and reduce human utilization. The general processes responsible for rock coast cliff erosion are well known and have been extensively discussed elsewhere

Rock Coasts, Fig. 1 The Glamorgan Heritage Coast, UK

(Sunamura 1992; USACoE 2002; Woodroffe 2002; Trenhaile 1997). Quantifying erosion controls is however rather difficult (Van Jones et al. 2015).

An extensive body of literature supports the significance of mechanical action within the wave erosional system (cf. Sunamura 1992). Realistically, failure depends upon many additional factors, such as hydro-geological processes and ground water seepage through the cliff mass. The retreat rate of rock cliffs varies but depends upon the:

Strength of the Rock Material Forming the Cliff

Axiomatically the harder the rock, the slower is the erosion rate. Rock and joint strength parameters (Table 1) can be derived from field measurement, such as Schmidt hammer readings and tilt tests, and laboratory analyses, for instance, uniaxial compression/tensile strength, point loading tests with values incorporated into standard rock mechanics formulae, such as given below:

$$\mathrm{JRC} = (\alpha - \varphi_b)/\log_{10}[(\mathrm{JCS}/\sigma_n)] \quad (1)$$

$$\varphi_b = (\varphi_b - 20) + 20\,({}^{r}/{}_{R}) \quad (2)$$

$$\sigma_n = \gamma_h \cos^2\alpha \quad (3)$$

$$t_p = \sigma_n \tan\,[\varphi_b + \mathrm{JRC}\cdot\,\log_{10}(\mathrm{JCS}/\sigma_n)] \quad (4)$$

where JCS = Joint Compressive Strength, e.g. via Schmidt hammer, JRC = Joint Roughness Coefficient (varies from 0 - very rough to 20, α = joint tilt angle at failure, φ_b = residual angle of friction along the joint, σ_n = mean value of normal stress induced by the sliding block weight, r = uniaxial compressive strength for wet rock samples, R = uniaxial compressive strength for dry rock samples, h = block thickness, γ = bulk density, and t_p = peak shear strength.

Rock Coasts, Table 1 Geomorphic rock mass strength classification for limestone/shales in Lias age rocks, Glamorgan Heritage Coast, Wales (GHC), UK (after Selby 1980; Fig. 1)

Parameter	Limestone	Shale
Intact rock strength	18	5
Weathering	9	5
Joint spacing	21–28	15–21
Orientation	14	14
Width	6	2
Continuity	4	4
Totals	78–85	48–54

Basal Wave Energy

Coastal cliff erosion is a complex system and variations in the geological, erosional, and weathering environment are reflected in the general cliff erosion rates derived from field and laboratory observations. Many investigations have established the links between basal erosion, notching (Fig. 2), cliff instability, and recession (Sunamura 1992; Rosser et al. 2013). Cliff surface deterioration and cliff base erosion are related especially to the assailing force of waves. Quasi-periodic wave erosion is more efficient when high tides coincide with storms whereby basal erosion by waves produce notching, and a laterally extending cliff base hollow. They are clear indicators of cliff erosion.

Three main processes affect a cliff's base:

- Cumulative hydraulic action related to breaking waves, water spray, and high speed droplets. Hydraulic forces that include compression, tension, impact, and shearing actions, which combine to achieve wave quarrying; all of these result in repeated stress placement on rock surface layers.
- Turbulent water currents that lift boulders, pebbles, and sand from the shore platform and beach.
- Shell feeding algae and other organism living in the intertidal band.

Mathematically**,** the major factors of basal erosion are given by Sunamura's (1992) equation:

$$x = f(F_w, s_r, t) \tag{5}$$

where x is the basal cliff erosion distance, F_w is the wave induced force, s_r is cliff material resistance, and t represents time.

If F_W is ≤ 0 no erosion occurs; when $F_W > 0$ erosion takes place.

Amount of Abrasive Material Available at the Cliff Base

Almost by definition, the loose sediment associated with cliff erosion occurs in the pebble-boulder range, which, if in sufficient quantity, is the best beach that nature could envisage to retard erosion. Beach sediment, usually in the pebble-boulder range, can accentuate erosion processes by either being an abrasive agent (boulders can smash into a cliff face) or can hinder it to form a protective beach. Increasingly strong wave action produces large hydraulic forces that are accentuated by the abrasive force of rock fragments hurled at the cliff base. The latter set up "*impact stresses on the rock surface, the stress increasing as the mass and/or angle of velocity of the impacting particles are increased"* (Sunamura 1992, p. 78). If the water depth in front of the cliff is higher than approximately half the wavelength, sediment is moved at the base and abrasion does not occur and the cliff becomes more stable (Plunging cliff: C type in Sunamura rock coast classification; Fig. 3).

Rock Coasts, Fig. 2 Golfo di Orosei, Sardinia: Active notch at the sea level and last interglacial fossil notch at approx. 8 m a.m.s.l. in a limestone cliff

Mass Movement

The coastal zone has a high frequency of cliff mass movement failures, which reflect the ability of high energy waves to exploit the well-jointed/interbedding nature of "very strong" and "moderately weak" rock materials. Wave undercutting is a critical control of many toppling and joint block detachment forms of failure. The Factor of Safety reduces as the ratio of undercutting depth to distance from the cliff face of tension fractures increase and as thrust forces within joint systems increase due to water infill by wave and tide factors, freeze-thaw and clay infill expansion and contraction.

The main forms of cliff falls are: Toppling (Fig. 4 left), Translation (Fig. 4 center), Buckling, and Falls rock (Fig. 4 right, debris and Earth), where the bulk of the mass falls as a free body; in soft rocks, flows can occur, where movement is faster towards the upper area of a moving body, that is, no block movement. The first two are usually the predominant mechanisms. Toppling occurs when an eccentricity develops

R

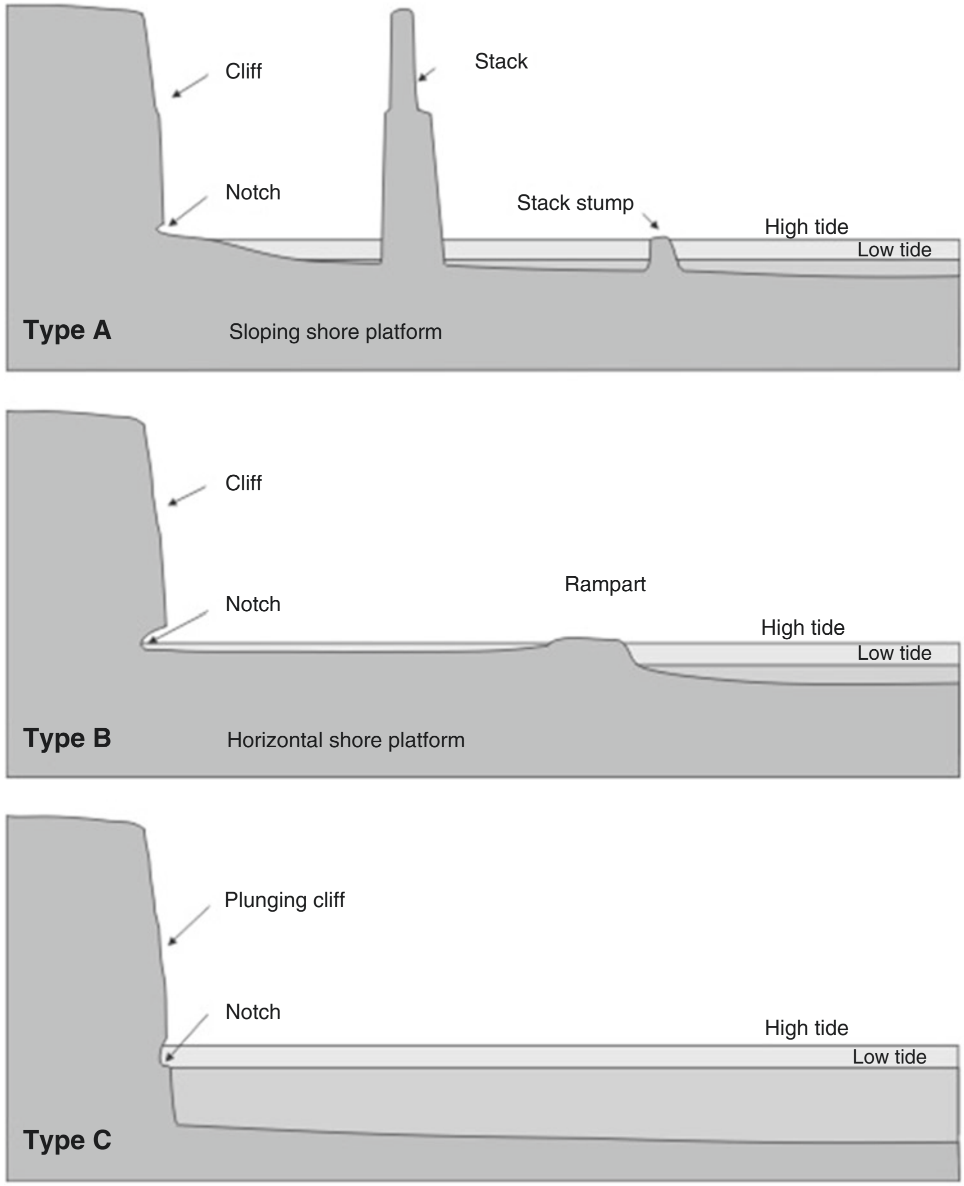

Rock Coasts, Fig. 3 Sunamura's rocky coast features classification: (**a**) sloping shore platform, (**b**) horizontal shore platform, (**c**) plunging cliff (from Pranzini 2004, modified)

so that overturning moments exceed resisting ones and little free fall movement occurs. A fulcrum is necessary along a hard rock band and it occurs when:

$$b/h < \tan ø \text{ and } \psi < ø \tag{6}$$

where b = block base dimensions; h = block height dimensions; ø = angle of frictional resistance; ψ = basal plane angle.

Sliding and toppling occur when

$$b/h < \tan \text{ and } \psi > ø \tag{7}$$

Shear resistance to toppling usually occurs along discontinuities orthogonal to the cliff strike. For translation to occur a hard rock band usually lies on top of a weaker rock unit and translation along a master joint is normal. The failure surface takes the path of least resistance through the rock mass, usually a curved surface.

Weathering

Weathering (chemical, hydrolysis, hydration, oxidation, and solution) and mechanical (frost, thermal stress, salt crystal growth, unloading, and swelling) decreases a rock's mechanical strength and coastal cliff deterioration due to temperature (nonuniform) variations mainly affecting surface rocks. Heat conductivity is a function of the rock's thermal properties, and discontinuous rocks are more vulnerable to thermal expansion/contraction. Rock composition differences cause

Rock Coasts, Fig. 4 (**a**) Toppling failure, Glamorgan Heritage Coast, UK (left); (**b**) Translation on glacial deposits, Poland (center); (**c**) Rock fall, Sardinia, Italy (right)

thermal conductivity anomalies resulting in large temperature gradients, which cause block cracking and displacement along joint/fault lines. Nivation processes by ice/water, salt crystallization, and so on reduce rock mass strength by entering rock discontinuities. Biological influences also can cause weathering. Plant growth can exert physical pressure on existing discontinuities. Marine organisms causing boring, for example, *Lithotrya, Lithophaga*, can also dislodge lithic material from a rock surface (Woodroffe 2002). Algae, fungi, and lichen can cause chemical alteration, especially in the tropics, as well as providing food for grazing organisms that can abrade the surface. This situation is estimated to reflect one-third of the mid-tidal zone at the Aldabra Atoll (Trudgill 1976). The importance of haloclasty (salt weathering) in cliff rock weathering is demonstrated by the ramparts that frequently border rock platforms on the seaward side, where the rock does not dry even at low tide due to constant exposure to spray. Salt does not precipitate and the process is not active leaving that ridge higher than the more sheltered platform (Fig. 5).

Parameter Interaction

Many models exist to show parameter interactions for soft coasts. Interaction of all the parameters discussed previously results in a rate of recession for the cliff mass as an erosion function, which can account for erosion forces and rock strength, as assumed by Sunamura (1992), Eq. (5), and also for the decrease of wave erosion intensity with cliff height. The variety of different mechanisms characterized by diverse time/space scales, process intensities, etc., in a general form can be expressed for the evolution of a 2-D cliff profile under marine influences (Williams et al. 1996; Belov et al. 1999) as:

$$(df/dt)^2 = k(z,t)\left\{(df/dy)^2 + (df/dz)^2\right\} \qquad (8)$$

where $f = f(y,z,t)$ is the function defining the cliff profile, $k(z,t)$ is the erosion function – the vertical distribution of erosion intensity and also temporal variation of storm-tide periodicity which modulates impact amplitude.

Rock Coasts, Fig. 5 Rock platform and rampart (Australia)

This equation is eikonal, an uncommon approach for geological literature, reflecting long-term cliff profile change in 2-D Cartesian coordinates. Cliff erosion defined by the erosion function is dependent on the nondimensional erosion amplitude parameter v, which in turn is contingent upon breaking wave energy, storm/tide cyclicity, and cliff geometry. While the speed of cliff retreat is also influenced by cliff geology, strength, and geomorphology of the rock mass, it is implicitly subsumed in v, as a complex parameter.

Conclusions

Pre-sea level rise morphological differences, rock variability in petrography and structure, diversity in climate, tidal range, and wave energy interact to make each rock coast segment a different case as far as landscape, processes, and erosion rate. Sunamura (1992) lists some 220 case studies from the

R

literature and gives cliff erosion rates: most of them are less than 1 cm/yr, with some cliffs almost stable for centuries, but sand, silt, clay, and generic glacial deposits can retreat as much as 10 m/yr. Values of coastal retreat for recently deposited pyroclastic material reach as high as 80 m/yr.

Since most of the processes are nonlinear with time, cliff failure events, or even single rock falls, are rarely forecasted, and this exposes people and values to a significant risk. Since cliffs are among the most attractive elements of coastal landscape monitoring, signage and restrictions are an integrant part of coastal management.

Cross-References

- ▶ Armor Stone
- ▶ Beach Replenishment
- ▶ Biological Weathering
- ▶ Boulders
- ▶ Chemical Weathering
- ▶ Classification of Rocks
- ▶ Climate Change
- ▶ Coast Defenses
- ▶ Erosion
- ▶ Factor of Safety
- ▶ Gabions
- ▶ Landforms
- ▶ Landslide
- ▶ Mass Movement
- ▶ Mechanical Properties
- ▶ Nearshore Structures
- ▶ Physical Weathering
- ▶ Risk Assessment
- ▶ Risk Mapping
- ▶ Rock Laboratory Tests
- ▶ Rock Mass Classification
- ▶ Rock Mechanics
- ▶ Rock Properties
- ▶ Sea Level
- ▶ Shear Stress
- ▶ Stabilization

References

Belov AP, Davies P, Williams AT (1999) Mathematical modeling of basal coastal cliff erosion in uniform strata: a theoretical approach. J Geol 107(1):99–109

Pranzini E (2004) La forma delle coste. Zanichelli, Bologna, 245pp

Rosser NJ, Brain MJ, Petley DN, Lim M, Norman EC (2013) Coastline retreat via progressive failure of rocky coastal cliffs. Geology 41(9):939–942

Selby MJ (1980) A rock mass strength classification for geomorphic processes: with tests from New Zealand and Antarctica. Zeit Fur Geomorph 24:31–51

Sunamura T (1992) Geomorphology of rocky coasts. Wiley, Chichester, 302pp

Trenhaile AJ (1997) Coastal dynamics and landforms. Oxford University Press, Oxford

Trudgill ST (1976) The marine erosion of limestone at Aldabra Atoll., Indean Ocean. Zeit Fur Geomorph Supp Band 26:164–200

USA US Army Corps of Engineers, CoE Coastal Eng (2002) Quantifying the erosion controls on erosion of a hard rock cliff. Mar Geol 363:230–242

Van Jones EC, Rosser NJ, Brain MJ, Petley DN (2015) Quantifying the erosion controls on erosion of a hard rock cliff. Mar Geol 363:230–242

Williams AT, Davies P, Belov AP (1996) Coastal cliff failures at Colhuw beach, Wales, UK. In: Breccia CA, Ferrante A (eds) Coastal environments. Computational Mechanics Publications, Southampton, pp 75–82

Woodroffe CD (2002) Coasts – form, Process and evolution. Cambridge University Press, Cambridge, 263pp

Rock Field Tests

Yonathan Admassu
Geology and Environmental Science, James Madison University, Harrisonburg, VA, USA

Definition

Rock field tests as discussed here do not refer to tests performed with portable devices that can be used in the field such as the Schmidt hammer or the point load test device. Rock field tests only refer to tests that have to be performed on the ground surface, underground openings, and boreholes to characterize deformability and *in situ* stress. The following is a summary of International Society for Rock Mechanics (ISRM)-suggested methods for rock field tests (Ulusay and Hudson 2007).

Introduction

Designing subsurface or on-surface civil engineering structures requires a sound knowledge of rock mass deformability and *in situ* stress of rock mass. Both deformability and *in situ* stress are controlled by discontinuities in rock and tectonic (paleo or active) stress at the site of proposed construction. Therefore, it is necessary to devise field-testing methods that can be performed inside underground openings, inside boreholes, and on the ground surface. Deformability of a rock mass is its response to change in stress due to loading by engineering/mining structures. It is estimated by applying stress using hydraulic jacks and monitoring displacements to quantify deformability. Examples of deformability tests inside underground openings or on ground surface include the plate test, radial jacking, and large flat jack, whereas the

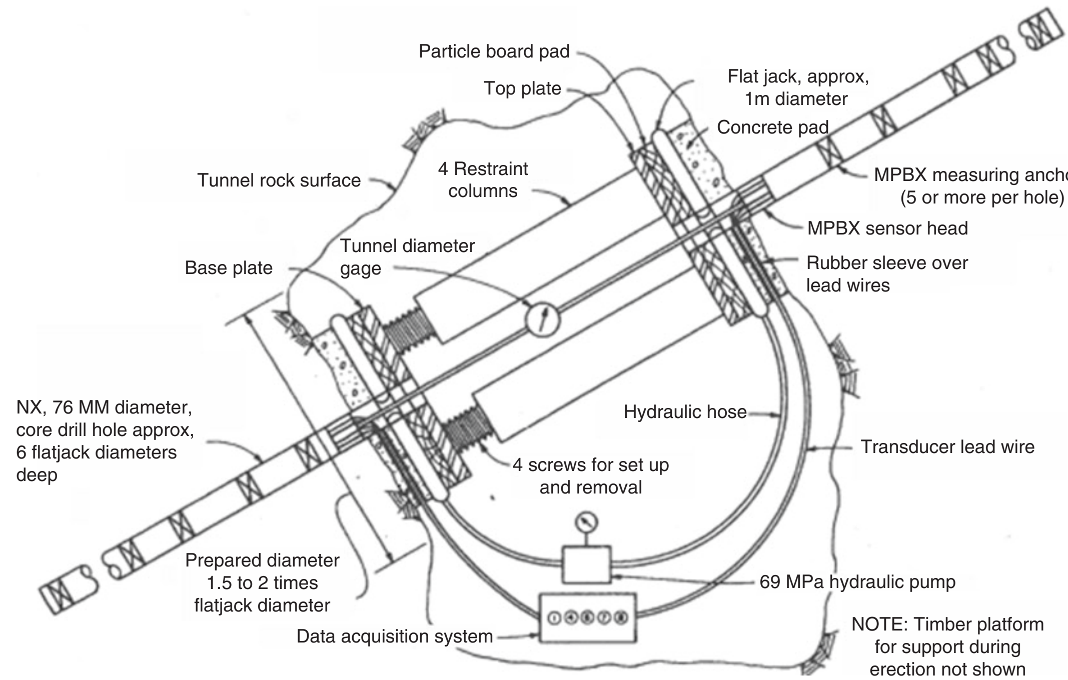

Rock Field Tests, Fig. 1 Plate test inside a tunnel

downhole plate test and flexible/stiff dilatometers can be used inside a borehole. *In situ* stress is another important rock mass parameter that needs to be measured as well. Three methods for *in situ* stress determination, the flat jack, overcoming, and hydraulic fracturing, are also discussed below. The flat jack and hydraulic fracturing methods involve application of induced pressure, whereas the overcoring is performed by relieving stress by coring around a rock in which a probe is installed.

Deformability Tests

Deformability of rock is a measure of strain (deformation) of intact rock and rock masses in response to change in stress. Deformability tests can be performed on the ground surface, on tunnel walls, or in boreholes. The plate test, radial jacking, and large flat jack are performed on tunnel walls and on ground surface. Downhole tests include downhole plate test and flexible/stiff dilatometers.

Deformability: Plate Test

The plate test is performed by placing two flat jacks (1 m in diameter) on flat surfaces inside a tunnel that are diagonally opposite to each other (Coulson 1979). A flat jack is made up of metal sheets attached around their edges and can be inflated using hydraulic fluids. The flat jacks are secured against a tunnel wall by load-transferring restraint columns that resist motion of the flat jacks into the tunnel opening (Fig. 1). Fluid pressure is applied into the flat jacks simultaneously to apply stress onto the area under the flat jacks. Strain due to loading is measured in boreholes drilled perpendicularly behind the loading plates. Up to five strain gauges known as MPBXs (multiple-position borehole extensometers) are installed in both boreholes to monitor strain during loading (Fig. 1). Setup and testing methods suggested by Coulson (1979) for the plate test are summarized below.

Setup The tunnel area for testing should be cleaned off of loose rocks. Boreholes that are diagonally opposite from each other should be drilled as deep as 10 m. The drilled cores should be carefully logged. The MPBXs should be placed inside the boreholes to measure the anticipated deformation. The flat jacks will be pressurized to apply stress over the top of the boreholes (Fig. 1). The area between the boreholes and the flat jack should be covered with concrete. Wood or resin should be placed as filler between the flat jacks and the steel plates on top of the load-transferring restraint columns.

Testing Loading is applied cyclically. Each loading should be followed by a 24 h period of zero pressure. Deformation measurements from the installed MPBX instruments should be continuously recorded. The duration of loading, maximum test pressure, and number of loading increments are dependent on the type of project. Deformation is calculated based on distance between the flat jack and the depth of the displacement sensor, load, and radius of loaded area, Poisson's ratio, and Young's modulus. The deformation modulus (E_d)

R

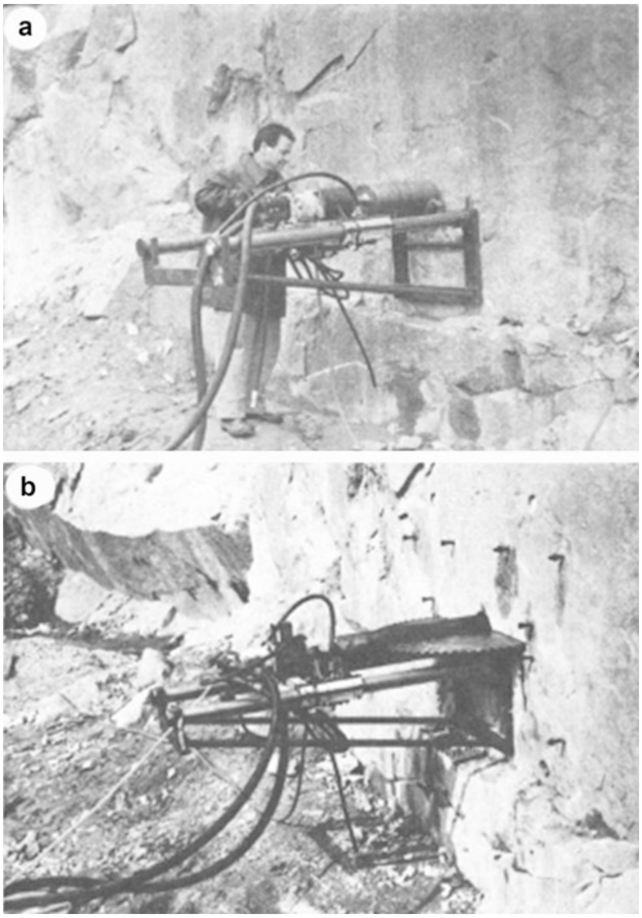

Rock Field Tests, Fig. 2 Cutting a slot to insert a flat jack

for the rock mass between two MPBXs at depths $z1$ and $z2$ behind the flat jacks is given by:

$$E_d = q\,(K_{z1} - K_{z2}/W_{z1} - W_{z2}),\ \ K_z = W_z(E/q)$$

where q is pressure applied, W_z is displacement in the direction of applied pressure, and E is Young's modulus.

Deformability: Large Flat Jack

This test is intended to measure *in situ* deformability of rock mass by inserting flat jacks into slots cut into rock using a rock saw or a series of overlapping drilled holes (Loureiro-Pinto 1986) (Figs. 2 and 3). The test can be performed on up to four coplanar slots simultaneously. Each flat jack consists of two steel sheets less than 1 mm thick, welded around the edges to be inflated by hydraulic fluid. Deformation is measured by measuring displacements at various places perpendicular to the slots. If the slot is made by line drilling, the semicircular gaps should be filled with concrete. Setup and testing methods suggested by Loureiro-Pinto (1986) for the test are summarized below.

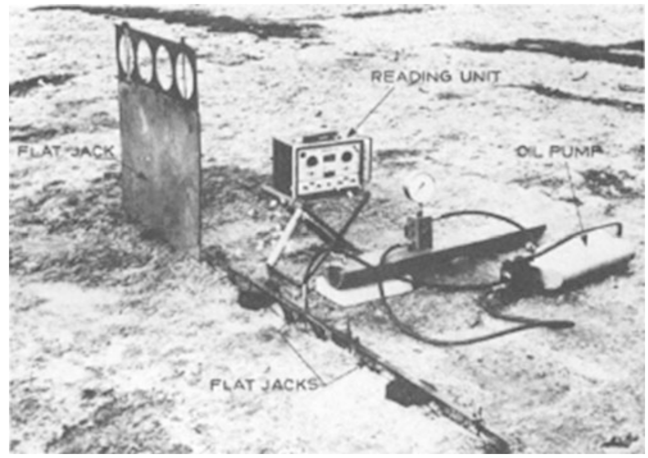

Rock Field Tests, Fig. 3 Inserting a large flat jack

Setup Test locations should preferably be in zones which will be affected by the intended work with due consideration given to the direction of anticipated maximum compressive stress. At least two coplanar slots should be used. Flat surfaces perpendicular to the chosen jack positions should be prepared inside an underground structure such as an adit or tunnel or on surface. The flat surface may be lined by concrete to aid in the installation of the cutting machine that should carefully be operated in order to avoid deviations. The slot cut by a rotary saw or line drilling should be smooth (+/−5 mm) and have a width between 5 and 10 mm larger than the flat jack.

Testing The deformation gauges (deformeters) must be calibrated before testing. Three loading/unloading cycles should be used. The test pressure should be at a minimum of 0.2 MPa and maximum of 120–150% of the maximum loading due to the proposed structure. Each loading should be performed at constant increments to permit accurate plotting of pressure and deformation. The variation in applied pressure should not vary by more than 2%. The modulus of deformation (E) is calculated as follows:

$$E = k(1 - v2)\,p/d$$

where p = increment of applied pressure

d = increment in slot opening corresponding to increment in pressure

v = Poisson's ratio

k = coefficient depending on stiffness, shape of flat jacks, location of measuring point, shape of the test chamber, and depth of crack that formed due to loading

Deformability: Radial Jacking Test

The radial jacking test is to measure deformability of rocks due to radial loading. The test is done in circular openings such as adits and tunnels. The load is uniformly distributed radially, and subsequent diametrical displacement within the ground opening is measured (Coulson 1979). Setup and testing methods suggested by Coulson (1979) for the test are summarized below.

Setup The test chamber is excavated to the required dimension and shotcreted. The geology, lithology and structural condition, and orientation of discontinuities should be documented. Holes to install extensometers should be drilled. Loading is done by placing flat jacks over the shotcrete surface. The flat jacks are placed on top of rigid steel rings that are attached to a frame of sufficient strength to resist movement into the opening. Wood planks are placed between the steel rings and the flat jacks. The setup allows the flat jacks exerting load only on both the steel rings and the shotcrete surface, but movement into the opening is resisted by the rigid rings. Deformation of the shotcrete surface can be measured by the extensometers anchored diametrically across the tunnel/adit opening. Multiple extensometers can be used, and the recorded displacement should be in reference to anchors placed well away from the zone of loading.

Testing Three loading and unloading cycles are recommended. For each cycle, pressure should be increased at the rate of 0.05 MPa/min. The displacement should be recorded until 80% of the anticipated displacement has been recorded. Each loading is followed by unloading to near zero pressure. The elastic moduli (E) and deformation moduli are given by:

$$E = p_2 r_2 / \Delta_e (m + 1/m)$$

$$V = p_2 r_2 / \Delta_t (m + 1/m)$$

where p_2 = pressure just below the shotcrete lining at radius of r_2
Δ_e = elastic displacement
Δ_t = total displacement
m = estimated Poisson's ratio

Deformability: Downhole Plate Test

This test is intended to measure *in situ* deformability of rock mass by applying perpendicular stress to a flattened borehole end and measuring displacements. The method allows measuring deformability at different depths with the primary loading axis coinciding with the borehole axis. The displacement due to loading should be measured. Setup and testing methods suggested by Coulson (1979) for the test are summarized below.

Setup The drilled hole for testing should at least have a diameter of 500 mm. The borehole end should be made flat (+−5 mm) and perpendicular to the drill axis (+−3 °). A circular loading plate of ~500 mm should be lowered to the borehole end. Casing may be necessary to stabilize the borehole as well as lowering the water table. A loading column to transmit force onto the loading plate should be assembled. The vertical displacement due to loading should be measured with respect to references placed on ground surface at greater than ten test borehole diameters.

Testing The range of loading is recommended to be within 0.3–1.5 q_0. q_0 is the stress due to the proposed structure. Three loading cycles with each loading increased equally over five increments are performed. The resulting displacement for each loading increment as a function of time should be recorded. If testing for deeper horizons is desired, the equipment should be removed, drilling should continue to the test level, and the borehole end should be prepared for another test. The deformation modulus is calculated as follows:

$$E = dq/d\rho \frac{\pi}{4} \,.\, D \left(1 - v^2\right) I_c$$

where q = applied pressure
ρ = settlement
v = Poisson's ratio
I_c = depth correction factor

Deformability: Downhole Flexible Dilatometer

This test is a downhole measurement of deformability using an inflatable cylindrical flexible membrane placed within a borehole at desired depths (Ladanyi 1987) (Fig. 4). Deformation is measured as a function of volume change of the membrane when it is inflated and pushes against the borehole wall. The other method of measuring deformation is by direct radial displacement measurements using transducers installed inside the dilatometer. This method allows deformability measurement in any direction, thereby characterizing anisotropy. Deformability using the flexible dilatometer can be measured at different depths in a drill hole. The measurement is however limited to the horizontal axis or perpendicular to the drill axis. The volume of rock to be tested is usually very small compared to radial or flat jacking methods. Results should be size and orientation adjusted. Setup and testing methods suggested by Ladanyi (1987) for the test are summarized below.

Setup Rotary diamond coring is required to provide smooth walls for testing. Casing may be needed to stabilize the borehole outside the testing zone. The test section should be checked with a downhole camera or a diameter gauge if there is any obstruction for the dilatometer probe. Testing depth interval could be at regular spacings or at selected sites with certain geologic attributes. The stiffness of the system should be calibrated to correct pressure and volume measurement.

R

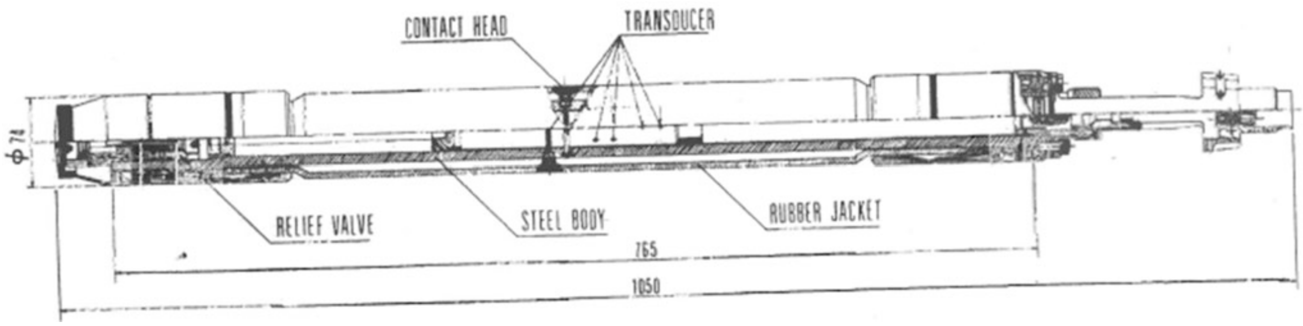

Rock Field Tests, Fig. 4 LNEC-type dilatometer

Testing The dilatometer probe is inserted at the test section. The probe is inflated until the membrane is in full contact with the borehole wall. Pressure is then to be increased incrementally to the maximum value. At the end of each increment, the dilation in terms of volume change (calculated in terms of pump fluid used) and the applied pressure should be recorded with respect to time for about 10 min. Up to three loading and unloading cycles are required. If the probe is equipped with radial displacement-measuring transducer, displacement can directly be measured at different orientations and recorded with respect to time. The deformation modulus (E_d) using just volume change is calculated as follows:

$$E_d = 2(1 + V_R)\, G_d, G_d = M_R\left(\pi La^2/\alpha\right)\, [(1 + B_c(1 - 2v_R)(/(1 - B_c]$$

where G_d = deformation modulus
α = pump constant (fluid volume displaced per turn)
L = length of cell membrane
a = inside radius of cylinder
b = outside radius of cylinder
$B_c = (a/b)^2$
V_R = Poisson's ratio

The deformation modulus (E_d) using radial displacement measurements is given by:

$$E_d = (1 + V_R)\, D\, \Delta p/\Delta D$$

where D = drill hole diameter and $\Delta p/\Delta D$ is the slope of change in pressure with respect to radial displacement.

Deformability: Downhole Stiff Dilatometer

The stiff dilatometer measures deformability using curved loading platens that can exert pressure at different orientations on the borehole wall and measure displacement (Fig. 5) (Yow 1996). The probe can be lowered to any desired depth within the borehole. It can also be rotated to measure deformability at different orientations. Highly fractured or weak rock masses can be problematic for the test. The stiff dilatometer suffers the same drawbacks as the flexible dilatometers in regard to the very small volume of rock that can be tested. Setup and testing methods suggested by Yow (1996) for the test are summarized below.

Setup The dilatometer displacement-measuring devices, linearly variable differential transformers (LVDTs), should be calibrated so that displacement readings read zero displacement at the borehole-drilled diameter. The borehole to be tested should be logged and location/orientation for test should be specified. The borehole should be checked carefully for irregular wall surfaces and varying diameters.

Testing The dilatometer can be lowered to any desired depth for testing. After each test, the dilatometer can be retracted and moved to a different location. It is best to start the test from the lowest most location and continue testing upward to the collar of the borehole. This avoids rock failure obstacles during testing that might affect the movement of the dilatometer inside the borehole. Once the dilatometer reaches the desired depth, the pressure on the platens can be increased until they touch the borehole wall. The displacement reading should be recorded and ideally with zero displacement. Loading can then continue in equal increments and corresponding displacement readings be recorded. Once the maximum pressure has been reached, the pressure should be allowed to dissipate in decrements that correspond to the increments. Displacement values should be recorded during unloading as well. Multiple loading/unloading cycles can be performed. Time-dependent deformability can be tested by maintaining the maximum pressure for an extended time and measuring displacement regularly. The next testing location should at least be 30.5 cm away from a previous test location. The modulus of deformation (E) can be calculated as follows:

$$E = 0.86^{*}0.93^{*}\Delta Q_h(D/\Delta D)\ T$$

where D = borehole diameter
ΔD = change in borehole diameter
ΔQ_h = pressure increment
T = coefficient depending on Poisson's ratio

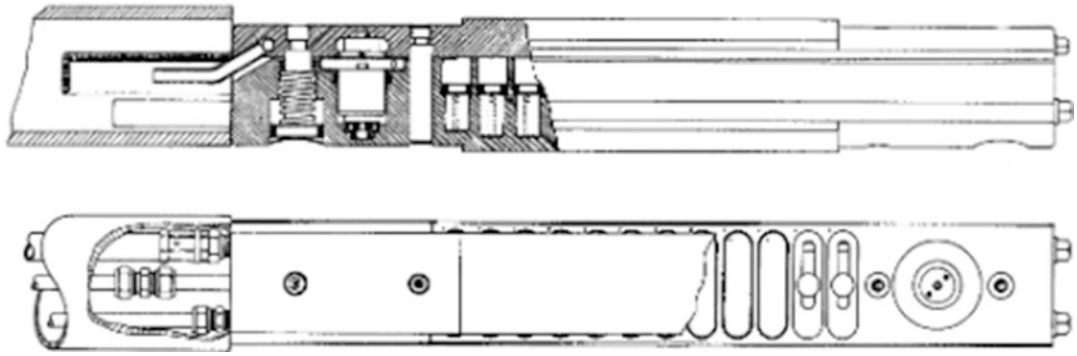

Rock Field Tests, Fig. 5 Line drawing showing a flexible dilatometer

In Situ Stress Test

Stress on underground rock mass generally increases with depth but is affected by geologic structures, tectonic forces, and residual stress from paleotectonics. The natural state of stress is termed an *in situ* stress, which can be much higher than the rock mass strength at a specific site causing problems to the stability of underground openings. Therefore, determining the *in situ* stress is essential for designing underground structures and foundations. The suggested methods for determining *in situ* stress include using the flat jack, overcoring, and hydraulic fracturing techniques.

In Situ Stress Test: Flat Jack

The flat jack method involves inserting pressure-expandable steel sheets welded along their edges into a slot cut into a rock mass. It is ideally installed in underground openings that are wide enough to allow installation (Fig. 6) (Kim and Franklin 1987). The flat jack is connected to a hydraulic pump. Displacement perpendicular to the flat jack is measured with reference to pairs of pins grouted into the rock on either side of the flat jack. Each measurement determines the state of stress perpendicular to the flat jack, and therefore, multiple orientations of flat jacks may be used to get a complete picture of *in situ* stress (Fig. 7). Setup and testing methods suggested by Kim and Franklin (1987) for the test are summarized below.

Setup The flat jack which is at least 0.1 m^2 has one inlet for the pressurizing fluid and another for bleeding. A rotary rock saw is needed to create a slot to install the flat jack. A series of overlapping boreholes can also be used as slot, but the space between the flat jack and rock needs to be grouted. Displacement measuring pins anchored symmetrically on either side of the flat jack should be around 12 mm in diameter and 150 mm in length. A minimum of six setups at different orientations are required. The site of flat jack installation should be cleared off of loose materials and should be flat. The distance between test sites should be at least three times the length of the flat jack.

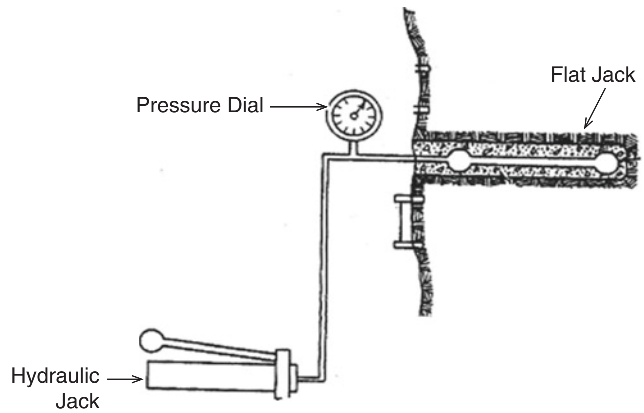

Rock Field Tests, Fig. 6 Cross-sectional view of a flat jack placed in a slot

Testing Pressure- and displacement-measuring devices should be calibrated. Distance measurement between each pair of the pins should be taken before the slot is cut. Another set of distance measurements should be taken immediately after the slot is made to capture the amount of slot closure. The flat jack is then inserted and grouted so that it will be held in place. Pressure into the flat jack is increased until the separation between the pins is the same as it was before the slot was cut. This pressure is termed the cancelation pressure. Readings of the pin separation are recorded during the pressure increment stage. The *in situ* stress perpendicular to the flat jack is approximately within 5% of the cancelation pressure.

In Situ Stress Test: Overcoring

The method of overcoring is used to determine *in situ* stress in a borehole. The technique involves inserting a probe with

R

strain gauges bonded to the inside wall of a borehole called a pilot hole. The pilot hole is then drilled again (overcored) by a larger diameter borehole relieving the stress experienced by the probe inside (Fig. 8) (Sjöberg et al. 2003). As the overcoring advances and the pilot hole experiences a relief in stress, the strain gauges in the pilot hole respond by extending outward proportional to the *in situ* stress and elastic property of the rock. If the elastic properties of the rock are known from lab tests, the strain recovery (difference in strain before and after overcoring) as a result of overcoring can be related with *in situ* stress. Various types of probes, the Borre probe, CCBO, CSIR, and USBM, have been described by Sjöberg et al. (2003); Sugawara and Obara (1999); Kim and Franklin (1987).

Setup Before testing, calibration of strain gauges and cleaning of the borehole should be accomplished. The depth of testing, where the pilot hole should be located, is specified in advance. Drilling is advanced to the top of the specified zone of testing, and a smaller pilot hole (~50% of the original hole) is then drilled. The pilot hole core is analyzed for its homogeneity and the presence of open fractures. The ideal zone of testing should be where the rock is homogenous and free of open fractures. If the rock quality is unacceptable, drilling at the normal diameter should advance further. If the rock quality of the pilot hole core is found acceptable, the pilot hole should be cleaned by flushing water downhole before installing the probe.

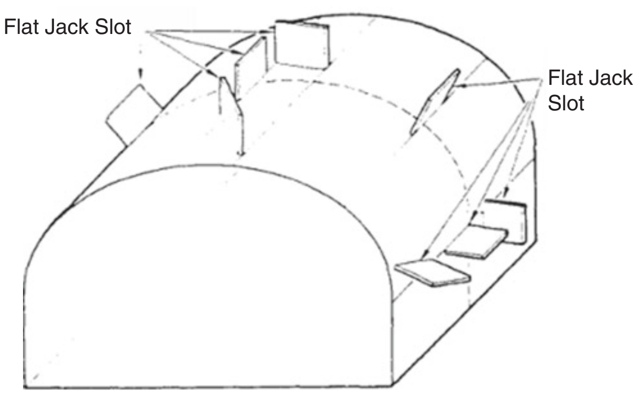

Rock Field Tests, Fig. 7 Layout of flat jack slots

Testing For the testing to begin, a probe with strain gauges is installed inside the pilot hole. The strain gauges can be oriented perpendicular, parallel, and at 45 ° to the borehole axis and are glued to the pilot hole wall. Once the glue has hardened, overcoring can begin. The overcored section is broken off at the base and brought to surface to record length of sample, lithology, rock fabric, and uniformity of thickness. After the probe has been removed from the sample, the hollow core with a minimum length of 24 cm is subject to biaxial loading to determine Young's modulus and Poisson's ratio. A three-dimensional stress tensor is calculated based on multidirectional strain data from the strain gauges, orientation of the borehole, and elastic constants of the rock assuming that the rock is homogenous, isotropic, and linear elastic. For details of calculation, the reader is referred to Sjöberg et al. (2003).

In Situ Stress Test: Hydraulic Fracturing

The hydraulic fracturing method of determining *in situ* stress is based on the relationship between the fluid pressure needed to open new fractures or reopen existing fractures, rock property, and *in situ* stress. The zone to be tested is blocked from the rest of the borehole by placing inflated rubber packers on top and bottom to block vertical escape of the hydraulic fluid (Fig. 9) (Haimson and Cornet 2003). Once the packers are inflated and the test zone is securely

Rock Field Tests, Fig. 8 Installation procedure for overcoring starting with drilling to the test level (*leftmost*), drilling a pilot hole and installing the probe inside the pilot hole, and finally overcoring around the pilot hole (*rightmost*)

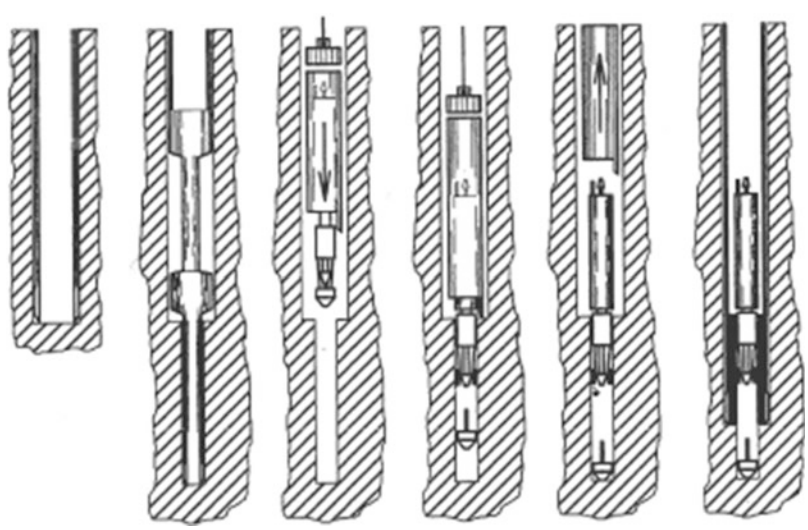

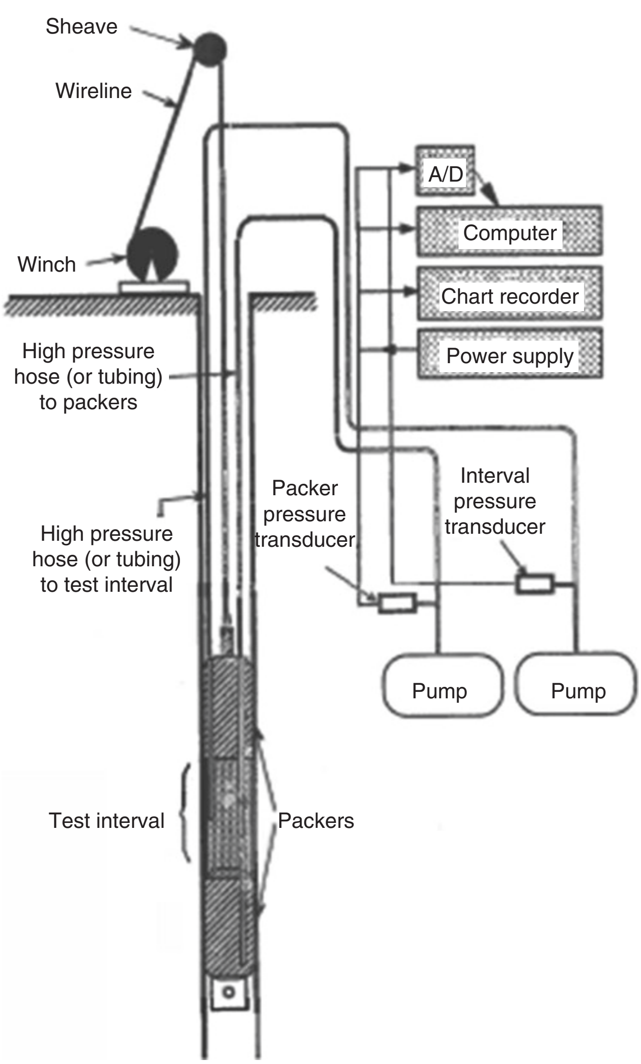

Rock Field Tests, Fig. 9 Hydraulic fracturing test equipment setup

sealed, fluid pressure is raised until a new fracture opens or a pre-existing fracture reopens. Pumping is stopped and pressure is allowed to decay. Cycles of raising pressure to the point of fracture reactivation and subsequent decay can be repeated. The fracture orientation before and after the test is captured using an impression packer or downhole geophysical methods.

Setup After selecting the zone of testing, the straddle packers are placed leaving a zone six times the borehole diameter in between. For tests relying on generating new fractures, the selected test zones should be devoid of fractures. The packers are inflated by a pump on surface or an attached pump controlled remotely. The hydraulic fluid is transferred from surface through high-pressure tubing to the test zone. Pressure gauges on surface are used to monitor real-time pressure change. Hydraulic pumps capable of generating up to 100 MPa at a flow rate of up to 10 liter/minute are needed. Oriented impression packer which has an outer layer of soft semi-cured rubber is inflated inside the zone of testing to capture the orientation of the fractures as imprints on its surface. Other geophysical tools such as borehole cameras or electrical imaging systems can be used to obtain fracture orientations from the test zone.

Testing Testing can be based on opening a new fracture or reopening existing fractures that have multiple orientations. The test zone's intrinsic permeability may be evaluated by an initial pressurized slug test. The pressure within the testing interval is raised by maintaining a constant flow rate until it reaches a point where a new fracture opened or pre-existing fractures reactivated. This pressure is termed the breakdown pressure. Pressurization can also be applied in a stepwise manner where flow rate varies and the maximum pressure for each flow rate is maintained for about 5 min. After the breakdown pressure is reached, pumping is stopped without venting the pump, and decay in pressure is monitored in real time until the fractures are closed reaching the shut-in pressure. The pump is vented after about 10 min of reaching the shut-in pressure. Cycles of repressurizing and decay may continue. The methods of *in situ* stress calculations vary depending on the test type, opening new fracture or reopening existing fractures. For cases where new fractures within 15 ° to the borehole axis, the least horizontal stress axis (σ_h) is equal to the shut-in pressure, and its direction is normal to the new hydraulically induced fracture. The maximum horizontal stress (σ_H) is given by:

$\sigma_H = T + 3(\sigma_h - P_0) - (P_b - P_0) - P_0$, where T is rock tensile strength, P_b is the breakdown pressure, and P_0 is pore pressure.

The direction of σ_h is perpendicular to σ_h.

If the test was performed on pre-existing fractures, the normal stress supported by the fracture ($\sigma_m{}^n$) is given by:

$$\sigma^m{}_n = \sigma\,(X_m)\,n_m n_m$$

where X_m is the location of the mth test, $\sigma^m{}_n$ is the measured normal stress supported by the fracture plane with normal n_m, and $\sigma\,(X_m)$ is the stress tensor at X_m. For details of calculation, the reader is referred to Haimson and Cornet (2003).

Summary

Deformability and *in situ* stress of rock masses are affected by discontinuities in rock and tectonic (paleo or active) stress. Therefore, it is necessary to devise field-testing methods that have been discussed above. Rock field tests can be performed inside underground openings, inside boreholes, and on the ground surface by applying stress using hydraulic jacks and monitoring displacements. Deformability tests inside underground openings or on ground surface include the plate test, radial jacking, and the large flat jack, whereas the downhole plate test and flexible/stiff dilatometers can be used inside a borehole.

Designing underground structures heavily relies on accurate determination of *in situ* stress in addition to rock deformability. *In situ* stress is mainly a function of depth, but tectonic forces (active or paleo) can also affect the state of stress. Three methods, the flat jack, overcoring, and hydraulic fracturing, are discussed above. The flat jack method is performed by relieving *in situ* stress by opening a slot into rock and applying induced stress to reopen the slot to its original width, thus estimating *in situ* stress. Overcoring is performed by installing a probe inside a drilled hole (pilot hole) and advancing a larger diameter core drilling around the pilot hole. As the larger hole advances, the pilot hole experiences a stress relief and deforms as a function of *in situ* stress and its mechanical properties. The principle of using hydraulic fracturing is to use the magnitude of fluid pressure injected into a section of a borehole to reopen existing fractures or create new ones as a proxy for determining *in situ* stress.

Cross-References

▶ Boreholes
▶ Deformation
▶ Extensometer
▶ Hydraulic Fracturing
▶ Jacking Test
▶ Modulus of Deformation
▶ Modulus of Elasticity
▶ Poisson's Ratio
▶ Pore Pressure
▶ Pressure
▶ Shear Modulus
▶ Young's Modulus

References

Coulson J (1979) Suggested methods for determining in situ deformability of rock. Int J Rock Mech Min Sci 16(3):195–214

Haimson B, Cornet F (2003) ISRM suggested methods for rock stress estimation—part 3: hydraulic fracturing (HF) and/or hydraulic testing of pre-existing fractures (HTPF). Int J Rock Mech Min Sci 40(7):1011–1020

Kim K, Franklin J (1987) Suggested methods for rock stress determination. Int J Rock Mech Min Sci Geomech Abstr 24(1):53–73

Ladanyi B (1987) Suggested methods for deformability determination using a flexible dilatometer. Int J Rock Mech Min Sci 24(2):123–134

Loureiro-Pinto J (1986) Suggested method for deformability determination using a large flat jack technique. Int J Rock Mech Min Sci Geomech Abstr 23(2):133–140

Sjöberg J, Christiansson R, Hudson J (2003) ISRM suggested methods for rock stress estimation—part 2: overcoring methods. Int J Rock Mech Min Sci 40(7):999–1010

Sugawara K, Obara Y (1999) Draft ISRM suggested method for in situ stress measurement using the compact conical-ended borehole overcoring (CCBO) technique. Int J Rock Mech Min Sci 36(3):307–322

Ulusay R, Hudson J (2007) The complete ISRM suggested methods for rock characterization, testing and monitoring: 1974–2006. International Society for Rock Mechanics, Commission on Testing Methods, ISRM Turkish National Group, Ankara

Yow J (1996) Suggested method for deformability determination using a stiff dilatometer. Int J Rock Mech Min Sci Geomech Abstr 23(2):13

Rock Laboratory Tests

Tatiana Rotonda[1] and Paolo Tommasi[2]
[1]Department of Structural and Geotechnical Engineering, Sapienza Università di Roma, Rome, Italy
[2]Institute for Environmental Geology and Geo-Engineering, National Research Council, Rome, Italy

Definition

Tests performed in the laboratory to determine physical or mechanical properties of intact rocks and rock discontinuities.

Introduction

Rock Laboratory tests are carried out to determine rock properties. Since rock properties are a key input for rock mechanics design in civil, mining, and petroleum engineering, this entry is mainly based on documents by the International Society for Rock Mechanics (ISRM). The ISRM Commission on Testing Methods, since 1974, has published the ISRM Suggested Methods (SMs) covering different aspects of rock mechanics. The SMs are collected in books ("yellow" book, Brown 1981; "blue" book, Ulusay and Hudson 2007; and "orange" book, Ulusay 2015). A complete list of ISRM SMs is included in the "orange" book.

The scope of the SMs is to achieve some degree of standardization of testing procedures and to consider the result of tests, wherever obtained, as reliable as possible. Currently, the ISRM SMs are considered the fundamental documents on which all national standards for rock engineering applications, where they exist, are based.

Another important collection of testing standards, covering the same field of application as the ISRM and more, are produced by the ASTM International (American Society for Testing and Materials).

Rock properties are relevant not only in rock engineering, but also when rock is used as a construction material, such as masonry blocks of new and historical buildings, dimension stones, rock armors for coastal defense, rocks for Earth-structures, etc. Depending on the particular application, tests and related properties can be quite different from those proposed for rock engineering. In this field of application, standards have been formulated by the European Committee for Standardization (EN standards), ASTM International, etc. The description of these tests is beyond the scope of the present entry apart from exceptions of general interest.

Throughout, for each test, reference is made to the standard number if it exists (e.g., ASTM D854 or EN 13383-2) or to the author (e.g., ISRM 1974) and extensively reported in the reference list. In ASTM standards, the year of release is omitted. If two standards do not differ significantly, only one reference is given. Readers who are more acquainted with a different standard, can compare it with that referenced in the text. For the ASTM standards, the reader is addressed to the latest version of the ASTM annual book (ASTM 2015).

As laboratory tests are aimed to measure rock properties and some tests determine more than one property, this entry is divided into subentries, each referring to a rock property rather than a test. This has the added advantage of grouping some tests, so that a tedious list of tests is avoided.

The content of the present entry does not presume to provide detailed instructions on the test procedures or to be exhaustive of the rock laboratory tests. The reader is invited to refer to the above-mentioned ISRM documents. Moreover, not only are rock laboratory tests numerous but the work of the ISRM Commission on Testing Methods is always in progress and further SMs on different tests or updated procedures will be published.

Preparation and Identification of Specimens

Preparation of specimens requires great care to minimize damage and irregularities that introduce artefacts in test results. For most of the tests, cylindrical specimens (ASTM D4543) are required; they are prepared usually in the laboratory by overcoring cores or drilling block samples. Ends of specimens are then squared with a diamond saw and finished through a grinding machine. Some lithotypes, very sensitive to water (e.g., swelling or slaking marls and shales), require special care in specimen preparation.

The minimum size, diameter *D*, or height *H*, of cylindrical specimens for determining strength, deformability, sound velocity, and permeability is related to the size of the largest grain in the rock, whenever possible, by a ratio of at least 10:1, in order to consider the specimen homogeneous with respect to the measured property. The same criterion should apply to the ratio between specimen diameter and macropores.

For most tests, specimens can be tested dry or fully saturated or at their natural moisture content. Drying of specimens may be carried out using a desiccator or a low temperature oven. Particular care is required especially for crystalline rocks that should not reach temperatures over 50 °C, less than the recommended temperature of 105 °C (ISRM 1979a). Otherwise, microcracking could induce damage in specimens intended for mechanical testing. Specimens are saturated in water under vacuum for a given period and kept there up to testing. Detailed procedures are described in ISRM (1979a).

Specimens should be subjected to a preliminary petrographic examination and then grouped into sets of lithologically homogeneous specimens. The homogeneity of the statistical sample is relevant in interpreting the results of the mechanical tests.

For each set, a detailed petrographic description (see e.g., ISRM 1978a) is recommended prior to testing. Macroscopic analysis should regard rock texture (including grain size and anisotropy), approximate mineralogical composition, weathering grade and defects (pores, fissures). For many applications, a microscopy analysis with polarized-light can provide useful information on microtexture, mineralogical composition, microporosity, intimate weathering, etc. Moreover, a synthetic description of each specimen is required, including angle of foliation/lamination and presence of apparent defects, as their orientation with respect to load could influence the investigated rock property.

For joint specimens, a detailed description of filling thickness/type and joint surface conditions is to be provided. The latter includes mineralogical composition, if different from the surrounding rock, weathering and shear features such as polishing and striae.

Physical Properties

Physical properties include density, porosity, water content, and water absorption of the rock material. Density can be referred to the solid phase (grain density ρ_s) and to the material at its natural water content (bulk density ρ), in dry conditions (dry density ρ_d), and in saturated conditions (saturated density ρ_{sat}).

Grain density ρ_s is calculated by dividing mass (M_s) and volume of powders, the latter being measured through the flask pycnometer (ISRM 1979a and ASTM D854) or, more conveniently, through a helium pycnometer (ASTM D5550). Measurement of grain density requires particular accuracy when the content of heavy minerals (i.e., mafic) is appreciable and variable.

Bulk and dry densities are calculated by dividing the measured total (M) or dry (M_s) mass of a cylindrical specimen, conforming to strict geometrical requirements ISRM (1979a), to its volume V, which is obtained from calliper measurements of height H and diameter D. For a good estimate of ρ_d, many specimens are required to be oven dried at low temperatures.

When cylindrical specimens cannot be easily prepared, especially in weak rocks, volumes of lumps can be measured through the buoyancy method (ISRM 1979a) or the displacement of mercury or microscopic particles (Webb 2001). The former procedure is suitable for rock materials that do not swell or slake when oven dried or immersed in water. The latter two techniques require that the rock material does not have macropores on its external surface volume.

Measurements of ρ_d and ρ_s are particularly important for the determination of porosity n, which can be calculated as $n = 1 - \rho_d/\rho_s$. Porosity could control strength and deformability of intact rocks, especially when high.

Saturated density ρ_{sat} requires measurement of the mass of the cylindrical specimen M_{sat}, saturated by de-aired water under vacuum, and is calculated as M_{sat}/V. Effective porosity (i.e., including only pores saturated by water) can thus be derived as $1 - [(\rho_{sat} - \rho_d)/\rho_w]$, where ρ_w is the density of the water.

Measurement of ρ_d, ρ, and ρ_{sat} is crucial in low-density rocks when dynamic stiffness is derived from sound velocity measurements (see section "Sound Velocity").

Water content w_n is measured as $(M - M_s)/M_s$, according to ISRM (1979a). It is worth noting that on site wax-coating of block samples yields a representative measurement of natural water content, whereas measurement on core samples is altered by water absorption during coring. It is recommended to measure natural water content only on rocks at *in-situ* conditions.

For many applications (e.g., quality assessment of aggregates for earth structures and rip-rap/armour-stone rocks), the absorption coefficient, that is, the mass of water retained by rock pores upon immersion in water divided by the dry mass of the sample, is determined (e.g., according to the EN 13383-2 standard).

Hardness and Abrasiveness

Abrasiveness is a rock property expressing the resistance to wear of the rock material. Hardness is a measure of the extent to which the surface of a solid resists a permanent change of shape obtained in different ways. Therefore, it is a "concept of material behavior" (ISRM 1979b) rather than a property.

Both abrasiveness and hardness depend on the type of minerals and their abundance, as well as on the bond strength between crystals/clasts.

Abrasiveness

The measure of abrasiveness is a major issue in such matters as:

(a) Mechanized tunnelling
(b) Rock drilling
(c) Performance of rock aggregates (from gravelly to blocky) used as armourstone or in highway/railway construction, rockfill dams, etc.

A number of SMs have been proposed to measure the effect of wear, most of which were reviewed by ISRM (1979b) but little has been done since then.

Wear of aggregate rock is usually evaluated through tests where revolving drums contain an assigned amount of rock fragments of prescribed size with or without a charge of steel balls. The former case includes the Los Angeles test (ISRM 1979b) and the Micro-Deval test (e.g., EN1097-1), whereas the latter includes the Deval and Mill Abrasion tests, no longer recommended for rock characterization. In these tests, abrasiveness is expressed as the loss in weight, that is, the weight of the material produced by abrasion passing through the 1.7-mm (or 1.6-mm) sieve, divided by the original weight.

For (a) and (b) applications, the problem can also be viewed as the ability of the rock to abrade cutting/drilling tools.

A different approach proposes to measure the wear of a steel tool simulating the wear of TBM (Tunnel Boring Machines) cutters. The Cerchar test, object of a SM by ISRM (Alber et al. 2014), measures the wear on the conical tip of a steel stylus (conforming to geometrical and hardness specifications) that moves on an irregular rock surface under a given normal force and displacement rate. The test yields the *CAI* index, which is the width of the flat wear surface in mm, multiplied by 10.

Hardness

Hardness tests included in the SMs by ISRM measure the rebound height of a standard "hammer" on a rock surface (Shore scleroscope SS, Schmidt hammer SH) or the indentation load and depth of a tool in the rock specimen. The SS and SH are nondestructive tests that differ for hammer dimension, weight, and drop mode (free fall for the SS and spring release for the SH). Rebound height can be correlated to uniaxial compressive strength (*UCS*) and Young modulus (the latter only with the SH test).

The SS (Altindag and Güney 2006) has a 5.94-mm-diameter hammer and is used on core/cubic specimens with a volume close to (and not less than) 80×10^3 mm^3. Even though many measurements on the whole specimen face are averaged, the reduced hammer diameter seems to restrict its use to rocks that are relatively homogeneous at this small scale.

The SH (Aydın 2009) has a hammer diameter of 15 mm and therefore is less sensitive to small-scale inhomogeneity. This is applicable to rocks in the *UCS* range of 20–150 MPa. Two types of SH instruments are easily available, with different impact energy: L-type (0.735 N·m) and N-type (2.207 N·m). Tests are potentially nondestructive for rocks having $UCS > 80$ MPa. Core and block samples have to conform to specific sizes and are to be clamped to a steel block of prescribed weight and shape (for core samples). The SH is also used on discontinuities to estimate compressive strength and weathering conditions of their surfaces, which affect shear strength of joints.

The indentation test (Szwedzicki 1998) is used to characterize/classify the rock with reference to hardness, especially with respect to drillability and cuttability and when only small rock lumps are available. Indentation hardness can also be correlated to *UCS* and tensile strength. The depth h of a crater produced by penetration of a conical tool, with specified geometry and steel properties, into the saw cut rock surface is recorded together with the applied load P. The indentation hardness index *IHI* [kN/mm] is calculated as P/h.

Durability

Rock durability is the resistance offered by a sample to weakening and disintegrating under repeated changes in environmental conditions. Durability is typically related to moisture and temperature changes (i.e., drying and wetting) but also to freezing, thawing and salt crystallization. This property is relevant for rockfill structures (e.g., dams, road embankments), rocks in marine environment, and building/dimension stones.

ISRM (1979a) edited a SM on the slake-durability test (Franklin and Chandra 1972), which is intended to evaluate the resistance of rock samples to slaking when subjected to cycles of drying and wetting.

The equipment consists of a drum made of a 2-mm square wire mesh which can resist temperatures up to 105 °C and can be immersed in water.

A representative sample of ten rounded (roughly spherical in shape) lumps with a mass in between 40 and 60 g is placed in the drum. After an initial drying in the oven until a constant mass is reached, the total mass of the drum plus rock lumps is measured.

The drum is then placed in rotation, through a motor drive at a constant revolution speed, partially submerged in a slaking fluid, for 10 min. The residual total mass is dried to a constant mass and then measured. A second cycle of wetting and drying is run and masses are measured. The drum mass is also measured to obtain the net mass of the rock lumps.

The second cycle slake-durability index is calculated as the net mass after the second cycle of wetting and drying over that after the initial drying. If successive cycles are operated, durability indexes can be calculated at the end of each cycle.

The slaking fluid can be tap or sea-water, or any fluid of interest for the final design.

Slake-durability is dependent on mineralogical composition. It is measured especially in rocks containing clay minerals. This test does not exclude the possibility of slaking in rocks with significant clay content subjected to prolonged wetting.

Strength of Intact Rock

Strength is one of the most significant mechanical properties of rock materials, as it is the capacity of sustaining loads, which is a major issue in all engineering applications. Rock materials fail under deviatoric stresses (uniaxial and triaxial compressive tests) and tensile stresses (direct and indirect tensile tests, point load test, beam bending tests). Weak rocks can yield under hydrostatic stresses (triaxial compressive tests), but their capacity of sustaining loads increases at increasing strains.

A common occurrence in the various tests is the decrease in strength as the size of the tested rock specimen increases. This is due primarily to the fact that the larger the specimen, the higher the probability of encountering defects, which initiate failure. As a result, special care is required in choosing specimen size.

Uniaxial Compressive Strength

The uniaxial compression test, the simplest and most common test among the laboratory tests, is mainly aimed to determine the uniaxial compressive strength (*UCS*).

The internationally recognized procedure for carrying out the test devoted to the measurement of uniaxial compressive strength and deformability is provided by ISRM (1979c). This SM was complemented by a successive SM (Fairhurst and Hudson 1999), which is devoted to determine the stress-strain behavior of intact rock in uniaxial compression. ASTM (ASTM D2938), too, recommends a standard procedure.

The measured uniaxial compressive strength is mainly intended to characterize the intact rock for engineering purposes. As *UCS* can be considered the most important index property, the test is also useful for strength classification (see "Rock Properties").

Specimens, in the shape of right circular cylinders, must conform to strict geometrical requirements.

In order to reduce the effect of restraint at the specimen ends, some precautions have been devised. Both specimen ends are confined by steel platens in the form of discs having a diameter not dissimilar to the diameter of the specimen. Test specimens are quite slender, having a height to diameter ratio (H/D) of 2.0–3.0; moreover, this high value allows the complete development of shear planes through the specimen volume.

To ensure uniform stress, specimen ends have to be flat. Moreover, a spherically seated upper loading platen is used to reduce the effect of oblique specimen ends on test results.

Unjacketed specimens are compressed, under a loading machine, parallel to their longitudinal axis in unconfined stress conditions. This loading condition leads specimen to failure under deviatoric stresses. The compressive strength is the peak stress, calculated as the maximum compressive force sustained by the specimen over its initial cross-sectional area.

As the compressive strength of rocks is quite variable, a minimum number of five specimens is recommended.

Uniaxial compressive strength is very sensitive to the water content of the specimen, similarly to other rock properties. Generally, rock strength in dry conditions is higher than that in saturated conditions. Thus, specimens have to be tested at the same water content, chosen as appropriate to the design for which the test data are required.

For a comprehensive review of the uniaxial compression test, see Hawkes and Mellor (1970).

Tensile Strength

Tensile strength is usually measured in uniaxial (direct) or diametral compression (indirect) tests on cylindrical specimens. Conceptual and experimental issues are reviewed by Mellor and Hawkes (1971) and Perras and Diederichs (2014). The testing procedure is reported in detail by ISRM (1978c).

In direct tests, the specimen ends have a height to diameter ratio (*H/D*) not lower than 2.5. Their ends are either cemented to the load platens (ISRM 1978c) or clamped through opposite devices connected to the loading machine (e.g., Gorski 1993). The latter set-up is better suited to rocks of medium to high strength. The tensile strength *TS* is equal to the axial load at failure divided by the cross-sectional area of the specimen.

In the indirect test, also known as the Brazilian test, diametral load is applied through two curvilinear loading jaws that increase the contact area, thus reducing contact stresses and hence avoiding local ruptures. The ratio *H/D* of the specimen, according to ISRM (1978c), is set to 0.5.

On the diameter plane aligned with the compressive load, the state of stress at failure, calculated from the elasticity theory in plane strain conditions, is biaxial. It can be considered to be constant along a wide zone across the specimen center (Fig. 1) and equal to (tensile stresses are negative according to the Geotechnical Engineering convention):

$$\sigma_x = -\frac{2P_{\max}}{\pi DH}; \quad \sigma_y \sim -3\sigma_x \tag{1}$$

where $P_{\max}$ is the load at failure. The Brazilian tensile strength *BTS* is equal to the absolute value of the tensile stress σ_x at failure.

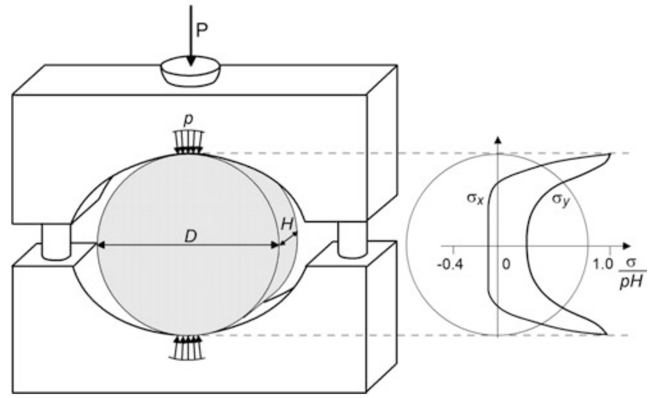

Rock Laboratory Tests, Fig. 1 Scheme of indirect (Brazilian) test. On the right, the distribution of horizontal σ_x and vertical σ_y stresses is shown, where *p* is the distributed load acting on the contact area

Since the state of stress acting in many engineering problems is multiaxial and the experimental set-up of the indirect test is much easier than that of the direct test (e.g., preparation of specimens for clamping or effectiveness of platen-specimen bonding), indirect tests are extensively performed in the practice.

On the other hand, tensile strength from indirect tests is often overestimated (Perras and Diederichs 2014) because failure develops along an imposed surface (not necessarily the weakest).

For dimension stones, a beam-bending test is commonly carried out. In the flexural strength test, the specimen, in the shape of a slab, is loaded according to a quarter-point loading configuration, along two lines, each 25% of the span from each support.

Triaxial Compressive Strength

Knowledge of the variation in strength of intact rocks under a confining state of stress is fundamental in many applications in rock engineering. The most common state of stress applied in triaxial tests is cylindrical, with the principal stresses under the condition $\sigma_1 > \sigma_2 = \sigma_3$. This is obtained through triaxial tests on cylindrical specimens, which provide data for determining the shape of the strength envelope and the parameters of the strength criterion of the intact rock. Detailed testing procedures are reported by ISRM (Kovari et al. 1983).

Specimens, which must conform to the same requirements of uniaxial tests, are tested in high-pressure cells. Figure 2 reports the schematic view of a common triaxial cell used in many laboratories (Hoek cell), where the axial and radial stress are applied independently.

The cell containing the specimen is placed under a loading machine. Typically a radial confining pressure $\sigma_r = \sigma_2 = \sigma_3$ is applied by pressurized oil acting on a thick rubber membrane surrounding the specimen (Franklin and Hoek 1970). The axial stress $\sigma_a = \sigma_1$ is equal to the axial load applied at the

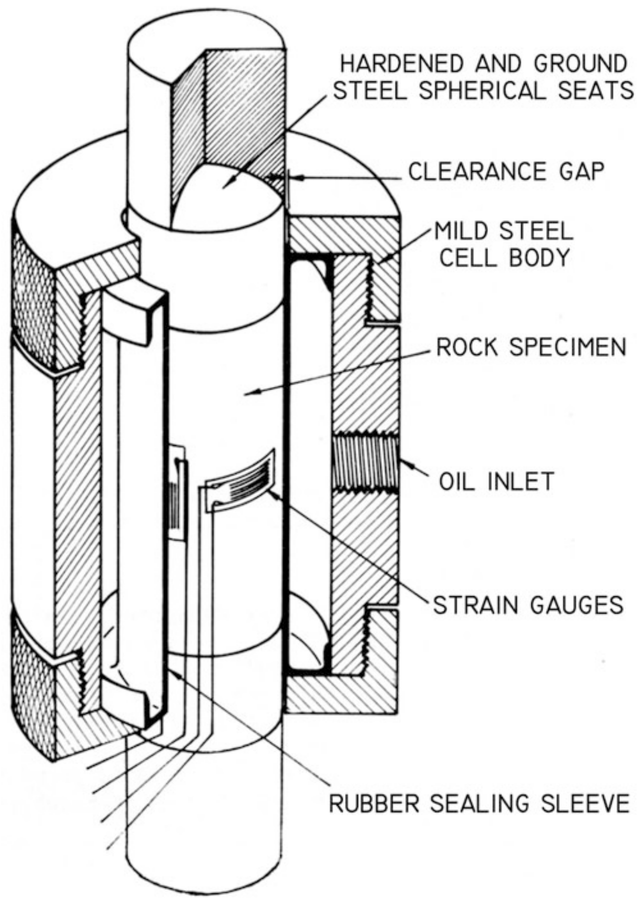

Rock Laboratory Tests, Fig. 2 Triaxial test cell (Franklin and Hoek 1970, modified)

specimen ends divided by the cross sectional area of the specimen.

The most common test is the "individual test." The specimen is initially subjected to an isotropic stress state $\sigma_r = \sigma_a = p$. Successively, a deviatoric stress is applied by increasing σ_1 until failure, which determines the peak strength ($\sigma_{1,\mathrm{peak}}$). When a stiff or a servo-controlled loading machine is used, after peak, axial strains are increased until σ_1 stabilizes; the related stress is the residual strength ($\sigma_{1,\mathrm{res}}$).

Experimental values of $\sigma_{1,\mathrm{peak}}$ (and $\sigma_{1,\mathrm{res}}$ when available) obtained at different values of the radial stress p, together with *UCS* from uniaxial tests, are plotted on the plane of the principal stresses (Fig. 3). Strength data are then enveloped with different models according to the selected failure criterion.

Multiple or continuous-failure tests can also be performed (Kovari et al. 1983) to obtain further information on strength behavior from a single specimen of brittle rock. The procedure requires that the load is applied with a stiff or a servo-controlled testing machine and that axial strain is thoroughly measured. In multiple-failure tests, a single specimen is tested at different (increasing) isotropic stresses p_i, until peak strength $\sigma_{1,\mathrm{peak},i}$ for each value of p_i is reached. Damage due to successive failures is assumed to be significantly lower than that due to the increment in strength at the higher radial stresses. Successively, the strength envelope in the desired range of confining stresses is obtained by interpolating pairs $p_i - \sigma_{1,\mathrm{peak},i}$.

In hard rocks, strains are measured through electric strain gauges glued to the specimen (Fig. 2). The positions of the strain gauges must prevent damage to electric wires connecting strain gauges to the data logger. In soft rocks, external displacement transducers mounted on the load platens can be used for the measurement of the sole axial strains. Axial displacements at the platen-specimen joint and between the spherical seat halves have to be estimated and subtracted from measured values.

Testing procedures are designed for dry specimens. Moisture effects can be accounted for by preparing sets of specimens at different moisture content and running tests at different confining pressures on each set.

Point Load Strength

The point load strength test (Franklin 1985) measures the resistance of a specimen compressed between two conical platens yielding a strength index (*PLI*) of intact rocks. The *PLI* index is used for the characterization of rock materials and for the classification of rocks, similar to the uniaxial compressive strength. The test also measures a strength anisotropy index of the rock, which is the ratio of *PLI*s obtained in the directions of the greatest and the least values. The test is not recommended for weak rocks, where *UCS* is less than approximately some tenths of MPa.

Similarly to the Brazilian test, the test induces tensile failure under the application of a compressive loading. The loading system is not required to have a high capacity, compared to that required to break a specimen under a compressive state of stress, and therefore the testing machine can be also portable (Fig. 4). This feature together with the little or no specimen preparation indicates that the test was originally intended to obtain a strength index for intact rocks directly on site (Broch and Franklin 1972).

The specimen, in the form of core, small block, or irregular lump, is broken by applying a compressive load through a pair of spherically truncated, conical platens, with specified shape and material. On core specimens, load is applied along a diameter (diametral test) or along the axis of the cylindrical specimen (axial test).

The point load strength index (*PLI*) is calculated as the maximum compressive force P_{max} over the squared "equivalent core diameter" D_e, which is the core diameter for a diametral test. For axial, block, and lump tests, the equivalent core diameter is derived from the minimum cross-sectional area of a plane through the platen contact points.

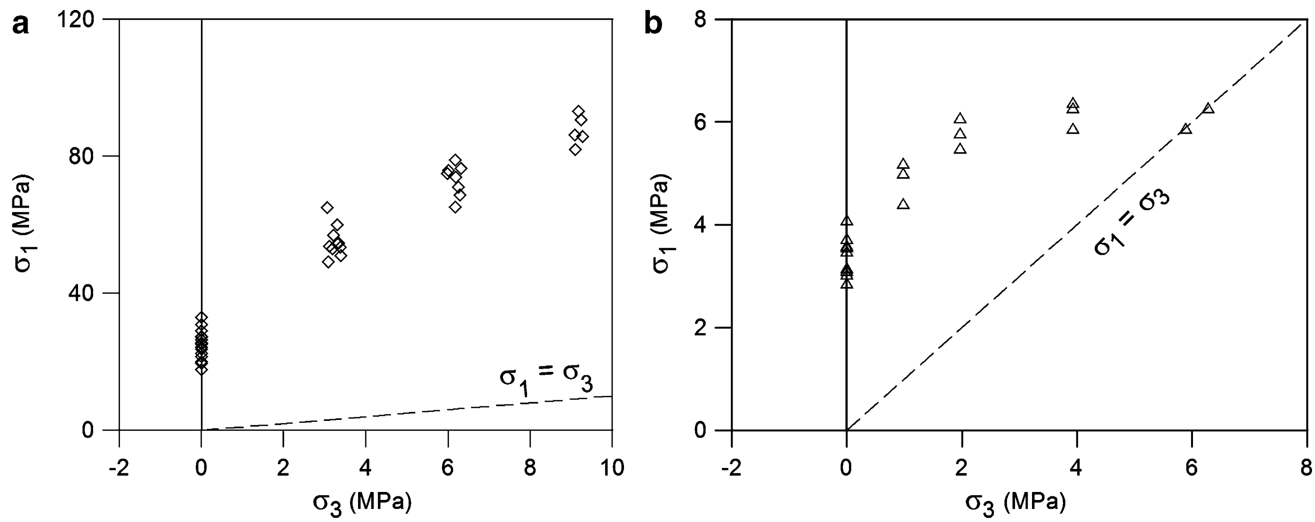

Rock Laboratory Tests, Fig. 3 Results of uniaxial and triaxial tests: (**a**) hard brittle rock; (**b**) soft rock. Note the different scales of the two plots

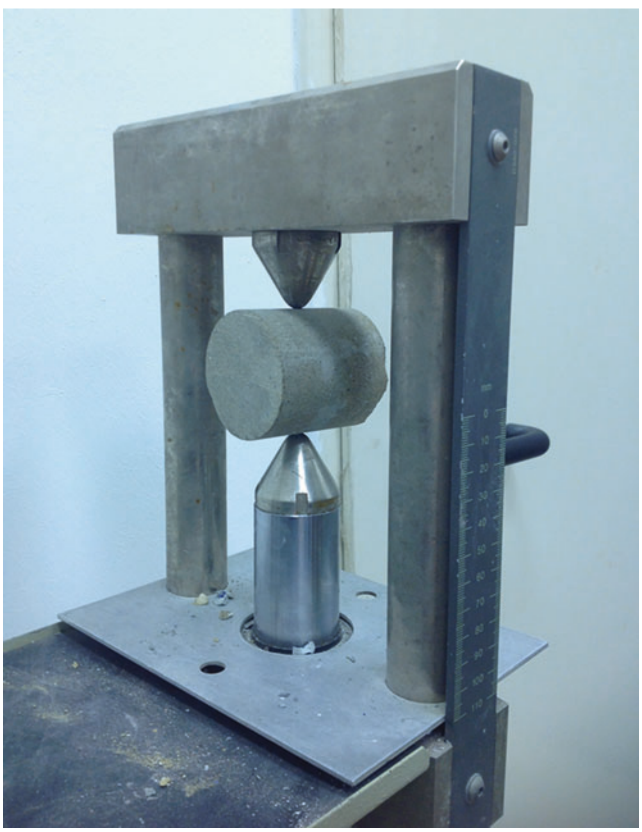

Rock Laboratory Tests, Fig. 4 Point load strength test (diametral test)

The influence of the specimen size on rock strength requires to correct the index *PLI* when the equivalent core diameter of the specimen is quite different from the conventional value of 50 mm, very similar to the widespread NX diameter (54 mm). The size-corrected strength index PLI_{50} can be calculated as:

$$PLI_{50} = \left(\frac{D_{\mathrm{e}}\,[mm]}{50}\right)^{0.45} \frac{P_{\max}}{D_{\mathrm{e}}^{2}} \tag{2}$$

Due to the possibility of testing specimens of different shapes and of testing both in the laboratory and the field, researchers have proposed using this test to estimate *UCS*, although the failure mode is different in the two tests. Many empirical relations between *UCS* and *PLI*, for different rock types, have been obtained by researchers, so that this indirect test is now widely accepted for estimating *UCS* (Broch and Franklin 1972; Bieniawski 1975). It has been found, on average, that the uniaxial compressive strength *UCS* is about 20–25 times the index *PLI*. Tests on many different types of rock, however, show that the ratio between the two strengths can vary between 15 and 50, especially for anisotropic rocks. For low to medium-strength rocks, the ratio can be significantly less than 20 (Singh et al. 2012).

Fracture Toughness

The analysis of the stress distribution in the neighborhood of a crack tip considers three basic plane modes of distortion. The modes called I and II correspond to the two deformation conditions most typically measured. Modes I and II are plane strain distortions where the points on the crack surface are displaced normal and parallel, respectively, to the plane of the crack (Fig. 5). The intensity of loading at the crack tip, for the condition of crack propagation, is quantified by the stress intensity factors. These factors, depending on the type of material, correspond to the material property called fracture toughness.

Three ISRM Suggested Methods for determining mode I static fracture toughness K_{IC} have been presented. ISRM (Franklin et al. 1988) proposes to carry out a test on chevron

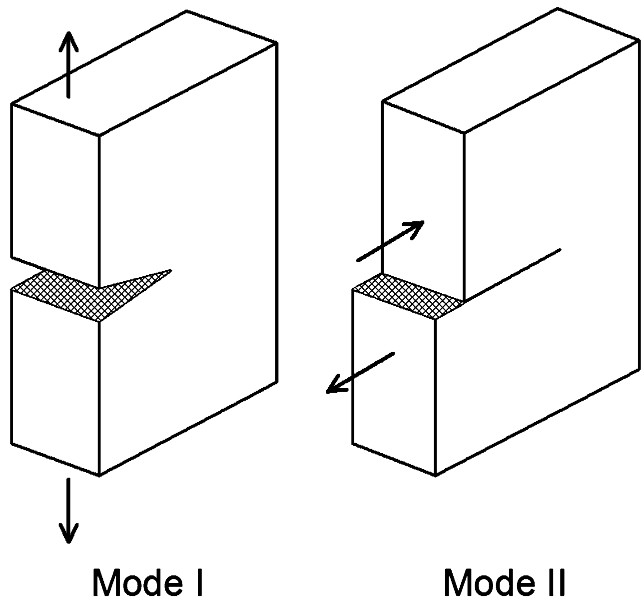

Rock Laboratory Tests, Fig. 5 Two deformation conditions of a crack

bend (CB) specimens and on short-rod (SR) specimens. Then ISRM (Fowell 1995) suggests performing the test on cracked chevron-notched Brazilian disk (CCNBD) specimens. The last SM from ISRM (Kuruppu et al. 2013) recommends that mode I static fracture toughness is determined under steady loading using semicircular bend (SCB) specimens.

The SCB specimen has the shape of a semicircular disk with a notch at the center of the planar surface along the thickness direction. Recommended values of the specimen geometry and notch length are given. The load is applied according to a three-point bend scheme through three cylindrical rollers offering no frictional resistance. Two supporting rollers are at the base of the planar surface along the thickness direction, whereas at the bottom, a loading roller is attached to the top loading plate transferring a compressive load. Mode I fracture toughness K_{IC} is determined using the observed peak load, together with some geometrical factors.

ISRM (Backers and Stephansson 2012) concerns the measurement at different confining pressures, through the Punch-Through Shear with Confining Pressure (PTS/CP) experiment, of the mode II plain strain fracture toughness K_{IIC}. The specimen is a right circular cylinder with two circular notches at both the end surfaces of the cylindrical specimen. The jacketed specimen is placed in a loading cell so that a confining pressure can be applied. An axial load is independently applied. The mode II fracture toughness may be evaluated, as a function of the confining pressure, from the peak load achieved during testing.

The measurement of the fracture toughness finds its field of application where the process of crack propagation is relevant: from the breaking ability of cutting tools to stability problems under the approach of the fracture mechanics.

Static and Dynamic Elastic Properties

Elasticity is the capacity to recover deformations when loads are applied to a body. Linearly, elastic bodies present linear relationships between applied stresses and resulting strains (Hooke's law), whose coefficients are the elastic constants. In intact rocks, these are related to the stiffness of the components (crystals or clasts) and to the presence of defects, such as pores and cracks, at the macroscopic and microscopic scale.

Behavior of intact rock is typically nonlinear when subjected to large stresses, and therefore, elastic properties are defined only for appropriately small stress ranges.

Most rocks behave as isotropic materials, whose response is independent of the orientation of the applied stress. Other rocks behave anisotropically. The most common type of anisotropy, affecting schistose and some types of sedimentary rocks, is transverse isotropy, corresponding to a full rotational symmetry around one axis. For isotropic and transversely isotropic materials, the number of independent elastic constants are 2 and 5, respectively. For other types of symmetry, the elastic constants are up to 21.

Elastic properties may be determined from static measurements of stress and strain or by dynamic methods. In the latter case, elastic wave speeds (seismic or ultrasonic velocities) are commonly measured.

Stress-Strain Curve for Intact Rock

The stress-strain curve of an intact rock specimen is obtained in uniaxial and triaxial compression tests. For general purposes, the complete curve, including pre and post-peak behavior, is determined under an uniaxial compressive load (Fairhurst and Hudson 1999; ASTM D3148).

The complete curve for rocks was previously obtained using a stiff testing machine, whereas today servo-controlled testing machines are used. The control system operates in axial strain or radial strain, measuring the feedback signal at high loop-closure rates. When rock is expected to show a ductile behavior, the control variable is the axial strain. However, the choice between axial or radial strain as the control variable has to be considered when brittle behavior is expected. The most widely used control variable is the axial strain, whereas if a reduction of the axial strain is expected after the peak, only the radial strain provides the complete stress-strain curve.

According to ISRM (Fairhurst and Hudson 1999), a more stringent rule is required in preparing specimens, whose diameter is at least 20 times the largest grain or crystal in the rock.

To measure strains over a large volume, direct contact extensometers (two axial diametrically opposed and one circumferential) are recommended. If strain gauges are used, their length should be more than ten grain/crystal diameters.

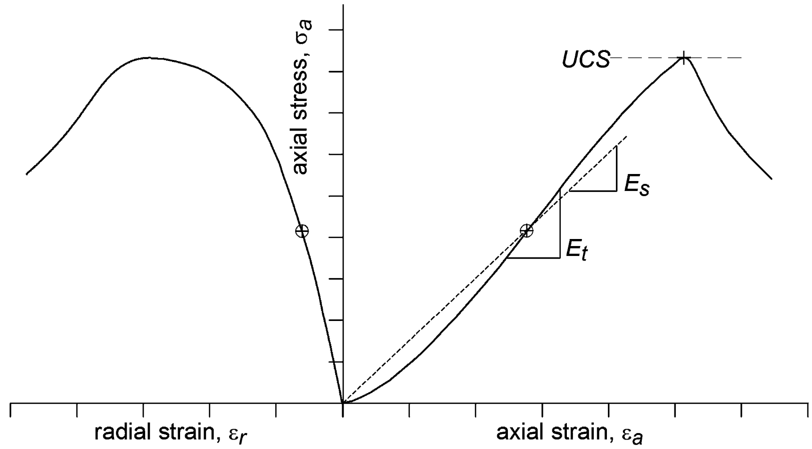

Rock Laboratory Tests, Fig. 6 Complete stress-strain curve for a rock specimen showing the compressive strength *UCS*, the tangent E_t and secant E_s Young's moduli

Specimens are subjected to a uniaxial compressive load and the test is also suited to determine *UCS*.

Uniaxial stress conditions allow calculation of the engineering elastic constants. For an isotropic rock, the elastic properties are: Young's modulus *E* of the rock, defined as the ratio of the change in axial stress to the change in axial strain, and Poisson's ratio ν, calculated as the ratio of the change in radial strain to the change in axial strain.

As the stress-strain behavior is by no means elastic, conventional Young's moduli (Fig. 6) are defined: the tangent Young's modulus E_t, generally measured at a stress level equal to 50% of the *UCS*; the secant Young's modulus E_s, generally measured from zero stress to a stress level equal to 50% of the *UCS*.

Tangent and secant of Poisson's ratios ν are calculated similarly to Young's moduli.

Sound Velocity

The ISRM SM for determining sound velocity (ISRM 1978b) proposes different approaches, which utilize waves generated at different frequency ranges.

An updated SM from ISRM (Aydın 2014) covers the high (100 kHz–2 MHz) and low (2–30 kHz) frequency ultrasonic pulse techniques. Two pulse techniques are proposed according to whether a single transducer (pulse-echo technique) or a pair of transducers (pitch-catch technique) is used. In the pitch-catch technique, the two transducers can be arranged in different positions; the most frequently used is the direct transmission configuration (transducers located at the ends of the specimen) (Fig. 7), where direction and length of the wavefront are known with greater certainty. This is also the set-up recommended by ASTM (D2845).

The test provides the velocities of compressional (longitudinal, P) and shear (transversal, S) waves in rock specimens of virtually infinite extent, compared to the wavelength of the pulse used.

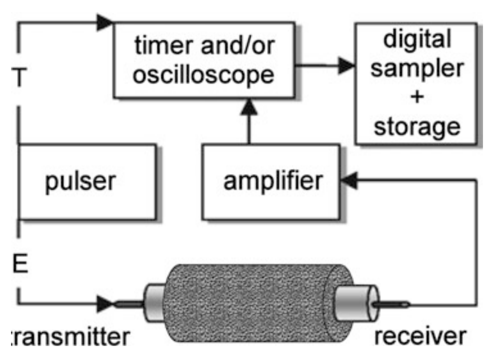

Rock Laboratory Tests, Fig. 7 Layout of the direct transmission configuration and components of the ultrasonic apparatus (E transmitter excitation signal, T timer trigger signal) (Modified from Aydın 2014)

The simplest ultrasonic apparatus includes a signal generator, an arrival timer in the form of a threshold trigger and/or an oscilloscope for visual analysis of the waveform, amplifiers and filters for signal enhancement, and a data acquisition unit (Fig. 7). The oscilloscope displays both the direct pulse and the first arrival of the transmitted pulse, thus measuring travel time. Note that as the first transmitted arrival is the P-wave, its detection is relatively easy, but the S-wave arrival may be masked by the reflections of the P-wave.

Blocks or cylinders are the typical shapes of the specimens. In the pulse transmission technique, the receiver is positioned on a plane opposite to the plane to which the transmitter is pressed through a low stress (about 10 kPa) to assure a good contact. A thin layer of coupling medium, such as high-vacuum grease or glycerin, between specimen and transducer ensure also an efficient transmission of the signal. The velocities of either P or S-waves (V_P, V_S) are calculated by dividing the transmitter-receiver distance to the measured travel time.

In isotropic rocks, the relations between the velocities V_P, V_S, and the dynamic elastic moduli (E_{dyn}, G_{dyn}, ν_{dyn}), where ρ is the specimen density, are the following:

$$
\begin{aligned}
V_{\mathrm{P}} &= \sqrt{\frac{E_{\mathrm{dyn}}}{\rho}\frac{1-v_{\mathrm{dyn}}}{(1+v_{\mathrm{dyn}})(1-2v_{\mathrm{dyn}})}} \\
V_{\mathrm{S}} &= \sqrt{\frac{G_{\mathrm{dyn}}}{\rho}} = \sqrt{\frac{1}{\rho}\frac{E_{\mathrm{dyn}}}{2(1+v_{\mathrm{dyn}})}}
\end{aligned}
\tag{3}
$$

From these, two independent dynamic elastic moduli can then be calculated.

In transversely isotropic rocks, the measurements of velocities in the directions normal and parallel to the symmetry plane help determine four of the five elastic constants.

The dynamic elastic moduli are expected to differ from the static constants.

Dynamic elastic properties are affected by the microstructural characteristic, such as size and shape distribution of voids and grains and their relative arrangements. The influence of microfissures on the elastic properties is greater for the dynamic than for the static properties, and therefore, dynamic measurements are especially suited to study the effect of microfissures. Anisotropy is also investigated through these measurements.

Strength and Stiffness of Discontinuities

Especially, when a rock mass is modelled as a discontinuous medium, strength and stiffness of discontinuities are required. Currently, scale effects are only accounted for by *in situ* direct shear tests, but their high costs have made laboratory direct shear tests of relatively small discontinuity specimens a standard practice.

Both constant-normal-load (CNL) or constant-normal-stiffness (CNS) tests can be used. The former are adequate for near-surface problems, whereas the latter are preferred when joint behavior at relevant normal stress is to be analyzed and normal stresses do not remain constant during shearing. Testing procedures of both CNL and CNS tests are described in detail by the ISRM SM (Muralha et al. 2014). More details on CNS tests can be found in Indraratna and Haque (2000). The procedure for CNL tests is also the object of the D5607 ASTM standard. In the following sections, attention is focused on CNL tests, more extensively used also at construction sites. The ISRM SM mentions the possibility of determining stiffness parameters but does not provide detailed indications.

Direct shear devices on rock discontinuities are similar to those utilized for soil laboratory tests (Fig. 8). Specimen preparation requires great care in the position of the discontinuity, which must coincide with the shear plane.

The test is subdivided into two phases: a normal load is applied and maintained constant, a shear load is then applied. Normal σ_n and shear τ stresses, as well as normal u_n and shear u_s displacements, are measured. Stresses are the average values calculated as the force over the area of overlap of the two specimen halves.

After peak strength is attained and the maximum shear displacement allowed by the apparatus is reached, further shearing cycles are performed in order to obtain ultimate shear strength (residual strength is usually reached at very large shear displacements). Direction of shearing should not be changed because strong asymmetry of asperity and formation of rock chips on the joint surface might alter original joint conditions. Typical results of shear tests on discontinuities are plotted in Fig. 9.

Usually, a single specimen gives peak strength at a unique value of the normal stress. Moreover, the ultimate strength at different values of normal stress, progressively higher, can be obtained.

Both the ISRM SM and the ASTM standard prescribe a device that applies shear displacements at a constant rate. However, a "portable" shear box is widely used, especially at construction sites, which applies shearing through load increments. When using this apparatus, an adjustable pressure maintainer for the normal load is preferable. The apparatus, specimen preparation, and testing procedure are described by Ross-Brown and Walton (1975).

R

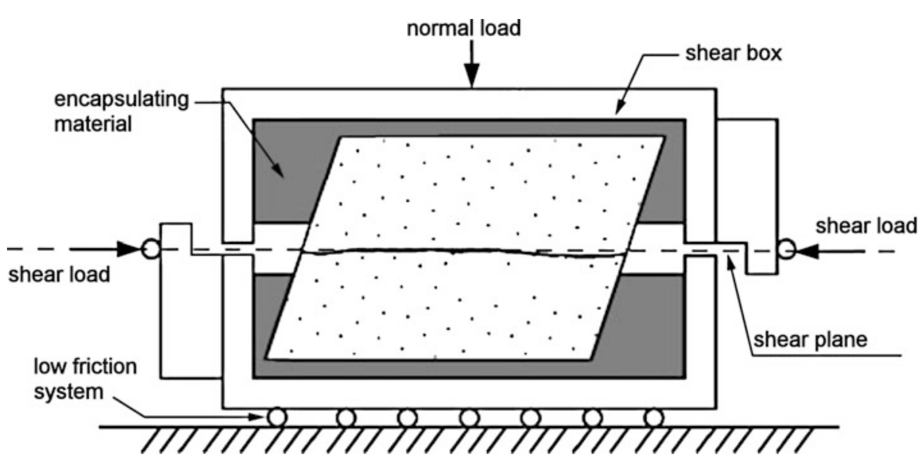

Rock Laboratory Tests, Fig. 8 Typical scheme of a shear box accommodating a core rock specimen with a joint (Modified from Muralha et al. 2014)

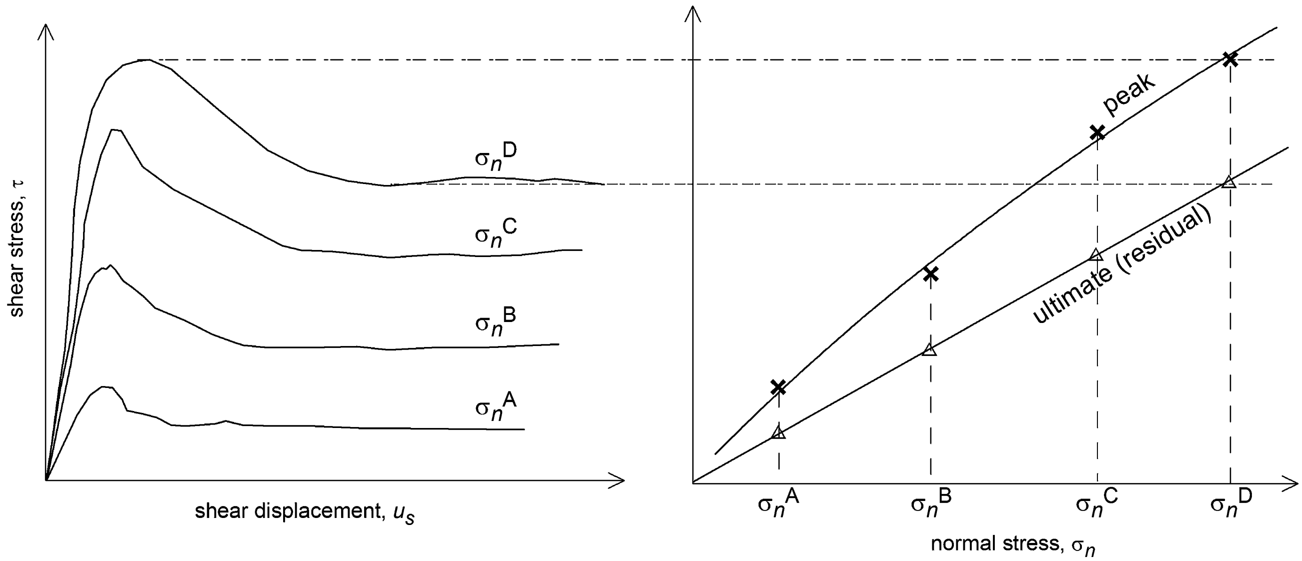

Rock Laboratory Tests, Fig. 9 Shear stress vs. shear displacement and normal stress vs. shear stress curves for CNL tests (Muralha et al. 2014, modified)

Major uncertainties in portable-box tests derive from measurements of u_n during shearing and from reconstructing the $\tau - u_s$ behavior immediately after peak. Due to rotations of the upper half of the box, determination of dilation is affected by uncertainties that can be limited by averaging measures of four transducers mounted on top of the box corners. Evidence of post-peak behavior of joints with strain-softening behavior is actually difficult.

Regardless of the device, prior to testing, roughness of the joint surface should be measured (possibly also after the test) through a 2D or 3D profilometer (Muralha et al. 2014).

The 2014 ISRM SM is mainly intended to describe tests on clean discontinuities (without infilling) with negligible tensile strength. The SM recommends that, in the case of infilling, complete dissipation of excess pore pressures due to consolidation must occur before shearing. Conversely, the ASTM standard also includes clay-filled joints, noting that the test yields the undrained shear strength. This strength should be taken with caution because it also reflects partial saturation of the infilling. A realistic estimate of the shear strength of a clay-filled joint in drained conditions requires a shear box allowing immersion of the test joint in water and adoption of shear displacement rates that are sufficiently low to allow dissipation of excess pore pressures during shearing.

Since joint tests produce scattered results, a number of specimens with comparable surface conditions retrieved from the same joint or from joints of the same set is required (5 according to ISRM). Where a limited number of joint specimens is available, peak strength at different normal stresses can be obtained from the same joint specimen with a multistage procedure (Muralha et al. 2014).

Normal stiffness can be determined through *ad hoc* normal loading tests or during the normal loading stage preceding shearing. The normal stress is measured simultaneously to the normal displacement. The resulting $\sigma_n - u_n$ curve (Fig. 10a) is nonlinear and can be used to calculate secant or tangent normal stiffness at different values of σ_n.

Similarly, tangent or secant shear stiffness and dilation can be calculated from the $\tau - u_s$ and $u_n - u_s$ curves, respectively (Fig. 10b). A detailed discussion on different aspects of joint deformability can be found in Bandis et al. (1983).

Permeability of Intact Rock

Permeability is a rock property necessary for analyzing hydro-mechanical problems. It describes the capacity of porous materials to be passed through by a fluid (“primary” permeability). In rock masses, water flow is mainly controlled by the aperture of open discontinuities. But flow through intact rock could be relevant when the *in situ* state of stress closes discontinuities, or when the primary permeability of the intact rock is high.

Primary permeability of rocks can be measured with various methods. A standard test method (ASTM D4525) is designed to measure the permeability to air of a small sample of rock, but the same procedures can be applied with a gas.

Permeability is measured by flowing air through the specimen. A permeameter arranges the cylindrical specimen, which is laterally isolated from flowing through a sleeve, allowing a directional flow from one end to the other. The end confining plugs of the permeameter could preferentially have a port for the flow of the air and another for a static

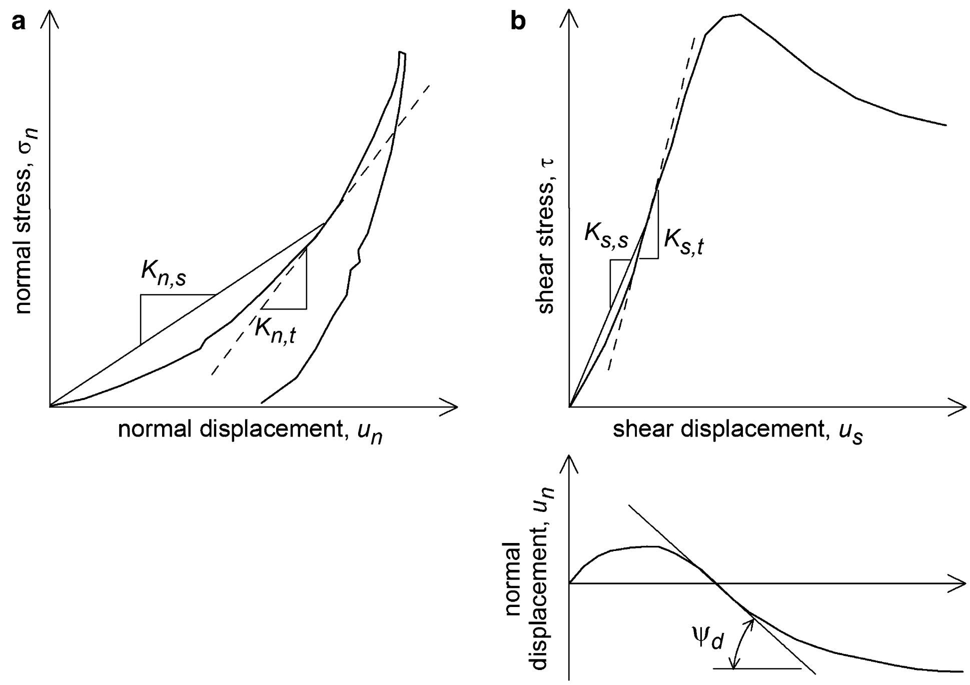

Rock Laboratory Tests, Fig. 10 Definition of normal secant $K_{n,s}$ and tangent $K_{n,t}$ stiffnesses (**a**), shear secant $K_{s,s}$ and tangent $K_{s,t}$ stiffnesses and angle of dilatancy ψ_d (**b**) of rock discontinuities

pressure line, thus permitting the specimen to be tested under loading.

The apparatus includes at least a pressure transducer for measuring the air pressure differential across the ends of the specimen and a microflowmeter for measuring the flow rate of the air.

By way of example, the Hoek cell can be used as a permeameter. It can be equipped with rigid end caps, screwed to the body of the cell; alternatively, two permeable steel platens can be used thus allowing application of a triaxial state of stress.

Three or more tests are performed on a specimen at different air pressure values, from the higher to the lower. At a fixed entrance pressure, the flow rate is measured, so that the coefficient of permeability is calculated as a function also of the air viscosity and of the geometry of the specimen.

Swelling Properties

Swelling affects both argillaceous rocks and rocks containing clay and sulfate minerals (anhydrite and gypsum). In clay-anhydrite rocks, two different swelling mechanisms are involved: the swelling of clay due to hydration of clay particles (the phenomenon lasts some days) and the swelling due to transformation of anhydrite into gypsum (long times are required). Therefore, it is important to determine the mineralogical composition of the rock in order to choose the correct testing procedure.

ISRM SM (Madsen 1999) suggests three different procedures according to their scope. All the tests should be carried out on specimens having the same density and water content as those at the time of sampling. Immediately after recovery, the samples should be carefully wrapped with a waterproof liner such as a thin plastic sheet, followed by an aluminum foil and sealed with paraffin or similar. The specimens, prepared in the laboratory avoiding the use of water, are circular discs whose thickness is 2–3 times shorter than the diameter.

The first test measures the time-dependent axial swelling stress of a radially confined rock specimen. The specimen is arranged in a rigid steel ring having the specimen diameter and is sandwiched between two porous steel plates. Then the specimen is located in a container. A loading plate, placed on top of the porous plate, transmits the load at the loading piston. The assembly is inserted in a rigid frame where the swell heave is resolved in an axial load and vice versa.

After a minimum axial stress is applied, the container is filled with water, thus covering the specimen. The axial stress and displacement are measured and recorded as a function of elapsed time. If rock contains only clay minerals, small amounts of strain can be compensated in a stepwise manner by increasing the axial force. If rock contains anhydrite minerals, strains due to the transformation of anhydrite into gypsum cannot be compensated. The test proceeds until the maximum axial force developed by the specimen can be determined or estimated.

The second test measures the axial and radial free swelling strain developed in unconfined stress conditions. The specimen is located in a container. It is confined by a thin flexible steel band, used to determine the radial swelling deformation, and is sandwiched between two porous steel plates.

After the assemblage, the container is filled with water to a level above the top of the specimen. Then the axial swelling displacement is recorded as a function of time elapsed, until a maximum (or constant) value is reached. The increase in circumference is measured at the end.

The third test measures the axial swelling strain necessary to reduce the axial swelling stress of a radially constrained rock specimen. The test is practicable only on purely argillaceous rocks. This test is quite similar to the first, but the specimen is initially loaded stepwise up to a desired axial stress (*in situ* stress conditions). The container is then filled with water to cover the top porous plate. A succession of heaves and axial load decrements are measured, until no displacement can be observed for the particular load decrement.

Summary

Laboratory testing to determine rock properties is important to various civil, mining, and petroleum engineering activities. Collected samples must be prepared and identified carefully prior to undertaking tests. Typical laboratory tests involve determination of physical properties (density, porosity, water content), hardness and abrasiveness, durability, strength (uniaxial compressive strength, tensile strength, triaxial compressive strength, point load strength, fracture toughness), static and dynamic elastic properties (stress-strain curve for intact rock, sound velocity), strength and stiffness of discontinuities, permeability of intact rock, and swelling properties.

Cross-References

▶ Abrasion
▶ Armor Stone
▶ Building Stone
▶ Clay
▶ Compression
▶ Consolidation
▶ Deformation
▶ Density
▶ Deviatoric Stress
▶ Dilatancy
▶ Durability
▶ Effective Stress
▶ Elasticity
▶ Failure Criteria
▶ Field Testing
▶ Geotechnical Engineering
▶ Hooke's Law
▶ International Society for Rock Mechanics (ISRM)
▶ Mechanical Properties
▶ Normal Stress
▶ Petrographic Analysis
▶ Poisson's Ratio
▶ Pore Pressure
▶ Rock Mechanics
▶ Rock Properties
▶ Saturation
▶ Sedimentary Rocks
▶ Shale
▶ Shear Strength
▶ Shear Stress
▶ Soil Laboratory Tests
▶ Strain
▶ Strength
▶ Stress
▶ Voids
▶ Young's Modulus

References

Alber M et al (2014) ISRM suggested method for determining the abrasivity of rock by the Cerchar abrasivity test. Rock Mech Rock Eng 47:261–266

Altindag R, Güney A (2006) ISRM suggested method for determining the Shore hardness value for rock. Int J Rock Mech Min Sci Geomech Abstr 43:19–22

ASTM (2015) Annual book of ASTM standards. American Society for Testing and Materials Annual, Philadelphia, PA, 4(04.08). Soil and Rock (I): D420 D5876

Aydın A (2009) ISRM suggested method for determination of the Schmidt hammer rebound hardness: revised version. Int J Rock Mech Min Sci Geomech Abstr 46:627–634

Aydın A (2014) Upgraded ISRM suggested method for determining sound velocity by ultrasonic pulse transmission technique. Rock Mech Rock Eng 47:255–259

Backers T, Stephansson O (2012) ISRM suggested method for the determination of mode II fracture toughness. Rock Mech Rock Eng 45:1011–1022

Bandis SC, Lumsden AC, Barton NR (1983) Fundamentals of rock joint deformation. Int J Rock Mech Min Sci Geomech Abstr 20:249–268

Bieniawski ZT (1975) The point-load test in geotechnical practice. Eng Geol 9:1–11

Broch E, Franklin JA (1972) The point-load strength test. Int J Rock Mech Min Sci Geomech Abstr 9:669–676

Brown ET (ed) (1981) Rock characterization, testing and monitoring: ISRM suggested methods. Pergamon Press, Oxford

Fairhurst CE, Hudson JA (1999) Draft ISRM suggested method for the complete stress-strain curve for intact rock in uniaxial compression. Int J Rock Mech Min Sci Geomech Abstr 36:279–289

Fowell RJ (1995) ISRM suggested method for determining mode I fracture toughness using cracked chevron notched Brazilian disc (CCNBD) specimens. Int J Rock Mech Min Sci Geomech Abstr 32:57–64

Franklin JA (1985) ISRM suggested method for determining point load strength. Int J Rock Mech Min Sci Geomech Abstr 22:51–60

Franklin JA, Chandra R (1972) The slake-durability test. Int J Rock Mech Min Sci Geomech Abstr 9:325–328

Franklin JA, Hoek E (1970) Developments in triaxial testing technique. Rock Mech 2:223–228

Franklin JA et al (1988) ISRM suggested methods for determining the fracture toughness of rock. Int J Rock Mech Min Sci Geomech Abstr 25:71–96
Gorski BP (1993) Tensile testing apparatus. U.S. Patent and Trademark Office US 5193396-A, Washington, DC
Hawkes I, Mellor M (1970) Uniaxial testing in rock mechanics laboratories. Eng Geol 4:179–285
Indraratna B, Haque A (2000) Shear behaviour of rock joints. Balkema, Rotterdam
ISRM (1978a) Suggested method for petrographic description of rocks. Int J Rock Mech Min Sci Geomech Abstr 15:41–45. In: Brown ET (ed) (1981) Rock characterization, testing and monitoring. ISRM suggested methods. Pergamon, Oxford
ISRM (1978b) Suggested methods for determining sound velocity. Int J Rock Mech Min Sci Geomech Abstr 15:53–58. In: Brown ET (ed) (1981) Rock characterization, testing and monitoring. ISRM suggested methods. Pergamon, Oxford
ISRM (1978c) Suggested methods for determining tensile strength of rock materials. Int J Rock Mech Min Sci Geomech Abstr 15:99–103. In: Brown ET (ed) (1981) Rock characterization, testing and monitoring. ISRM suggested methods. Pergamon, Oxford
ISRM (1979a) Suggested methods for determining water content, porosity, absorption and related properties and swelling and slake durability index properties. Int J Rock Mech Min Sci Geomech Abstr 16:141–156. In: Brown ET (ed) (1981) Rock characterization, testing and monitoring. ISRM suggested methods. Pergamon, Oxford
ISRM (1979b) Suggested methods for determining hardness and abrasiveness of rocks. Int J Rock Mech Min Sci Geomech Abstr 15:89–97. In: Brown ET (ed) (1981) Rock characterization, testing and monitoring. ISRM suggested methods. Pergamon, Oxford
ISRM (1979c) Suggested methods for determining the uniaxial compressive strength and deformability of rock materials. Int J Rock Mech Min Sci Geomech Abstr 16:135–140. In: Brown ET (ed) (1981) Rock characterization, testing and monitoring. ISRM suggested methods. Pergamon, Oxford
Kovari K, Tisa A, Einstein HH, Franklin JA (1983) ISRM suggested methods for determining the strength of rock materials in triaxial compression: revised version. Int J Rock Mech Min Sci Geomech Abstr 20:283–290
Kuruppu MD, Obara Y, Ayatollahi MR, Chong KP, Funatsu T (2013) ISRM suggested method for determining the mode I static fracture toughness using semi-circular bend specimen. Rock Mech Rock Eng 47:267–274
Madsen FT (1999) ISRM suggested methods for laboratory testing of swelling rocks. Int J Rock Mech Min Sci Geomech Abstr 36:291–306
Mellor M, Hawkes I (1971) Measurement of tensile strength by diametral compression of discs and annuli. Eng Geol 5:173–225
Muralha J, Grasselli G, Tatone B, Blümel M, Chryssanthakis P, Yujing J (2014) ISRM suggested method for laboratory determination of the shear strength of rock joints: revised version. Rock Mech Rock Eng 47:291–302
Perras MA, Diederichs MS (2014) A review of the tensile strength of rock: concepts and testing. Geotech Geol Eng 32:525–546
Ross-Brown DM, Walton G (1975) A portable shear box for testing rock joints. Rock Mech 7:129–153
Singh TN, Kainthola A, Venkatesh A (2012) Correlation between point load index and uniaxial compressive strength for different rock types. Rock Mech Rock Eng 45:259–264
Szwedzicki T (1998) Draft ISRM suggested method for determining the indentation hardness index of rock materials. Int J Rock Mech Min Sci Geomech Abstr 35:831–835
Ulusay R (2015) The ISRM suggested methods for rock characterization, testing and monitoring: 2007–2014. Springer, Cham
Ulusay R, Hudson JA (2007) The complete ISRM suggested methods for rock characterization, testing and monitoring: 1974–2006. ISRM Turkish National Group, Ankara
Webb A (2001) Volume and density determinations for particle technologists. Micromeritics Instrument Corp. http://wvm.micromeritics.com/Repository/Files/Volume%20_and_density_determinations_for_particle_technologists.pdf. Accessed 10 Sept 2016

Rock Mass Classification

William H. Godwin
Carmel, CA, USA

Synonyms

Ground classification; Rock strength classification

Definition

A classification system that captures all relevant information on the composition and characteristics of a rock mass to provide initial estimates of support requirements and to provide estimates of the strength and deformation properties of the rock mass.

Characteristics

One of the earliest classification systems for rock was developed by Terzaghi (1946). The classification system was developed as a method of classifying rock masses and evaluating rock loads based on qualitative assessments.

The rock-quality designation (RQD) developed by Dr. Don U. Deere (Deere and Deere 1988) is a method of logging sound drilled rock core to calculate and quantify the percentage of "good" rock in a core run. RQD is a quantitative method of evaluating rock quality and is widely used as one of the parameters in other more numerical rock classification systems.

$$\mathrm{RQD} = \text{Sum of length of core pieces 4 inches or greater} \;/\; \text{Total length of core run} \times 100\%$$

The Rock Mass Rating (RMR) system developed by Bieniawski (1989) and the Quality Index (Q) updated by Barton (2002) provide overall comprehensive indices of

R

rock mass quality for the design and construction of excavations in rock.

The RMR system incorporates rock mass data regarding rock strength, RQD, discontinuity spacing, discontinuity condition, groundwater, and an adjustment for discontinuity orientation with respect to the excavation. These parameters are assigned numeric values based on their conditions and the summation of the numeric values for all the parameters is the rating of the rock mass.

The Quality Index (Q) uses parameters similar to the RMR system to evaluate the stability that can be expected for excavation within the rock mass. One of the differences between RMR and Q lies in the assessment of the *in situ* stress state in the Q system by use of the “Stress Reduction Factor.” The numerical value of the index Q varies on a logarithmic scale from 0.001 to a maximum of 1000 and is estimated from the following expression:

$$Q = (RQD/Jn) \times (Jr/Ja) \times (Jw/SRF),$$

where

Jn = joint set number
Jr = joint roughness number
Ja = joint alteration number
Jw = joint water reduction factor
SRF = stress reduction factor

The general relationship between Q and rock quality is provided in Table 1 below.

A new classification system, termed the Geotechnical Strength Index or GSI, Marinos et al. (2006), captures variability in geologic materials associated with faulting and extreme deformation associated with tunnels in rock. It is meant to provide reliable input data related to rock-mass properties required as input for numerical analysis or closed form solutions for designing tunnels.

Rock Mass Classification, Table 1 Relationship between Q and rock quality values

Q	Rock quality
400–1000	Exceptionally good
100–400	Extremely good
40–100	Very good
10–40	Good
4.0–10	Fair
1.0–4.0	Poor
0.1–1.0	Very poor
0.01–0.1	Extremely poor
0.001–0.01	Exceptionally poor

Cross-References

► Engineering Geological Maps
► Site Investigation

References

Barton NR (2002) Some new Q-value correlations to assist in site characterization and tunnel design. Int J Rock Mech Min Sci 39(2):185–216
Bieniawski ZT (1989) Engineering rock mass classifications: a complete manual for engineers and geologists in mining, civil, and petroleum engineering. Wiley, New York, p 251
Deere DU, Deere DW (1988) The rock quality designation (RQD), index in practice. In: Kirkaldie L (ed) Rock classification systems for engineering purposes. ASTM, Philadelphia. 1984
Marinos P, Hoek E, Marinos V (2006) Variability of the engineering properties of rock masses quantified by the geological strength index: the case of ophiolites with special emphasis on tunneling. Bull Eng Geol Env 65(2):129–142
Terzaghi K (1946) Rock defects and loads on tunnel supports. In: Proctor RV, White T (eds) Rock engineering with steel support. Commercial Shearing, Youngstown, pp 15–99

Rock Mechanics

D. Jean Hutchinson and Mark Diederichs
Department of Geological Sciences and Geological Engineering, Queen’s University, Kingston, ON, Canada

Definition

Rock mechanics is a subdiscipline within applied geology, geological engineering, and mining engineering focused on the physical mechanics of rock with applications in both dynamic structural geology and in engineering.

An understanding of rock behavior requires proficiency in engineering mechanics, material properties and physics, and engineering geology, including structural geology. Rock mechanics may be considered with soil mechanics as end members of geomechanics.

Rock is a natural material with substantial ranges in material properties: strong or weak, stiff or highly deformable, ductile or brittle, and durable to easily disaggregated and weathered. In the lower end of the strength range, rock will approach soil-like behavior. Physical strength is highly variable across rock types, ranging from soil-like values (less than 1 MPa for uniaxial strength) for weak mudstones to uniaxial compression strength up to 500 MPa for fine-grained basalt, for example (Brady and Brown 2005; Hoek 2006). Likewise, rock stiffness varies across at least two orders of magnitude (up to 100 GPa for poly-mineralic rocks and higher for single-mineral crystals or glass).

Rock Mechanics, Fig. 1 Silty limestone (micrite) rock mass exposed along a highway road cut, including intact rock blocks separated by discontinuities (subhorizontal bedding planes, two steeply dipping joint sets, and a few additional randomly oriented joints) (Photo by D. Jean Hutchinson)

Rock generally has limited void space between the mineral particles, and therefore can be of high unit weight and very low porosity and permeability, or it may have voids created at the time of formation of the rock (particularly for clastic sedimentary or clay-rich rocks, or vesicular basalt or scoria) or created subsequently by preferential weathering of various mineral components. Permeability in most rock masses is created by the presence of discontinuities separating blocks or fragments of intact rock (Fig. 1). The highest permeability rocks are generally those where water flow has dissolved mineral constituents creating macroscale, interconnected pathways, such as in karstic limestone.

The range of engineering properties depends on the origin of the rock material, whether sedimentary, igneous, or metamorphic, and upon the environment in which the rocks have existed. Engineering analysis of rock depends upon whether it will be used as a construction material or be used *in situ* for excavations at the ground surface and underground, or for foundation support. In some cases, whether due to application of high stress to rock *in situ* or the presence of weak rock, excavations may be subject to creep closure or violent rockbursting behavior.

In situ rock behavior is controlled by the solid material and the presence and orientations of discontinuities, including joints, shear zones, and faults – together these components make up the rockmass. The expected strength of the rockmass depends upon the spacing (frequency) and strength and stiffness characteristics of the discontinuities, the strength of the rock between the discontinuities, and the magnitude and orientation of applied stress. The response of the rockmass to excavation or foundation loading depends on the scale of the engineering work relative to the frequency of the discontinuities – a larger excavation in a given rockmass will be subject to more substantial deformation and potential for failure than a smaller excavation.

Rock mechanics, as part of dynamic structural geology, includes the physics of brittle fracture, strain weakening and ductile yield, as well as the rheology of "flow" and continuum deformation (in a geological context). It includes consideration of the relationship between stress and strain across all yield modes.

Rock mechanics, as part of geotechnical engineering and rock engineering, includes the considerations described above, and also involves acquiring and interpreting field, instrumentation, and laboratory data on soil, rock, and groundwater conditions; evaluating distribution of stresses, including the response of the rockmass within foundations to the pressure imposed; analyzing seepage and drainage, and slope stability and stabilization measures; and understanding the effect of creating underground excavations on the rockmass, including the generation of rockmass damage depending on the excavation method and rate, and the use of rock support systems. For underground excavations, engineering analysis is required to control the behavior of the rockmass. This may require limiting deformation (for example, in water supply tunnels, or large open pit slopes), preventing rockmass loss or failure into the excavation (for example, in caverns for hydropower generation or mining stopes), or minimizing the damage to control rockmass permeability (for nuclear waste disposal). Important considerations in design with rock are the expected design life for the excavation, whether public access will be allowed, whether enhanced drainage may improve stability (for large natural rock slides; Clague and Stead 2012), and whether rockmass support will be subject to deterioration by corrosion, creep, water inflow, and/or high stress levels. Long-term design considerations include review of support and drainage-system performance and rehabilitation requirements, the potential for eventual excavation collapse to induce subsidence that may lead to distress in the ground surface or damage to adjacent infrastructure.

In addition to theoretical aspects of strength and deformation resulting from load combinations, rock mechanics also involves knowledge of construction methods, geology, and hydrogeology. Rock strength can be tested in the laboratory considering both the strength of the intact rock over a range of confining stresses and the strength of the discontinuities. *In situ* testing, considering both the influence of the intact rock and discontinuities on the rockmass response, can be completed, but generally such testing tends to be restricted to a relatively small volume of the rockmass due to the scale of most engineering works in rock. The influence on rock mass behavior of the discontinuities can be estimated with rockmass classification systems, based on empirical data collected from excavations or slopes, providing estimates of stand-up times for unsupported tunnels and requirements for effective tunnel support. Analysis of expected rock response is increasingly supported by numerical simulations, which are initially developed considering site investigation data and the type and shape of opening to be excavated, and calibrated using monitoring data as the excavation proceeds. In this case, the observations of rock response in early stages of engineering projects in rock should be used to guide subsequent excavations, whether at the same time or on future projects.

The geological origins and history of rock formations are essential considerations, because materials with substantially different engineering characteristics are often found within larger-scale excavations, particularly tunnels or large slopes. Data may be collected from previous experience with construction in these materials, and from mapping and analysis of surface exposures and drill hole core of the same or similar rock types with similar types of joints and faults.

Rock mechanics provides the analytical tools to evaluate stresses, strains, and deformations in rock materials, depending upon the excavation method and support systems installed. It is a subdiscipline of geological engineering, mining engineering, and geotechnical engineering within civil engineering that typically requires collaboration with professionals with expertise in geology, engineering geology, and hydrogeology.

Cross-References

- ▶ Borehole Investigations
- ▶ Classification of Rocks
- ▶ Dewatering
- ▶ Effective Stress
- ▶ Excavation
- ▶ Foundations
- ▶ Geotechnical Engineering
- ▶ Groundwater
- ▶ Instrumentation
- ▶ Mass Movement
- ▶ Rock Laboratory Tests
- ▶ Rock Properties
- ▶ Shear Strength
- ▶ Shear Stress
- ▶ Site Investigation
- ▶ Subsurface Exploration

References

Brady BHG, Brown ET (2005) Rock mechanics for underground mining. Springer Science eBook. ISBN:1-4020-2116-X. https://miningandblasting.files.wordpress.com/2009/09/rock-mechanics_for-underground-mining.pdf. Accessed 23 Jan 2018

Clague JJ, Stead D (ed) (2012) Landslides: types, mechanisms and modeling. Cambridge University Press, New York. ISBN:978-1-107-00206-7

Hoek E (2006) Practical rock engineering. RocScience website, Hoek's Corner online book, 341 p. https://www.rocscience.com/documents/hoek/corner/Practical-Rock-Engineering-Full-Text.pdf. Accessed 23 Jan 2018

Rock Properties

Abdul Shakoor
Department of Geology, Kent State University, Kent, OH, USA

Definition

Engineering properties of rocks are the indices used for comparing the engineering behavior of rocks tested under similar conditions, following standardized procedures.

Introduction

Rocks are significant in engineering construction because (West 1995):

1. They are important building materials with numerous applications in engineering construction.
2. Many engineering structures are built directly on rock, and their stability depends on the stability and quality of the foundation rock.

The engineering properties of rocks determine their behavior as construction materials and as structural foundations. There are two classes of rock properties: (a) intact rock properties and (b) rock mass properties. An intact rock contains no visible discontinuities (joints, bedding, foliation planes, etc.) whereas a rock mass is interrupted by discontinuities. Properties of intact rock are measured on small samples in the laboratory, whereas rock mass properties, being controlled by planes of weakness in the rock, are evaluated by studying large outcrops in the field.

Intact Rock Properties

Properties used for characterizing intact rock as a building material include: specific gravity, absorption, porosity, degree of saturation, unit weight (density), unconfined compressive strength, tensile strength, shear strength, Young's modulus, Poisson's ratio, and durability (Johnson and De Graff 1988; West 1995).

Specific Gravity, Absorption, Porosity, Degree of Saturation, and Unit Weight

Specific gravity is the ratio of the weight in air of a given volume of rock to the weight of an equal volume of water. In order to account for the presence of pores in a rock, the American Society for Testing and Materials (ASTM) (ASTM 2013) recommends using three different types of specific gravity in engineering practice. The laboratory test for determining specific gravity and absorption [ASTM D6473-10 (ASTM 2013); International Society for Rock Mechanics (ISRM) 2007)] requires that the rock specimen be weighed in air in a dry condition, weighed in air in a saturated condition, and weighed in water in a saturated condition. From these data, specific gravity and absorption values are obtained as follows:

$$\text{Bulk specific gravity } (\text{Sp G}_d) = A/B - C \tag{1}$$

$$\text{Bulk specific gravity } (\text{Sp G}_s) = B/B - C \tag{2}$$

(saturated, surface dried)

$$\text{Apparent specific gravity } (\text{Sp G}_a) = A/A - C \tag{3}$$

$$\text{Absorption} = \{(B - A)/A\}(100) \tag{4}$$

where:

A = mass of rock in air, oven dried for 24 h
B = mass of rock in air, saturated, surface dried
C = mass of rock in water, saturated

Porosity is the ratio of the volume of voids (Vv) to the total volume (Vt) of a rock, expressed as a percentage. It can be determined by using phase relations, as described in most soil mechanics textbooks. Porosity can range from 0.1% for dense rocks like diabase and quartzite to 5–25% for sandstone, and even higher for volcanic rocks like tuff (Gonzalez de Vallejo and Ferrer 2011).

Degree of Saturation is the ratio of the volume of water (Vw) to the volume of voids in a rock, expressed as a percentage. It can also be determined by using phase relations and ranges from 0% for completely dry rock to 100% for completely saturated rock.

The unit weight, or density, of rock is defined as the mass per unit volume and can be obtained by multiplying the bulk specific gravity by the density of water (1 g/cm^3; 1 Mg/m^3) or by dividing the mass by volume of a core sample. The general range of unit weight is 20–30 kN/m^3 (Gonzalez de Vallejo and Ferrer 2011).

Density, absorption, and degree of saturation show strong correlations with compressive strength (Shakoor and Bonelli 1991; Shakoor and Barefield 2009). Rocks with higher specific gravity and density and lower percent absorption, porosity, and degree of saturation have more desirable engineering properties.

Rock Strength

Depending upon the nature of applied stresses, rock strength can be described as unconfined compressive strength, tensile strength, and shear strength.

Unconfined Compressive Strength

The unconfined or uniaxial compressive strength is one of the most commonly used properties of rock (Bieniawski 1989). Either ASTM method D7012-13 (ASTM 2013) or ISRM method (ISRM 2007) is used to determine unconfined compressive strength. These test methods involve failing an NX-size (54 mm) core sample, with a length to diameter ratio of 2.0–2.5, under the application of vertical load. The strength is obtained by:

$$\sigma_c = P/A \tag{5}$$

where:

σ_c = unconfined compressive strength
P = failure load
A = cross-sectional area

Unconfined compressive strength of intact rock ranges from less than 1 MPa for weak rocks (shales, claystones, mudstones, etc.) to more than 350 MPa for rocks like granite, basalt, and quartzite (Johnson and De Graff 1988; West 1995; Gonzales de Vallejo and Ferrer 2011).

Table 1 shows the typical ranges of compressive strength for selected rock types. The large variation in strength within the same rock type is due to variation in petrographic characteristics. Compressive strength is greatly influenced by the texture, mineral composition, type and amount of cement, and degree of weathering (Johnson and De Graff 1988; Shakoor and Bonelli 1991). Among the igneous rocks, basalt and diabase exhibit higher average values of compressive strength than do granites because of their finer grain size and greater degree of grain interlocking. Also, the higher strength of quartzite can be attributed to a higher degree of grain interlocking. The high strength sandstone is characterized by a smaller percentage of straight grain-to-grain contacts (Shakoor and Bonelli 1991) and a higher percentage of siliceous cement.

Rock Properties, Table 1 Typical ranges of compressive and tensile strength values for selected rock types

Rock type	Compressive strength (MPa)	Tensile strength (MPa)
Granite	75–300	10–25
Diabase	100–350	15–55
Basalt	100–300	10–30
Quartzite	175–350	10–30
Sandstone	20–235	5–25
Shale/claystone/ mudstone	5–125	1–20
Limestone	50–250	5–30
Marble	100–200	10–20

Source: Farmer 1983; Johnson and De Graff 1988; West 1995; Gonzales de Vallejo and Ferrer 2011

The ASTM method D7012-13 for measuring compressive strength is time consuming and core samples required for the test are not always available. For this reason, several empirical tests for estimating compressive strength have been developed, of which point load and Schmidt hammer tests are the most frequently used. The point load test consists of placing an unprepared core sample or an irregular lump of rock between two conical platens and applying compressive load until the sample fails in tension (Broch and Franklin 1972; ASTM method D5731-08 (ASTM 2013); ISRM 2007). The three variations of the point load test include: (i) testing an irregular sample, (ii) testing a core sample axially, and (iii) testing a core sample diametrically. From the failure load P, and platen separation D, as indicated by the apparatus, the point load index I_s is determined as follows:

$$I_s = P/D^2 \qquad (6)$$

Unconfined compressive strength of a rock is related linearly to point load index by the following equation:

$$\sigma_c = k(I_s) \qquad (7)$$

The value of k depends on core diameter. For NX-size (54 mm) samples of most hard rocks, k is approximately 24 (Broch and Franklin 1972; Bieniawski 1989; Cargill and Shakoor 1990). For weaker rocks (shale, claystone, mudstone), the k values are significantly less (11–16). For irregular samples, Broch and Franklin (1972) have developed correction charts that can be used to normalize I_s values to 50 mm standard size.

The Schmidt hammer (Type L) is a portable device that can be used to estimate compressive strength in both the laboratory and the field. The hammer is pressed against the rock and a rebound number (N) is noted from the scale provided on the hammer sleeve. The rebound number has been correlated previously with unconfined compressive strength as shown in Fig. 1. The Schmidt hammer is considered to be a less reliable estimator of compressive strength than the point load test (Johnson and De Graff 1988; Cargill and Shakoor 1990).

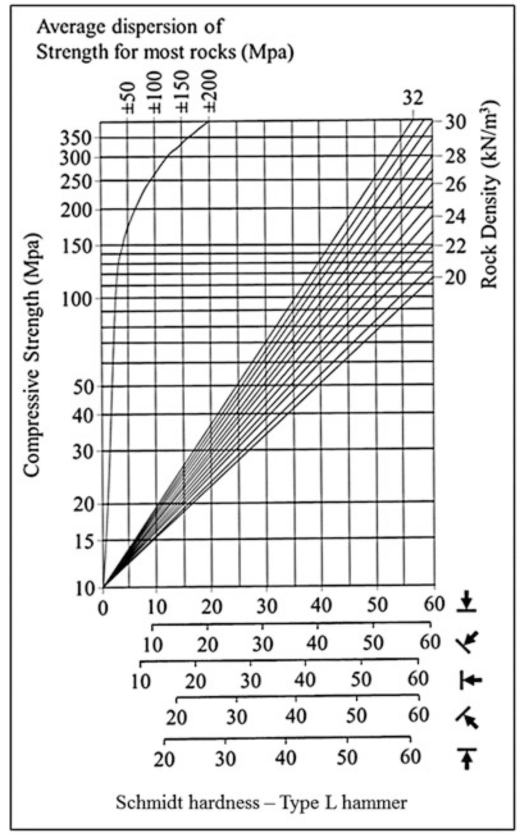

Rock Properties, Fig. 1 Relationship between Schmidt hammer rebound number and unconfined compressive strength (After Deere and Miller 1966)

Other indices of compressive strength include shore hardness, indentation hardness, and block punch strength index. Test procedures for determining these indices can be found in ISRM suggested methods (ISRM 2007).

Tensile Strength

The tensile strength of rocks is important in the design of roof spans for underground excavations or in situations where rocks are subjected to bending stresses. On average, tensile strength of rocks is approximately 10% of their compressive strength (West 1995), the range being 5–15%. Table 1 shows the ranges of tensile strength for some common rocks. The tensile strength can be determined either directly by applying a tensile load on a core sample, referred to as the direct pull test (ASTM D 2936-08 (ASTM 2013); ISRM 2007), or indirectly by applying a compressive stress on a disk-shaped sample and failing it in tension, called the Brazilian test (ASTM D3967-08 (ASTM 2013); ISRM 2007). Tensile strength is influenced by the same geologic parameters as compressive strength.

Shear Strength

Shear strength of rocks is evaluated by determining the shear strength parameters (c and φ). This is accomplished by establishing the Mohr envelope by either performing a direct shear test (ASTM D5607-08; ASTM 2013) or a triaxial test (ASTM D 2664-08; ASTM 2013; ISRM 2007). The cohesion value for rocks can range from less than 1 MPa for some weak argillaceous rocks (Hajdarwish et al. 2013) to as high as 48 MPa for stronger rocks like granite (West 1995), whereas friction angle can range from 10° for weak argillaceous rocks (Hajdarwish et al. 2013) to 70° or more for strong quartz-rich rocks (West 1995). Shear strength parameters are controlled by the same textural and mineralogical characteristics that influence compressive and tensile strengths, such as grain size, grain shape, degree of grain interlocking, type and amount of cement, percentage of clay size material, percentage of quartz, etc.

Elastic Properties

Elastic properties indicate deformational behavior of rocks. A cylindrical sample subjected to axial compression will decrease in length and increase in diameter. Upon removal of compressive force, some, but not all, of the deformation may be recovered. The recoverable deformation is the elastic deformation and the nonrecoverable deformation is the plastic deformation. In engineering, deformation is expressed as strain, the ratio of the change in dimension or volume to the original dimension or volume, expressed as a percentage. Figure 2 shows a typical stress-strain curve for rocks and elastic and plastic deformations. The two elastic properties that are used most frequently to evaluate the deformational behavior of rocks are Young's modulus and Poisson's ratio. Methods for determining these two properties have been standardized by ASTM (ASTM D7012-13; ASTM 2013) and ISRM (2007)

Young's Modulus

Young's modulus or modulus of elasticity (E) is the ratio of stress to strain:

$$E = \sigma/\varepsilon = (P/A)/(\Delta L/L) \tag{8}$$

where:

σ = stress
ε = strain
P = applied load in kg or Newtons
A = cross sectional are in cm^2
ΔL = change in length in cm
L = initial length in cm

E is the slope of the stress-strain curve shown in Fig. 2. Since the slope is variable, three different E values are shown in Fig. 2. These include the initial tangent modulus (E_i), the secant modulus at any point selected on the curve (E_s), and tangent modulus at any point selected on the curve (E_t). In engineering practice, E_{t50} and E_{s50}, tangent and secant modulus at 50% of the failure load, respectively, are frequently used. Young's modulus is a very valuable property for estimating the anticipated deformation under given loading conditions. In general, rocks with higher compressive strength also exhibit higher E values (Shakoor and Bonelli 1991) because both properties are controlled by the same petrographic characteristics. Average E values can range from 13.7 GPa for shales and claystones to 79.9 GPa for quartzites (Johnson and De Graff 1988; West 1995).

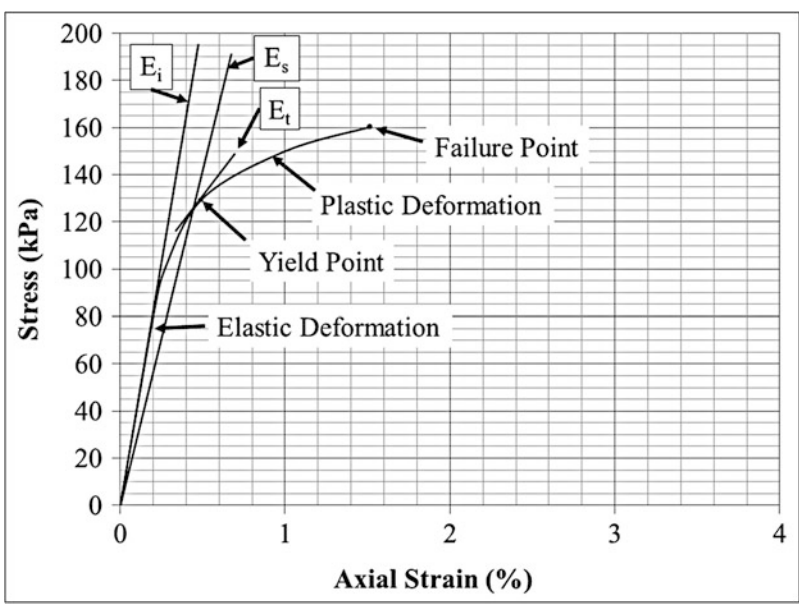

Rock Properties, Fig. 2 A typical stress-strain curve for rocks showing elastic versus plastic deformation and the three types of moduli of elasticity

R

Poisson's Ratio

Poisson's ratio (ν) compares lateral extension to vertical compression.

$$\nu = \text{lateral strain}/\text{vertical strain} = (\Delta D/\mathrm{D})/(\Delta L/\mathrm{L}) \quad (9)$$

where:

ΔD = change in diameter or lateral dimension in cm
D = initial diameter or lateral dimension in cm
ΔL = change in length in cm
L = initial length in cm

A perfectly elastic material has a Poisson's ratio of 0.33. The Poisson's ratio for rocks can range from 0.1 to 0.5 with values for most rocks falling between 0.15 and 0.25 (Johnson and De Graff 1988; West 1995).

Durability

Durability is the resistance of a rock to climatic changes such as heating and cooling, wetting and drying, and freezing and thawing, that is, to weathering and disintegration. Shale, especially clay shale, claystone, and mudstone frequently exhibit nondurable behavior upon wetting and drying. Several durability evaluation tests have been developed since the early 1970s, the most important of these being the slake durability index test developed by Franklin and Chandra (1972). Both ASTM (D4644-08; ASTM 2013) and ISRM (2007) have standardized the procedure for slake durability testing. The test consists of placing an oven-dried sample, consisting of 10–12 pieces, each weighing 40–60 g with a total weight of 450–500 g, in a 2 mm-meshed drum and rotating the drum through water for 10 min at a fixed speed. The sample that remains in the drum is oven-dried and weighed. The slake durability index (Id) is calculated as the ratio of the weight of the remaining sample to the initial weight, multiplied by 100. Repeating the test on the remaining sample provides the second-cycle slake durability index (Id_2). Id_2 can range from 0% for some claystone to nearly 100% for some silty shale or siltstone. Id_2 is frequently used as the standard for classification purposes.

Engineering Classification of Intact Rock

Classifications of intact rock, based on compressive strength and modulus ratio (Young's modulus/compressive strength), developed by Deere and Miller (1966), are given in Tables 2 and 3, respectively. The very high strength category in Table 2 includes rocks like basalt, diabase, and quartzite. Other igneous rocks, limestone, dolomite, and well-cemented sandstone are included in the high strength category, whereas schist and silty shale belong to the medium strength category. Clay shale, claystone, and mudstone fall in the low to very low strength categories. Since modulus ratio takes into account both the compressive strength and elastic modulus, it is considered to be more reflective of the engineering behavior of rocks than compressive strength alone. Marble has a distinctly high modulus ratio and that explains the historical use of marble as an excellent building stone. Granite, diabase, limestone, and dolomite mostly have medium values of modulus ratio, whereas foliated rocks can have modulus ratios ranging from low to high depending upon the direction of compression with respect to foliation.

Rock Properties, Table 2 Engineering classification of intact rock on the basis of unconfined compressive strength (After Deere and Miller 1966)

Class	Description	Uniaxial compressive strength (MPa)
A	Very high strength	Over 220
B	High strength	110–220
C	Medium strength	55–110
D	Low strength	27.5–55
E	Very low strength	Less than 27.5

Rock Properties, Table 3 Engineering classification[a] of intact rock on the basis of modulus ratio (E_t/σ_c) (After Deere and Miller 1966)

Class	Description	Modulus ratio[b]
H	High modulus ratio	Over 500
M	Medium modulus ratio	200–500
L	Low modulus ratio	Less than 200

[a]Rocks are classified by both strength and modulus ratio such as AM, BL, BH, CM, etc.
[b]Modulus ratio = E_t/σ_c
E_t = tangent modulus at 50% ultimate strength
σ_c = unconfined compressive strength

Rock Properties, Table 4 Durability classification based on second-cycle slake durability index (After ISRM 1979)

Second-cycle slake durability (Id_2)	Classification
0–30	Very low
30–60	Low
60–85	Medium
85–95	Medium high
95–98	High
98–100	Very high

Numerous durability classifications for clay-bearing rocks have been proposed by various researchers. Table 4 shows the ISRM (1979) classification based on Id_2.

Rock Mass Properties

The design and stability of large engineering structures such as dams, tunnels, highway cuts, and surface and underground mines depend on the properties of rock masses that are controlled by the presence of discontinuities such as bedding planes, joints, foliation, faults, and shear zones. Also, rock masses are significantly more anisotropic than intact rock.

There are seven aspects of discontinuities that are significant with respect to the stability of rock masses. These include geometry, continuity, spacing, surface irregularities, physical properties of adjacent rock, nature of infilling material, and groundwater (West 1995; Wyllie and Mah 2004).

Geometry deals with the orientation of the discontinuities and plays a fundamental role in the stability of rock slopes (Wyllie and Mah 2004) and roofs of underground openings (Hoek and Brown 1980).

Continuity indicates the persistence of the discontinuities. The more continuous the discontinuities, the weaker the rock mass.

Spacing represents the frequency of discontinuities, with spacing and continuity being interrelated. Table 5 shows a classification of discontinuities based on spacing by Deere (1964). Closely spaced discontinuities represent a weaker rock mass with greater potential for slope failure and deformation.

Surface irregularities contribute to increased resistance against failure by either overriding the irregularities or shearing through them (Patton 1966; West 1995; Wyllie and Mah 2004). When a discontinuity separates two different rock types, such as a bedding plane between sandstone and shale units, the properties of the weaker rock unit will control the shear strength along the discontinuity.

Infilling includes all soil-like material filling the discontinuities. The properties and thickness of the infilling material influence the resistance against shearing significantly (West 1995; Wyllie and Mah 2004).

Groundwater decreases the shear strength of a rock mass through buildup of pore pressure (Wyllie and Mah 2004; Gonzalez de Vallejo and Ferrer 2011).

Engineering Classification of Rock Mass

The following sections discuss briefly the various indices and classification schemes that describe the quality of rock mass and quantify its engineering behavior.

Percent Core Recovery

Percent core recovery is the ratio of the length of the core obtained to the length drilled, expressed as a percentage. It indicates both the quality of drilling and the soundness of the rock. A core recovery of 90% indicates a sound, homogeneous rock, a 50% recovery suggests rock with seams of weak, weathered material, and very low or no recovery means the rock is highly decomposed.

Rock Quality Designation (RQD)

Rock Quality Designation, developed by Deere (1964), is one of the most important and universally used indices of rock mass quality. It is defined as the ratio of the sum of NX-size core pieces that are equal to or greater than 10 cm to the total length drilled, expressed as a percentage. Table 6 shows the rock mass quality bands based on RQD. The RQD has been used to estimate Young's modulus (Coon and Merritt 1970), loads on tunnel support systems (Cording et al. 1975), and bearing capacity of foundation rock (Peck et al. 1974). However, while using RQD, one should keep in mind that: (1) RQD depends on the driller's experience; (2) schistose rocks may have a high RQD value but still contain many planes of failure; and (3) joints filled with clay seams may be widely spaced but can still result in failure.

Fracture Index

Fracture index or fracture frequency is the number of fractures per meter length of core (Farmer 1983). The higher the fracture index, the poorer is the quality of the rock mass.

Velocity Index

Comparing the square of the seismic wave velocity through a rock mass in the field (VF)2 to the square of seismic wave velocity through an intact rock sample in the laboratory (VL)2 is known as the velocity index or velocity ratio (Onedera 1963; Farmer 1983; Gonzalez de Vallejo and Ferrer 2011). As the fracture frequency in rock mass increases, the velocity index decreases. Conversely, a decrease in fracture frequency will result in an increase in velocity index. Table 7 (Farmer 1983) shows the relationship between rock mass quality, RQD, fracture frequency, and velocity index. For a given direction, the correlation between velocity index and RQD is 1:1 (Gonzalez de Vallejo and Ferrer 2011).

Rock Properties, Table 5 Descriptive classification of discontinuity spacing (After Deere 1964)

Bedding	Spacing	Joints
Very thin	< 5 cm	Very close
Thin	5–30 cm	Close
Medium	30 cm–1 m	Moderately close
Thick	1–3 m	Wide
Very thick	> 3 m	Very wide

Rock Properties, Table 6 RQD quality bands (After Deere and Miller 1966)

RQD (%)	Description
0–25	Very poor
25–50	Poor
50–75	Fair
75–90	Good
90–100	Very good

Rock Properties, Table 7 Relationship between RQD, fracture frequency, and velocity index (After Farmer 1983)

Quality classification[a]	RQD[a] (%)	Fracture frequency (per meter)	Velocity index $(v_F^2)/v_L^2)^b$
Very poor	0–25	>15	0–0.2
Poor	25–50	15–8	0.2–0.4
Fair	50–75	8–5	0.4–0.6
Good	75–90	5–1	0.6–0.8
Excellent	90–100	1	0.8–1.0

[a]Deere and Miller (1966)
[b]V_F is the wave velocity in the field; V_L is the velocity in the laboratory

Rock Mass Classification Systems

One of the earliest rock mass classifications for estimating tunnel supports was developed by Terzaghi (1946) who divided rock mass into categories such as intact rock, stratified rock, moderately jointed rock, blocky and seamy rock, squeezing rock, and swelling rock, based on discontinuity spacing and degree of weathering. However, the more frequently used quantitative classification systems that take into account a number of parameters include the Rock Structure Rating (RSR) developed by Wickham et al. (1972), the Geomechanics Classification or Rock Mass Rating (RMR) developed by Bieniawski (1973), and Rock Mass Quality or Q-system developed by Barton et al. (1974). The parameters considered in developing these classification systems include discontinuity spacing, discontinuity orientation, discontinuity surface properties, intact rock strength, and groundwater conditions. These parameters are assigned varying scores, based on the conditions they represent, which are then added or multiplied to obtain the final rating index.

The RSR system is based on three parameters designated A, D, and C that represent the general geology (rock type and structure), joint pattern (joint spacing and orientation), groundwater, and joint condition, respectively. The system is used specifically for designing support systems for mines and tunnels. The details of this system and its applications can be found in Wickham et al. (1972), Farmer (1983), and Bieniawski (1989).

The RMR classification divides rock mass into five classes (very good, good, fair, poor, and very poor) on the basis of RQD, intact rock strength, joint spacing, joint separation, joint continuity, joint orientation, and groundwater inflow. The RMR has been related to modulus of deformation (Bieniawski 1989) as well as cohesion and friction parameters (Hoek and Brown 1980). Complete details of RMR system are provided in Hoek and Brown (1980), Farmer (1983), and Bieniawski (1989). High RMR scores indicate very good to good quality rock mass, and low RMR scores represent poor to very poor quality rock mass.

The Q-system of the Norwegian Geotechnical Institute (NGI), developed specifically to evaluate tunnel roof stability and design of support system, uses six parameters to obtain the Q value as follows:

$$Q = (RQD/J_n)\ (J_r/J_a)\ (J_w/SRF) \tag{10}$$

where:

RQD = rock quality designation
Jn = number of joint sets
Jr = joint roughness
Ja = joint alteration
Jw = water inflow in joints
SRF = stress reduction factor

In the equation for Q value, RQD/J_n represents the block size, J_r/J_a the inter-block shear strength, and J_w/SRF the active state of stress (loosening load during excavation, squeezing load in incompetent rock, residual stress relief in competent rock). The higher the Q value, the better the quality of rock mass with respect to tunneling. Tables for assigning scores to various parameters comprising the Q-system can be found in Hoek and Brown (1980), Farmer (1983), and Bieniawski (1989).

Summary

There are two classes of rock properties: (i) intact rock properties and (ii) rock mass properties. Intact rock properties include specific gravity, absorption, porosity, degree of saturation, unit weight, unconfined compressive strength, tensile strength, shear strength, Young’s modulus, Poisson’s ratio, and durability. These properties are determined in the laboratory, and they are controlled by the petrographic characteristics of the rock. Properties of intact rock are used to evaluate the suitability of a rock for use as construction material. Rock mass properties, controlled by discontinuities, include percent core recovery, rock quality designation (RQD), fracture index, and velocity index. Rock mass properties are measured in the field on rock outcrops, and they are used to evaluate the quality of a rock mass for structures such as dams, tunnels, mine openings, and building foundations. Classification systems, based on intact rock properties and rock mass properties, have been developed to classify intact rock and rock mass into categories ranging from very good quality rock or rock mass to very poor quality rock or rock mass. These quantitative classifications provide the basis for evaluating the quality of rock as building material and for designing engineering structures on or inside the rock mass.

Cross-References

▶ Angle of Internal Friction
▶ Building Stone

▶ Dams
▶ Deformation
▶ Density
▶ Durability
▶ Engineering Properties
▶ Mechanical Properties
▶ Modulus of Deformation
▶ Modulus of Elasticity
▶ Poisson's Ratio
▶ Shear Strength
▶ Velocity Ratio
▶ Young's Modulus

References

American Society for Testing and Materials (ASTM) (2013) Annual book of ASTM standards: soil and rock 4.08 section 4. ASTM International, West Conshohocken

Barton N, Lien R, Lunde J (1974) Engineering classification of rock masses for the design of tunnel support. Rock Mech 6(4):189–236

Bieniawski ZT (1973) Engineering classification of jointed rock masses. Trans South Afr Inst Civ Eng 15(12):335–343

Bieniawski ZT (1989) Engineering rock mass classifications. Wiley, New York

Broch E, Franklin JA (1972) The point load strength test. Int J Rock Mech Min Sci 9:669–697

Cargill JS, Shakoor A (1990) Evaluation of empirical methods of measuring the uniaxial compressive strength. Int J Rock Mech Min Sci Geomech Abstr 27(6):495–503

Coon RF, Merritt AH (1970) Predicting in situ modulus of deformation using rock quality indexes. In situ testing for rock American Society for Testing and Materials Special Technical Publication. American Society for Testing and Materials (ASTM) self pub 477. pp 154–173

Cording EJ, Hendron AJ Jr, MacPherson HH, Hansmire WH, Jones RA, Mahar JW, O'Rourke TD (1975) Methods of geotechnical observations and instrumentation in tunneling. Report No UILU-ENG 75-2022 1 & 2, Department of Civil Engineering University of Illinois at Urbana-Champaign, Urbana Illinois, p 566

Deere DU (1964) Technical description of cores for engineering purposes. Rock Mech Eng Geol 1:16–22

Deere DU, Miller RP (1966) Engineering classification and index properties for intact rock. Technical Report No AFWL-TR-65-116, University of Illinois, Urbana, p 299

Farmer I (1983) Engineering behavior of rocks, 2nd edn. Chapman and Hall, New York

Franklin JA, Chandra A (1972) The slake durability test. Int J Rock Mech Min Sci 9:325–341

Gonzalez de Vallejo LI, Ferrer M (2011) Geological engineering. CRC Press/Taylor and Francis Group, London, p 678

Hajdarwish A, Shakoor A, Wells NA (2013) Investigating statistical relationships among clay mineralogy index engineering properties and shear strength parameters of mudrocks. Eng Geol 159:45–58

Hoek E, Brown ET (1980) Underground excavation in rock. The Institution of Mining and Metallurgy, London, p 527

International Society for Rock Mechanics (ISRM) (1979) Suggested methods for determining water content porosity density absorption and related properties and swelling and slake durability index properties. Int J Rock Mech Min Sci Geomech Abstr 16(2) Parts 1 and 2:143–156

International Society for Rock Mechanics (ISRM) (2007) In: Ulusay R, Hudson JA (eds) The complete ISRM suggested methods for characterization testing and monitoring: 1974–2006. ISRM Turkish National Group, Ankara, p 628

Johnson RB, De Graff JV (1988) Principles of engineering geology. Wiley, New York, p 497

Onodera TF (1963) Dynamic investigations of foundation rocks in situ. In: Proceedings of 5th US rock mechanics symposium. University of Minnesota, Minnesota, pp 517–533

Patton FD (1966) Multiple modes of shear failure in rock. In: Proceedings of 1st international congress of rock mechanics, Lisbon, pp 509–513

Peck RB, Hanson WE, Thornburn TH (1974) Foundation engineering. Wiley, New York, p 514

Shakoor A, Bonelli RE (1991) Relationship between petrographic characteristics engineering properties and mechanical properties of selected sandstones. Bull Assoc Eng Geol 28(1):55–71

Shakoor A, Barefield EH (2009) Relationship between unconfined compressive strength and degree of saturation for selected sandstones. Environ Eng Geosci XV(1):29–40

Terzaghi K (1946) In: Proctor RV, White T (eds) Rock tunneling with steel supports. Commercial Shearing and Stamping Company, Youngstown, pp 15–99

West TR (1995) Geology applied to engineering. Prentice-Hall, Englewood Cliffs, p 560

Wickham GE, Tiedemann H, Skinner EH (1972) Support determinations based on geologic predictions. In: Proceedings of 1st rapid excavation tunneling conference. American Institute of Mechanical Engineers, pp 43–64

Wyllie DC, Mah CW (2004) Rock slope engineering – civil and mining, 4th edn. Spon Press/Taylor and Francis Group, New York, p 431

Run-Off

Jeffrey R. Keaton
Amec Foster Wheeler, Los Angeles, CA, USA

Definition

Run-off, also referred to as runoff or surface runoff, is the term used to refer to that part of precipitation in the water cycle that moves on the ground surface downslope or downstream away from the location where it first accumulated as rain or snow. Surface water run-off is part of the water cycle that also includes evaporation, infiltration, and storage (USGS 2016). Run-off is estimated from rainfall based on an empirical approach that is known as the rational method (Goyen et al. 2014)

$$q = C\,A\,p \tag{1}$$

where q is the peak unit discharge in m^3/s from a drainage basin at a point of interest, C is a dimensionless coefficient that represents the amount of run-off as a decimal fraction of precipitation, A is the drainage basin area in m^2 above the point of interest, and p is representative rainfall intensity in mm/hr for a meaningful duration and a desired return period. The duration for the rainfall intensity may be the time of

R

concentration (the time required for water to flow from the most distant point in the drainage basin to the outlet defined as the point of interest). The unit discharge for several precipitation return periods (2 y, 5 y, 10 y, 25 y, 50 y, 100 y, 200 y) would be of interest for flood routing and flood hazard studies.

$$Q = C\,A\,P \tag{2}$$

where Q is total discharge volume in m^3 for a duration of interest, often one year, and P is total precipitation that falls during the period of interest. Thus, P might be the annual precipitation averaged to represent the drainage basin area. The total discharge would be of interest for water resources information.

The value of the C coefficient depends on the ground conditions in the drainage basin (vegetation, bare soil, exposed bedrock, urbanized pavement, and rooftops) that tends to vary with time and may be seasonal. The value of C also depends on the duration of the precipitation; C in a particular drainage basin would be lower for a rainfall event associated with a 2-year return period than for a 50-year rainfall event.

References

Goyen A, Phillips BC, Pathiraja S (2014) Project 13: urban rational method review. Australian rainfall & runoff report P13/S3/001, Engineers Australia. http://www.arr.org.au/wp-content/uploads/2013/Projects/ARR_Project_13_Stage3_report_DRAFT.pdf. Accessed May 2016

USGS (2016) The water cycle. U.S. Geological Survey webpage. http://water.usgs.gov/edu/watercycle.html. Accessed May 2016